

A PARACHUTE DESIGN STUDY
FOR A MARS ENTRY VEHICLE

REPORT NO. FR-3707B

September 1964

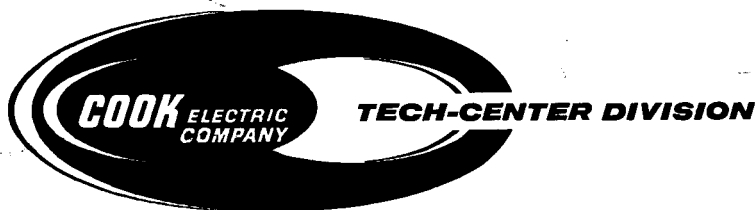
FACILITY FORM 602	N 65 15325	
	(ACCESSION NUMBER)	(THRU)
	141	1
	(PAGES)	(CODE)
	CR 60290	30
	(NASA CR OR TMX OR AD NUMBER)	(CATEGORY)

GPO PRICE \$ _____

OTS PRICE(S) \$ _____

Hard copy (HC) 4.00

Microfiche (MF) 1.00



640 OAKTON STREET MORTON GROVE, ILLINOIS, 60053

PHONE: 312 967-6600

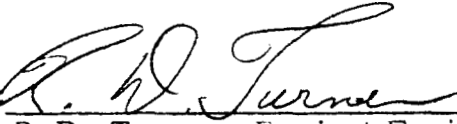
TWX: 312 967 5177

A PARACHUTE DESIGN STUDY
FOR A MARS ENTRY VEHICLE

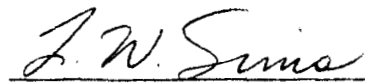
FR-3707B

JFL CONTRACT NO. 950741


Prepared by


R.D. Turner, Project Engineer

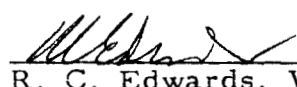
APPROVED BY:


L. W. Sims, Program Manager
Aerospace Technology Section
Tech-Center Division

10/5/64
Date


L. J. Lorenz, Manager
Aerospace Technology Section
Tech-Center Division

10/5/64
Date


R. C. Edwards, Vice President
Director, Cook Research Laboratories
Tech-Center Division

Date

(Prepared by Tech-Center Division, A Division of Cook Electric Company,
6401 W. Oakton Street, Morton Grove, Illinois)

A PARACHUTE DESIGN STUDY
FOR A MARS ENTRY VEHICLE

REPORT NO. FR-3707B

September 1964

R. D. Turner

Tech-Center Division
Cook Electric Company
Morton Grove, Illinois

(Prepared for Jet Propulsion Laboratory California
Institute of Technology, under Contract No. 950741)

ABSTRACT

15325
An investigation, sponsored by NASA and subcontracted by the Jet Propulsion Laboratory, was performed to determine the feasibility of decelerating an entry vehicle in the Mars atmosphere with a parachute system. The study was to define an optimum system which would provide the maximum deployment altitude, minimum terminal velocity and maximum descent time consistent with practical weight limitations. The basic entry vehicle weight considered was 350 pounds which included 100 pounds for the sum of the payload and second stage parachute.

The success of recent high supersonic parachute tests allowed consideration of supersonic deployment Mach numbers. To obtain the most desirable system, three first stage deployment Mach numbers (3, 4.5, and 6) were studied with three parachute weight allowances (21, 35, and 45.5 pounds) for the worst atmospheric profile. Fabric temperature limitations were considered. For each parachute weight-allowance, five first stage parachute sizes were investigated to study the effect on the system performance and to obtain the effect of varying the ratio of first stage weight to total parachute weight. The optimum system was found to be a 12 foot projected diameter Hyperflo parachute for first stage deceleration and a 59.3 foot nominal diameter extended skirt parachute for the terminal stage. These parachutes have a combined weight of 35 pounds and represent a first stage weight to total parachute weight of 35 percent. The first stage deployment Mach number chosen for this system was 3.0. The total parachute system weight was estimated to be 54 pounds or 15.4 percent of the entry vehicle weight. This optimum parachute system's performance was investigated for entry angles between -90 and -20 degrees, several atmospheric profiles, and a range of entry velocities.

For entry vehicles weighing more than 350 pounds (up to 5000 pounds) the ratio of total parachute weight to entry vehicle weight exceeded the 10 percent obtained for the 350 pound vehicle. The scaling used in determining the sizes of parachutes for the higher entry vehicle weights was based on maintaining the same ballistic coefficient for each stage of deceleration, thereby maintaining the same terminal velocity. This scaling procedure imposed the requirement of using large first stage parachutes, which increased the canopy stresses. This increased stress and opening load for the first stage parachute mainly accounted for the increased percentage of parachute weight (18 percent for 5000 pound vehicle) with larger entry vehicle weights.

Ant

FOREWORD

The work presented in this report was performed at the Tech-Center, a Division of the Cook Electric Company, Morton Grove, Illinois, under the authority of Contract No. NAS 7-100, Subcontract 950741. Mr. J. M. Brayshaw, Jr., Jet Propulsion Laboratory, served as the Technical Monitor.

The study was performed under the general direction of Mr. L. E. Benitez, Vice President and General Manager, and Mr. R. C. Edwards, Vice President, Director, Cook Research Laboratories.

The technical effort was carried out by the Aerospace Technology Section, under the direction of Mr. L. J. Lorenz, Section Manager, and Dr. R. J. Benjamin, Director of Engineering. Mr. L. W. Sims was Program Manager, and Mr. R. D. Turner was Project Engineer.

Other staff members who assisted with the project include Messrs. P. A. Minerva, (Computer Analysis) and F. A. Ruprecht, H. Loellbach, E. Biedron (Parachute Technical Advisors).

TABLE OF CONTENTS

<u>Section</u>	<u>Page</u>
I. INTRODUCTION	1
II. PROGRAM OBJECTIVES AND ENVIRONMENTAL CONDITIONS	2
A. Parachute Selection	13
B. Deployment Conditions	14
C. Parachute Filling Time Relationships	20
1. Hyperflo Filling Time	21
2. Reefed Extended Skirt Parachute Filling Time	24
3. Time to Fill From Reefed Condition for Extended Skirt Parachute	26
III. PARAMETRIC INVESTIGATION TO DETERMINE OPTIMUM PARACHUTE SYSTEM	29
A. Parachute Sizing	29
B. Trajectory Computations	36
C. Sensing System Requirements and Description	57
D. System Sequencing and Weight Breakdown for the Decelerator System	83
E. Description of Development Testing and Cost Estimates for Designing and Testing the Decelerator System	90
1. Sensing System	90
2. Effects of Sterilization and Long Time Vacuum on Materials	90
3. Mortar System Design	91
4. Hyperflo Parachute Tests	91
5. Effects of Sterilization and Long Time Vacuum on Pyrotechnic Charges	91
6. Second Stage Parachute Testing	92
7. System Tests	93
IV. EFFECT OF INCREASING THE ENTRY VEHICLE WEIGHT	96
V. SUMMARY AND RECOMMENDATIONS	108

APPENDICES

I. EQUATIONS USED IN DETERMINING THE TIME TO FILL FROM REEFED INFLATION TO FULL OPEN FOR A 14.3 PERCENT FULLY EXTENDED SKIRT PARACHUTE	110
--	-----

TABLE OF CONTENTS (Cont'd)

<u>Section</u>	<u>Page</u>
II. EQUATIONS USED FOR DETERMINING MATERIAL STRESS FOR FIRST AND SECOND STAGE PARACHUTES . . .	118
III. EQUATIONS USED IN DETERMINING MORTAR WEIGHTS . .	123
IV. SUPPLEMENTAL INFORMATION	126

LIST OF ILLUSTRATIONS

<u>Figure</u>	<u>Page</u>
1a. Density Variation With Altitude for Model Atmospheres A Through F	3
1b. Temperature Variation With Altitude for Model Atmospheres A Through F	4
1c. Density Variation With Altitude for Model Atmospheres G Through K	5
1d. Temperature Variation With Altitude for Model Atmospheres G Through K	6
1e. Density Variation With Altitude for Model Atmospheres L Through P	7
1f. Temperature Variation With Altitude for Model Atmospheres L Through P	8
2. Entry Vehicle Axial Force Coefficient Variation With Mach Number	9
3. Effect on Entry Vehicle Trajectory by Deploying an 8.0 D_p Hyperflo at Mach Numbers of 3.0, 4.5, and 6.0	15
4. Effect on Entry Vehicle Trajectory by Deploying a 12.0 D_p Hyperflo at Mach Numbers of 3.0, 4.5, and 6.0	17
5. Effect of Deployment Mach Number on Maximum Fabric Temperature for Two Hyperflo 1st Stage Sizes	18
6. Dynamic Pressure Reduction and Nomex Material Strength Reduction Versus Calculated Material Temperature for Predicted Trajectory of Entry Vehicle With 8.0 D_p Hyperflo Deployed at Mach 6.0	19
7. Hyperflo Filling Time Parameter Versus Deployment Velocity.	22
8. Hyperflo Projected Frontal Area Versus Filling Time	23

LIST OF ILLUSTRATIONS (Cont'd.)

<u>Figure</u>		<u>Page</u>
9.	Reefed Extended Skirt Filling Time Parameter Versus Deployment Velocity	25
10.	Reefed Extended Skirt Projected Frontal Area Versus Filling Time	27
11.	Hyperflo Drag Coefficient Based on Projected Area Versus Mach Number	33
12.	Second Stage Descent Time Versus the Ratio of First Stage Weight to Weight Allowance for a Mach 3.0 Hyperflo Deployment	37
13.	Second Stage Descent Time Versus the Ratio of First Stage Weight to Weight Allowance for a Mach 4.5 Hyperflo Deployment	38
14.	Second Stage Descent Time Versus the Ratio of First Stage Weight to Weight Allowance for a Mach 6.0 Hyperflo Deployment	39
15.	Altitude Where Mach Number Equals 0.9 Versus First Stage Weight	41
16.	Maximum Second Stage Descent Time Versus Parachute Weight Allowance	42
17.	Impact Velocity Versus the Ratio of First Stage Weight to Weight Allowance for a Mach 3.0 Hyperflo Deployment . . .	43
18.	Impace Velocity Versus the Ratio of First Stage Weight to Weight Allowance for a Mach 4.5 Hyperflo Deployment . . .	44
19.	Impact Velocity Versus the Ratio of First Stage Weight to Weight Allowance for a Mach 6.0 Hyperflo Deployment . . .	45
20.	Predicted Maximum Parachute Fabric Temperature and Instantaneous to Full Open Drag Ratio Versus Time From Deployment. 12.0 Ft. D_p Parachute, G Atmosphere, -90 Degree Entry Flight Path Angle, Mach 3 Deployment . . .	58

LIST OF ILLUSTRATIONS (Cont'd.)

<u>Figure</u>		<u>Page</u>
21.	Predicted Maximum Parachute Fabric Temperature and Instantaneous to Full Open Drag Ratio Versus Time From Deployment. 12.0 Ft. D_p Parachute, G Atmosphere, -90 Degree Entry Flight Path Angle, Mach 4.5 Deployment	59
22.	Predicted Maximum Parachute Fabric Temperature and Instantaneous to Full Open Drag Ratio Versus Time From Deployment. 12.0 Ft. D_p Parachute, G Atmosphere, -90 Degree Entry Flight Path Angle, Mach 6.0 Deployment . . .	60
23.	Altitude and Mach Number History As a Function of Time for Optimum System Deployed in G Atmosphere -20 Degree Entry Flight Path Angle.	65
24.	Altitude and Mach Number History as a Function of Time for Optimum System Deployed in G Atmosphere -34 Degree Entry Flight Path Angle.	66
25.	Altitude and Mach Number History as a Function of Time for Optimum System Deployed in G Atmosphere -51 Degree Entry Flight Path Angle.	67
26.	Altitude and Mach Number History as a Function of Time for Optimum System Deployed in G Atmosphere -90 Degree Entry Flight Path Angle.	68
27.	Altitude and Mach Number History as a Function of Time for Optimum System Deployed in J Atmosphere -20 Degree Entry Flight Path Angle.	69
28.	Altitude and Mach Number History as a Function of Time for Optimum System Deployed in J Atmosphere -90 Degree Entry Flight Path Angle.	70
29.	Predicted Maximum Parachute Fabric Temperature and Instantaneous to Full Open Drag Ratio Versus Time From Deployment. 12Ft. D_p Parachute, G Atmosphere, -51 Degree Entry Flight Path Angle, Mach 2.7 Deployment	71

LIST OF ILLUSTRATIONS (Cont'd)

<u>Figure</u>	<u>Page</u>
30. Force Time Histories For Parachutes, G Atmosphere 90 Degree Entry Angle	72
31. Force Time Histories For Parachutes, G Atmosphere 20 Degree Entry Angle	73
32. Force Time Histories For Parachutes, J Atmosphere 90 Degree Entry Angle	74
33. Effect of Entry Angle on Second Stage Deployment Altitude for Three Atmosphere Profiles	76
34. Effect of Entry Angle on Second Stage Descent Time for Three Atmosphere Profiles	77
35. Effect of Entry Velocity on Second Stage Deployment Altitude for G Atmosphere 90 Degree Entry Angle	78
36. Effect of Entry Velocity on Descent Time for G Atmosphere 90 Degree Entry Angle	79
37. System Sequencing	84
38. Payload Weight As a Function of Impact Weight Assuming the Entry Vehicle Weight Is 350 Earth Pounds	89
39. Weight of First Stage Parachute As a Function of Projected Diameter and Weight of First Stage Plus Drogue Or Pilot Chute and Mortar	98
40. Nominal Diameter of Terminal Parachute As a Function of Entry Weight For Both Single and Clustered Parachute Arrangements	103
41. Weight of Terminal Parachute System As a Function of Parachute Nominal Diameter	104
42. Payload As a Function of Entry Weight	105

LIST OF ILLUSTRATIONS (Cont'd.)

<u>Figure</u>	<u>Page</u>
43. Variation of First and Second Stage Parachute Weight As a Function of Entry Weight Considering Both Single and Cluster Arrangements For the Terminal Recovery Phase	107
A-1 Idealized Canopy Shape	111
A-2 Projected to Nominal Area Ratio Versus Time Ratio For a Solid Flat Canopy	112
A-3 Ratio of Skirt Inflow and Vent Outflow Velocities to Free Stream Velocity Versus Time Ratio For a Solid Flat Canopy	114

LIST OF TABLES

<u>Table</u>		<u>Page</u>
I.	Model Atmosphere Compositions and Physical Parameters at Critical Altitudes	10
II.	Parachute Sizes and Weights For a First Stage Made With Nomex Material and a Second Stage Made With Dacron Material	34
III.	Determination of Merit Figures For the Parachute Systems In Contention	51
IV.	Aerodynamic Heating Results	56
V.	Results of Computer Analysis For the Optimum Parachute System	80
VI.	Parachute Design Characteristics	87
VII.	Decelerator Component Description As a Function of Entry Vehicle Weight	99

SECTION I

INTRODUCTION

Man's goal of gaining intimate knowledge of the planets and satellites which surround our earth is close to being attained. The Apollo program which will place man on our closest neighbor in space is in full swing and predictions of a landing as early as in the late 1960's have been made. The Mercury program has proved man's ability to travel in space and the deep space probe of the Mariner program has shown the ability of man to obtain scientific data from distances as far as the planet Venus. The recent Ranger flight has successfully demonstrated the capability of impacting a space craft with precise accuracy on the surface of the moon.

All of the above programs have advanced or are about to advance the knowledge of the close-by heavenly bodies. The ability to determine scientific data for another planet from earth-bound instruments is now being supplemented by the capability of making direct observations near the planet. One of the future programs which is presently being contemplated is the placing of scientific instruments on the planet Mars. This study deals with the design of a parachute decelerator system which will permit the controlled descent of a payload through the Mars atmosphere.

The problems associated with designing a parachute decelerator system with the capability of functioning over a range of possible atmospheric profiles as opposed to a known profile such as earth's, significantly complicates the design. A further complication is the fact that for the early flights the exact entry flight path angle of the capsule will not be known. As a result, the decelerator system must function not only in an atmosphere where the atmospheric parameters are uncertain but also over a range of altitudes which result from a variation of entry angle.

Considering the above factors, plus the fact that the planet's atmospheric density at the surface may be less than one-seventieth that of earth's, the problem is complex. In the performance of this study, the known characteristics of conventional and recently developed parachutes were investigated to derive an optimum system. Since it is imperative that the deployment altitude be as high as possible due to unknown terrain characteristics, the state-of-the-art in parachute technology was surveyed to obtain a parachute that would be capable of being deployed at the highest supersonic velocity. This high supersonic velocity requirement stems from the assumption that velocity decreases monotonically as altitude decreases.

SECTION II

PROGRAM OBJECTIVES AND ENVIRONMENTAL CONDITIONS

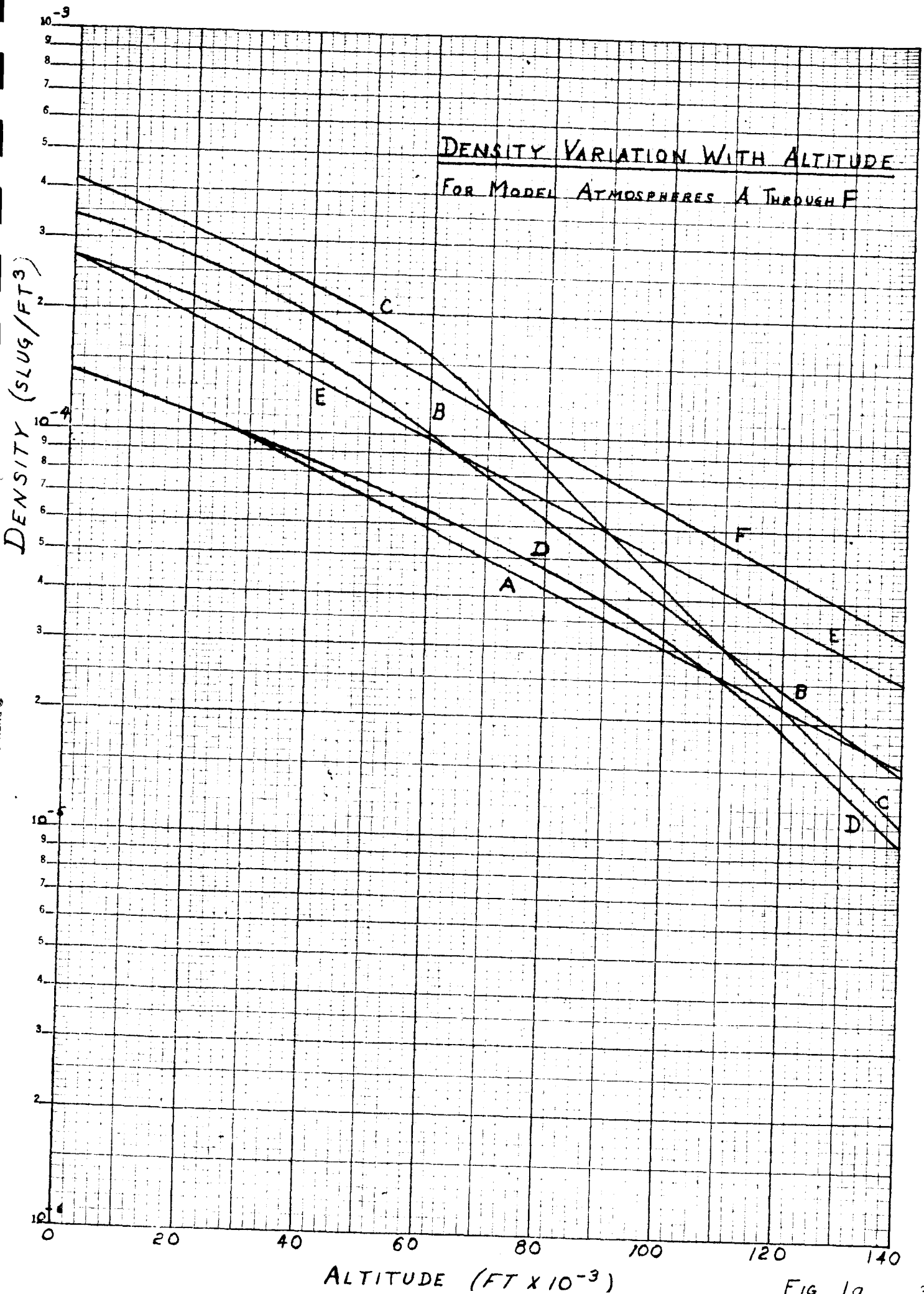
The purpose of this study was to define an optimum parachute system capable of providing a low-speed capsule descent to the Mars' surface in accordance with these design objectives:

- (i) Maximum parachute descent time
- (ii) Maximum deployment altitude consistent with descent time
- (iii) Minimum parachute oscillation
- (iv) Minimum weight
- (v) Minimum impact velocity

The atmospheric profiles provided by Jet Propulsion Laboratory (JPL) in which the deceleration system must be capable of operating are shown in Figure 1. Table 1 gives the composition of these atmospheres and pertinent factors which describe the physical parameters at critical altitudes.

Review of the model atmospheres shows that atmosphere G affords the lowest surface density and the next to largest inverse scale height (β). Atmosphere H, while having a smaller inverse scale height than G has a lower tropopause altitude and the same surface density as atmosphere G. This combination of factors made it difficult to determine which atmosphere would provide the most difficult profile for design of the recovery system. Six-degree-of-freedom trajectories computed by JPL for both G and H atmospheres showed that for any given Mach number in the Mach 6 and under range, G atmosphere affords the least altitude for deceleration. It is noted that the difference in altitude between G and H for the same Mach number is small, of the order of 4,000 feet at Mach 6 and 2,000 feet at Mach 3. In keeping with the program objectives atmosphere G was chosen as the design profile since atmosphere H affords no atmospheric parameter that would prove more severe in the decelerator design than does atmosphere G.

For the above computations a possible entry vehicle geometry selected by JPL for this study was a blunt shape (Sketched in Figure 2) with a hypersonic M/C_{DA} at zero-angle-of-attack of approximately 0.17. The entry weight of the capsule was 350 earth pounds with a zero-angle-of-attack axial force variation as shown in Figure 2. For all the computations performed it has been assumed that the initial angle-of-attack is 70 degrees at 800,000 feet.



TEMPERATURE VARIATION WITH ALTITUDE FOR MODEL ATMOSPHERES A THROUGH F

500

400

300

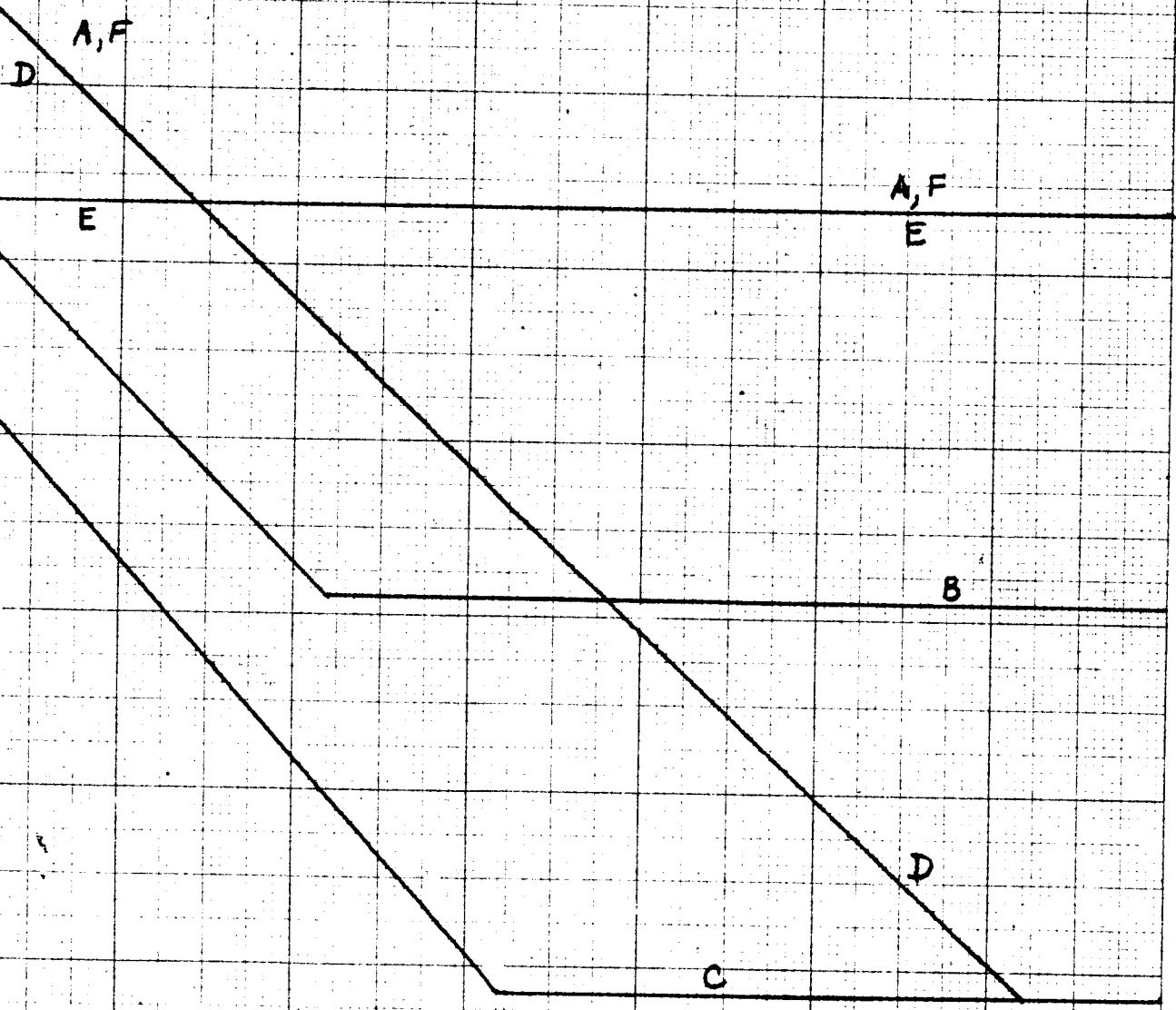
200

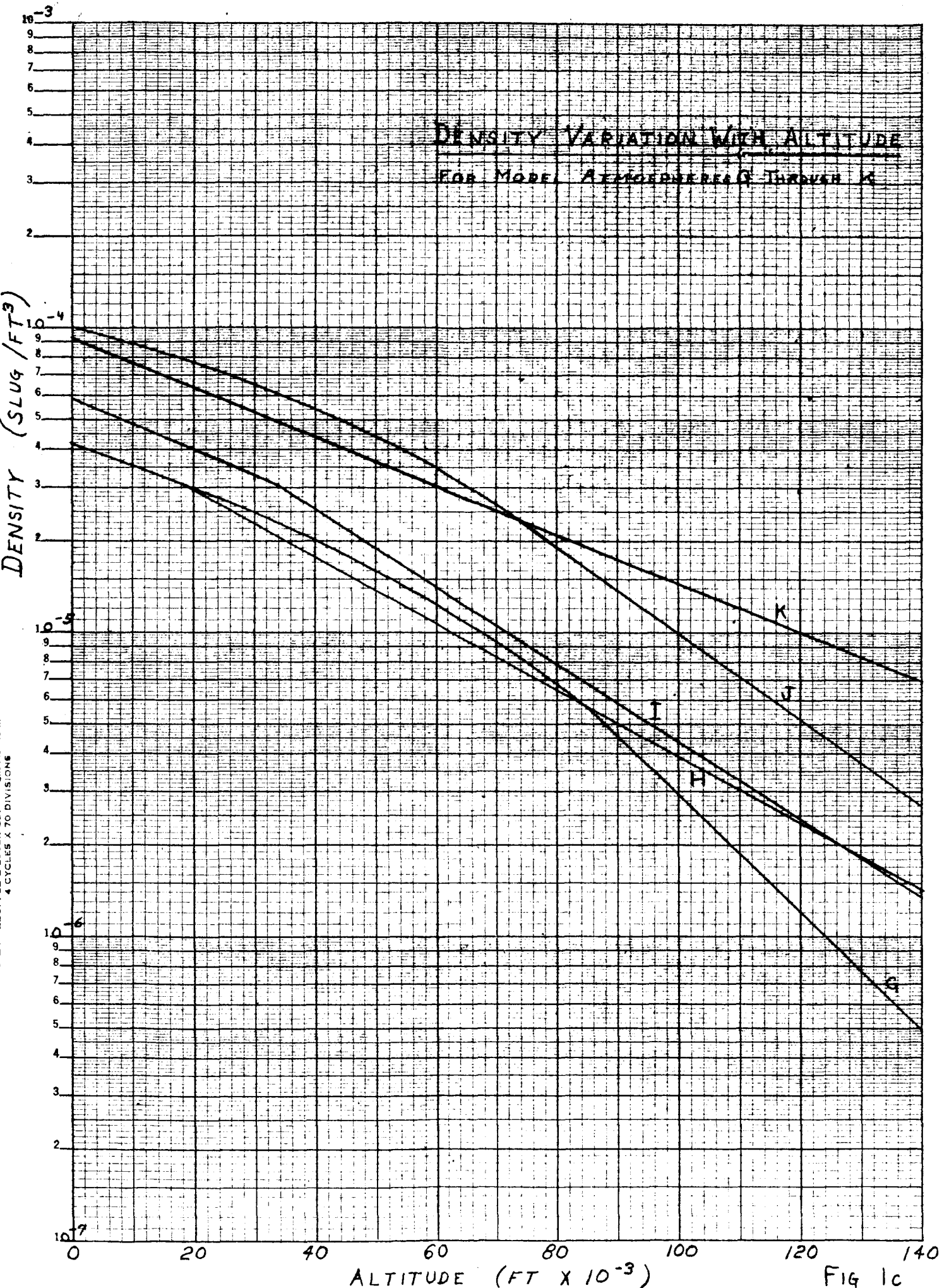
TEMPERATURE (°R)

0 20 40 60 80 100 120 140

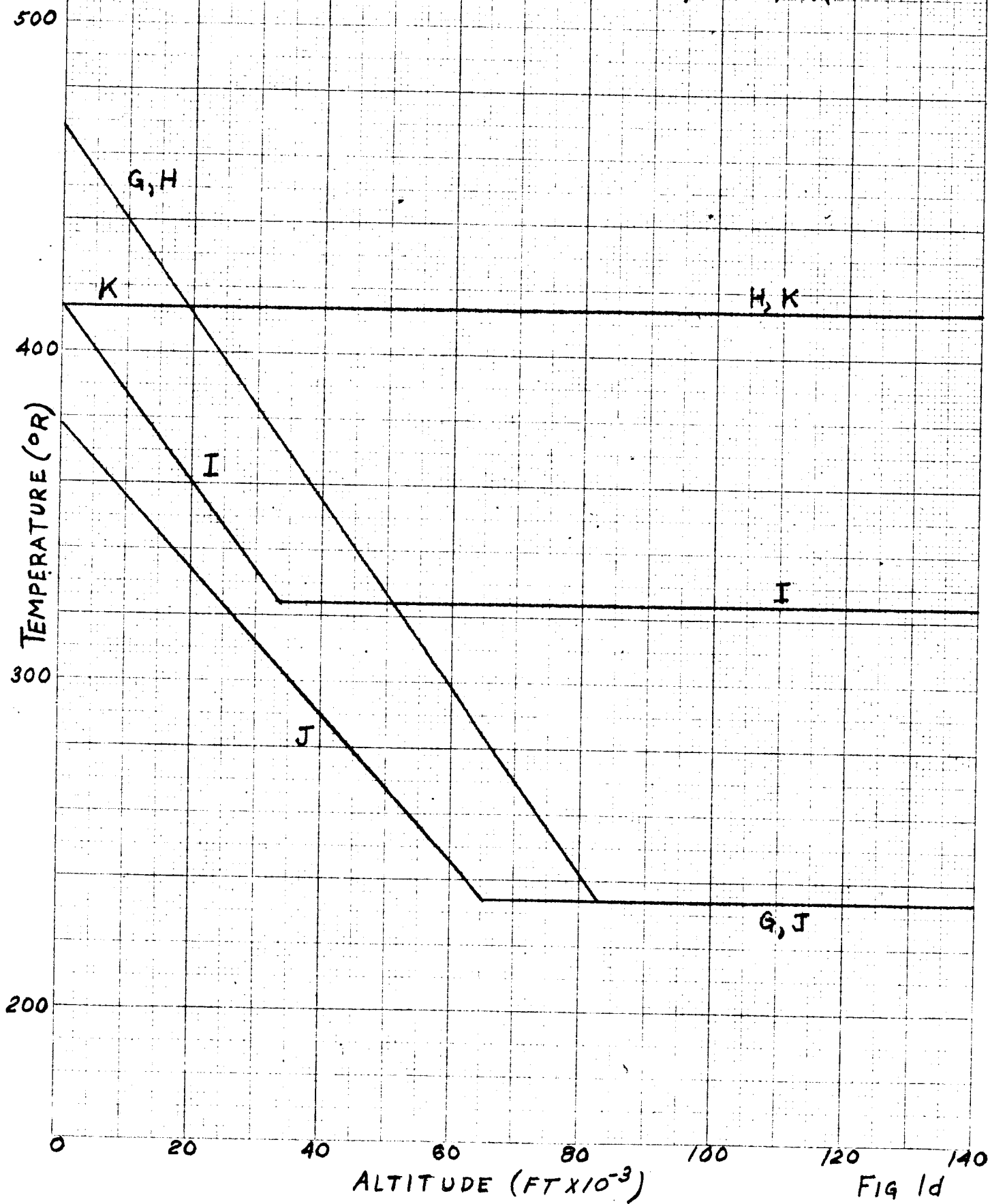
ALTITUDE (FT $\times 10^{-3}$)

Fig 1b



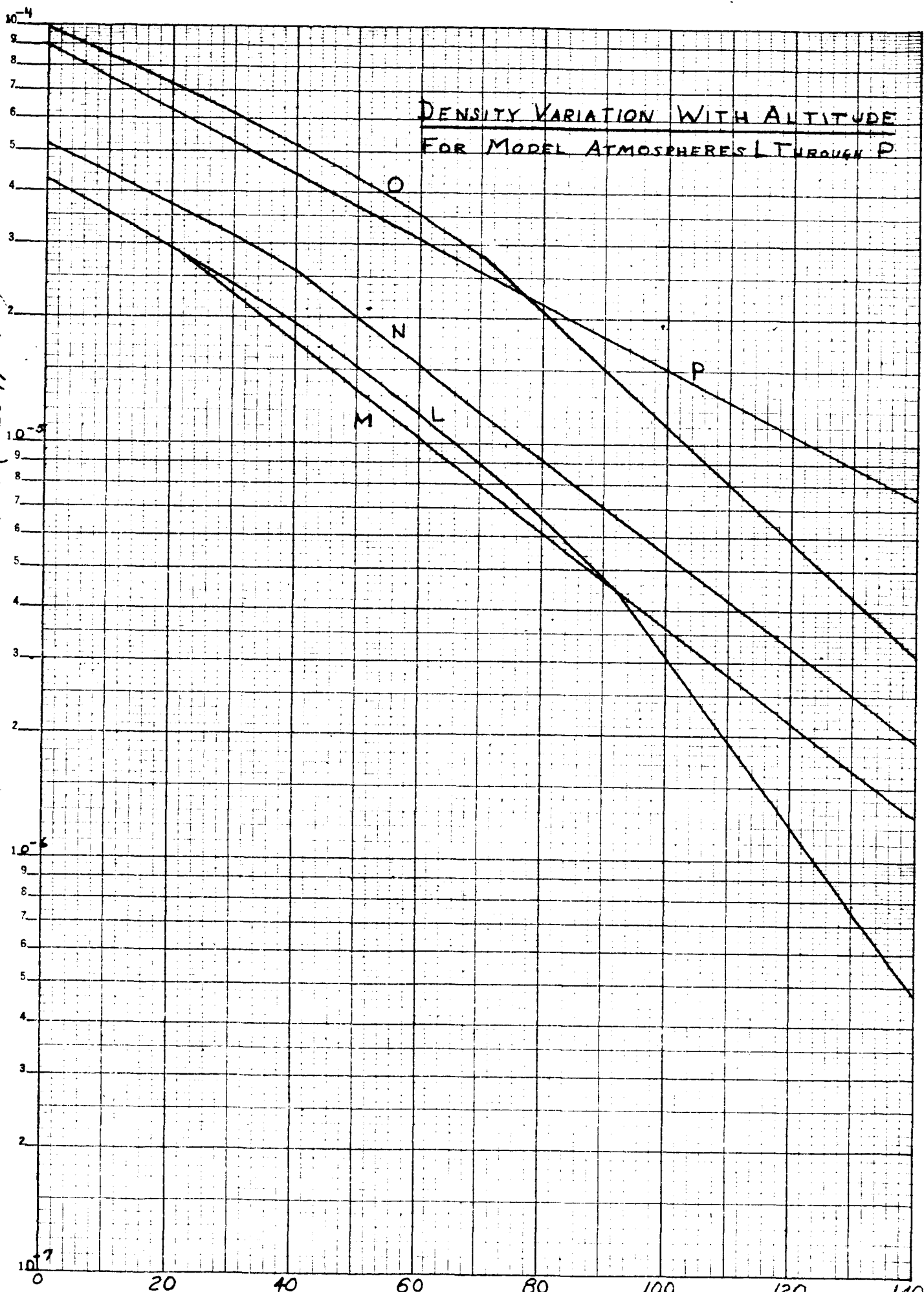


TEMPERATURE VARIATION WITH ALTITUDE FOR MODEL ATMOSPHERES G THROUGH K



DENSITY (SLUG/FT³)

DENSITY VARIATION WITH ALTITUDE
FOR MODEL ATMOSPHERES L THROUGH P



ALTITUDE (FT X 10⁻³)

Fig 1e 7

TEMPERATURE VARIATION WITH ALTITUDE FOR MODEL ATMOSPHERES L THROUGH P

500

400

300

200

TEMPERATURE (°R)

L, M

P

M, P

N

N

O

L, O

0 20 40 60 80 100 120 140

ALTITUDE (FT $\times 10^{-3}$)

Fig 1f

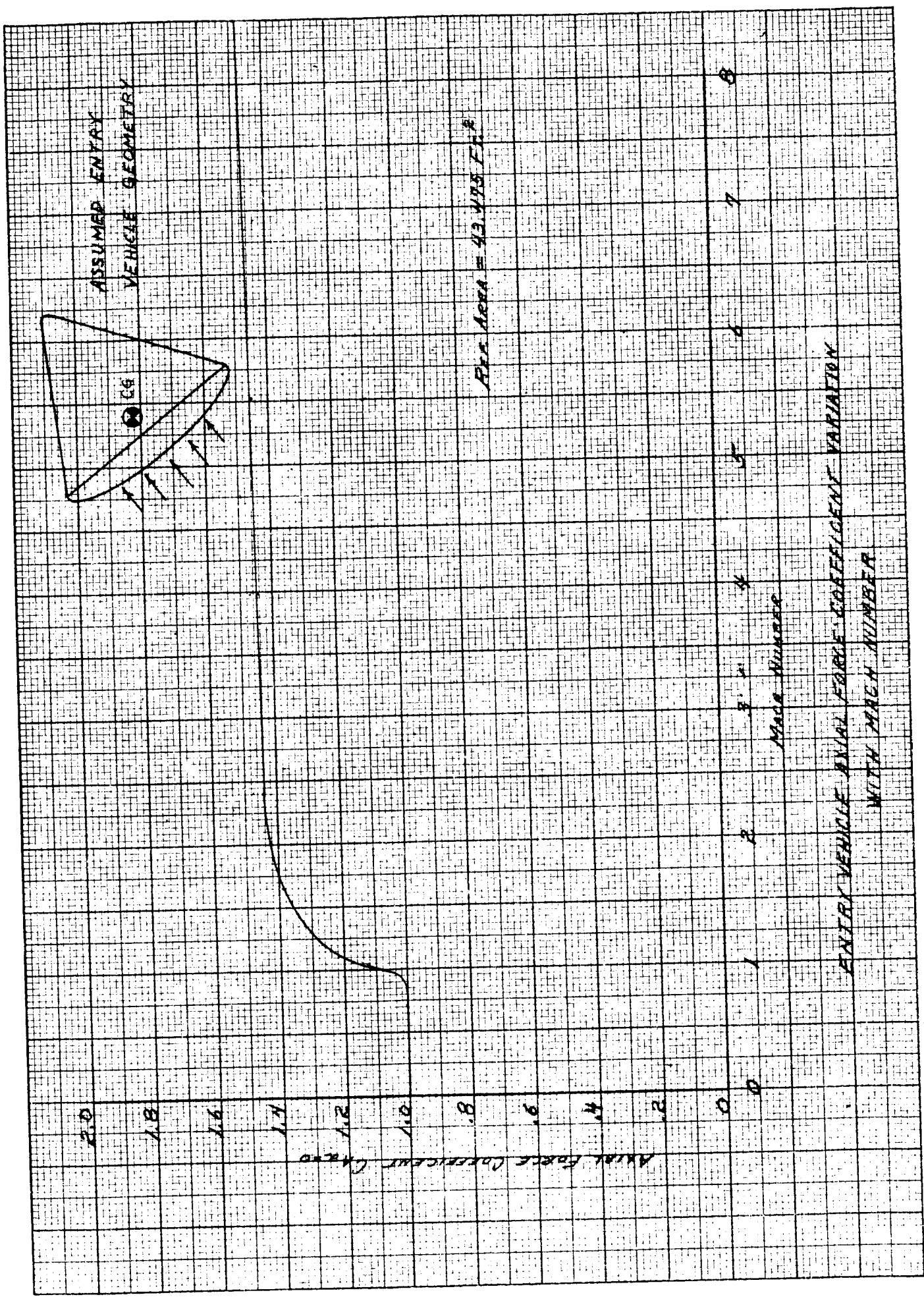


TABLE I

MODEL ATMOSPHERE COMPOSITIONS AND PHYSICAL PARAMETERS AT
CRITICAL ALTITUDE

Property	Symbol	Dimensions	A	B	C	D	E	F
Surface pressure	P_0	mb lbs/ft ²	54 113	94 196	136 284	54 113	94 196	136 284
Atmosphere temperature	T_s	°K °R	230 410	180 320	130 230	130 230	230 410	230 410
Surface temperature	T_0	°K °R	260 470	230 410	210 380	260 470	230 410	260 470
Acceleration of gravity at surface	g	cm/sec ² ft/sec ²	360 11.8	375 12.3	390 12.8	390 12.8	360 11.8	390 12.8
Composition (volume)		%						
CO ₂			7.2	1.9	0.7	7.2	1.9	0.7
A			6.0	0.85	0.6	6.0	0.85	0.6
N ₂			86.8	97.25	98.7	86.8	97.25	98.7
Molecular weight	M	mol ⁻¹	29.9	28.4	28.2	29.9	28.4	28.2
Specific heat ratio	γ		1.41	1.41	1.42	1.41	1.41	1.41
Adiabatic temp. lapse rate	Γ	°K/km °R/10 ³ ft	3.43 1.88	3.75 2.06	4.10 2.25	3.43 1.88	3.60 1.96	3.43 1.88
Tropopause altitude	h_T	km ft	8.75 28,700	13.33 43,700	19.50 64,000	37.90 124,000	0 0	8.75 28,700
Inverse scale height (Strat- osphere)	β	km ⁻¹ ft ⁻¹ x 10 ⁵	.056 1.7	.080 2.4	.110 3.4	.110 3.4	.056 1.7	.059 1.8
Surface density	ρ_0	gm/cm ³ x 10 ⁵ sl/ft ³ x 10 ⁵	7.5 14	14.0 27	22.0 43	7.5 14	14.0 27	18.0 34
Artificial surface density	ρ_0'	gm/cm ³ x 10 ⁵ sl/ft ³ x 10 ⁵	8.6 17	22 43	66 127	59 114	14 27	21 40
Density at tropopause	ρ_T	gm/cm ³ x 10 ⁵ sl/ft ³ x 10 ⁵	5.3 10	7.8 15	7.5 14	0.87 1.7	14 27	13 24

TABLE I (cont'd.)

MODEL ATMOSPHERE COMPOSITIONS AND PHYSICAL PARAMETERS AT
CRITICAL ALTITUDE

Property	Symbol	Dimensions	G	H	I	J	K
Surface pressure	P_o	mb lbs/ft ²	11 23.0	11 23.0	15 31.3	30 62.6	30 62.6
Stratosphere temperature	T_s	°K °R	130 234	230 414	180 324	130 234	230 414
Surface temperature	T_o	°K °R	260 468	260 468	230 414	210 378	230 414
Acceleration of gravity at surface	g	cm/sec ² ft/sec ²	375 12.3	375 12.3	375 12.3	375 12.3	375 12.3
Composition (volume)		%					
CO ₂			64.8	64.8	43.3	10.5	10.5
A			35.2	35.2	32.2	13.0	13.0
N ₂			0	0	24.5	76.5	76.5
Molecular weight	M	mol ⁻¹	42.6	42.6	38.8	31.3	31.3
Specific heat ratio	γ		1.37	1.37	1.39	1.40	1.40
Adiabatic temp. lapse rate	Γ	°K/km °R/ft x 10 ³	5.18 2.84	5.18 2.84	4.91 2.69	4.05 2.22	0
Tropopause altitude	h_T	km ft	25.09 82300	5.79 19000	10.19 33400	19.75 64800	0
Inverse scale height (Stratosphere)	β	km ⁻¹ ft ⁻¹ x 10 ⁵	.1478 4.506	.0835 2.546	.0972 2.963	.1085 3.308	.0613 1.869
Surface density	ρ_o	gm/cm ³ x 10 ⁵ sl/ft ³ x 10 ⁵	2.17 4.21	2.17 4.21	3.04 5.90	5.37 10.42	4.91 9.54
Artificial surface density	ρ_o'	gm/cm ³ x 10 ⁵ sl/ft ³ x 10 ⁵	13.60 26.40	2.52 4.89	4.35 8.44	14.20 27.55	4.91 9.54
Density at tropopause	ρ_T	gm/cm ³ x 10 ⁵ sl/ft ³ x 10 ⁵	0.332 0.643	1.55 3.02	1.62 3.14	1.66 3.23	4.91 9.54

TABLE I (cont'd.)

MODEL ATMOSPHERE COMPOSITIONS AND PHYSICAL PARAMETERS AT
CRITICAL ALTITUDE

Property	Symbol	Dimensions	L	M	N	O	P
Surface pressure	P_0	mb lbs/ft ²	11 23.0	11 23.0	15 31.3	30 62.6	30 62.6
Stratosphere temperature	T_s	°K °R	130 234	230 414	180 324	130 234	230 414
Surface temperature	T_0	°K °R	260 468	260 468	230 414	210 378	230 414
Acceleration of gravity at surface	g	cm/sec ² ft/sec ²	375 12.3	375 12.3	375 12.3	375 12.3	375 12.3
Composition (volume)		%					
CO ₂			100.0	100.0	38.3	11.8	11.8
N ₂			0	0	61.7	88.2	88.2
Molecular weight	M	mol ⁻¹	44.0	44.0	34.2	29.9	29.9
Specific heat ratio	γ		1.30	1.30	1.35	1.38	1.38
Adiabatic temp. lapse rate	Γ	°K/km °R/10 ³ ft	4.60 2.52	4.60 2.52	4.02 2.20	3.72 2.04	3.72 2.04
Tropopause altitude	h_T	km ft	28.25 92,600	6.52 21,400	12.44 40,800	21.50 70,500	0 0
Inverse scale height (Stratosphere)	β	km ⁻¹ ft ⁻¹ x10 ⁵	.1528 4.66	.0863 2.63	.0858 2.61	.1038 3.16	.0586 1.79
Surface density	ρ_0	gm/cm ³ x10 ⁵ sl/ft ³ x10 ⁵	2.24 4.35	2.24 4.35	2.68 5.20	5.14 9.97	4.69 9.10
Artificial surface density	ρ_0'	gm/cm ³ x10 ⁵ sl/ft ³ x10 ⁵	16.94 32.9	2.62 5.09	3.89 7.55	13.50 26.20	4.69 9.10
Density at tropopause	ρ_T	gm/cm ³ x10 ⁵ sl/ft ³ x10 ⁵	0.226 0.439	1.492 2.90	1.337 2.59	1.452 2.82	4.690 9.10

(A) Parachute Selection

Prior to selecting specific parachutes for the fulfillment of the above objectives, parametric weight allocations were made for the parachutes only (i. e., parachute weight and not total decelerator system weight). The values chosen for this study, based on previous experience and practical considerations, were 6, 10, and 13 percent of the entry vehicle weight. Converting these percentages to earth pounds results in weight allowances for the parachutes of 21, 35, and 45.5 pounds, respectively.

Once the above weights are defined a choice of the type of decelerator system must be made. The two choices available are a single-stage subsonic decelerator system or a two-stage system incorporating a first-stage supersonic decelerator. In considering a supersonic first stage, thought must be given to the range in Mach numbers over which test data has been obtained. To date the Hyperflo parachute configuration has been successfully free-flight tested to a Mach number of 4 and an altitude of 123,000 feet (Cree Parachute Test Program). This parachute configuration has also been wind tunnel tested to a Mach number of 6. All supersonic parachute testing to date, however, has been limited to pointed forebodies. The effects of a blunt forebody on a towed decelerator such as the one assumed herein has not been experimentally determined. It is believed by this contractor that the stability of the parachute will not be impaired but that some reduction in drag coefficient may occur. The magnitude of the decrement can not be readily assessed since wake information for blunt bodies in the Mach number range of interest are not available. This singling out of wake information as opposed to flow field information external to the wake is based on correlations performed during the development of the Hyperflo (Reference 1) which indicated that the drag coefficient of this parachute can be predicted using wake centerline values. This deficiency in experimental data has been noted by the Air Force Flight Dynamics Laboratory, Research and Technology Division at Wright Field. A contract with Cook Electric Company recently has been consummated that will provide experimental wind tunnel data for assessing the change in performance of the Hyperflo, if any, as a result of blunted forebodies. This study will cover a Mach number range of 1.5 to 6.

Based on the experimental data obtained to date which has included low subsonic aircraft drop test transonic sea level rocket sled tests, free-flight supersonic tests and supersonic wind tunnel tests, the Hyperflo parachute is a promising candidate for the supersonic decelerator. This testing history, although covering a large portion of the Mach number spectrum, has been limited in number of tests due to the relatively recent conception of the design. A second factor which makes this parachute design highly attractive is that it affords the least cloth area for a given projected frontal area of any of the parachute configurations used for supersonic deployment. These considerations led to the selection of the Hyperflo design as the parachute to be used if a supersonic first stage is to be incorporated in the design.

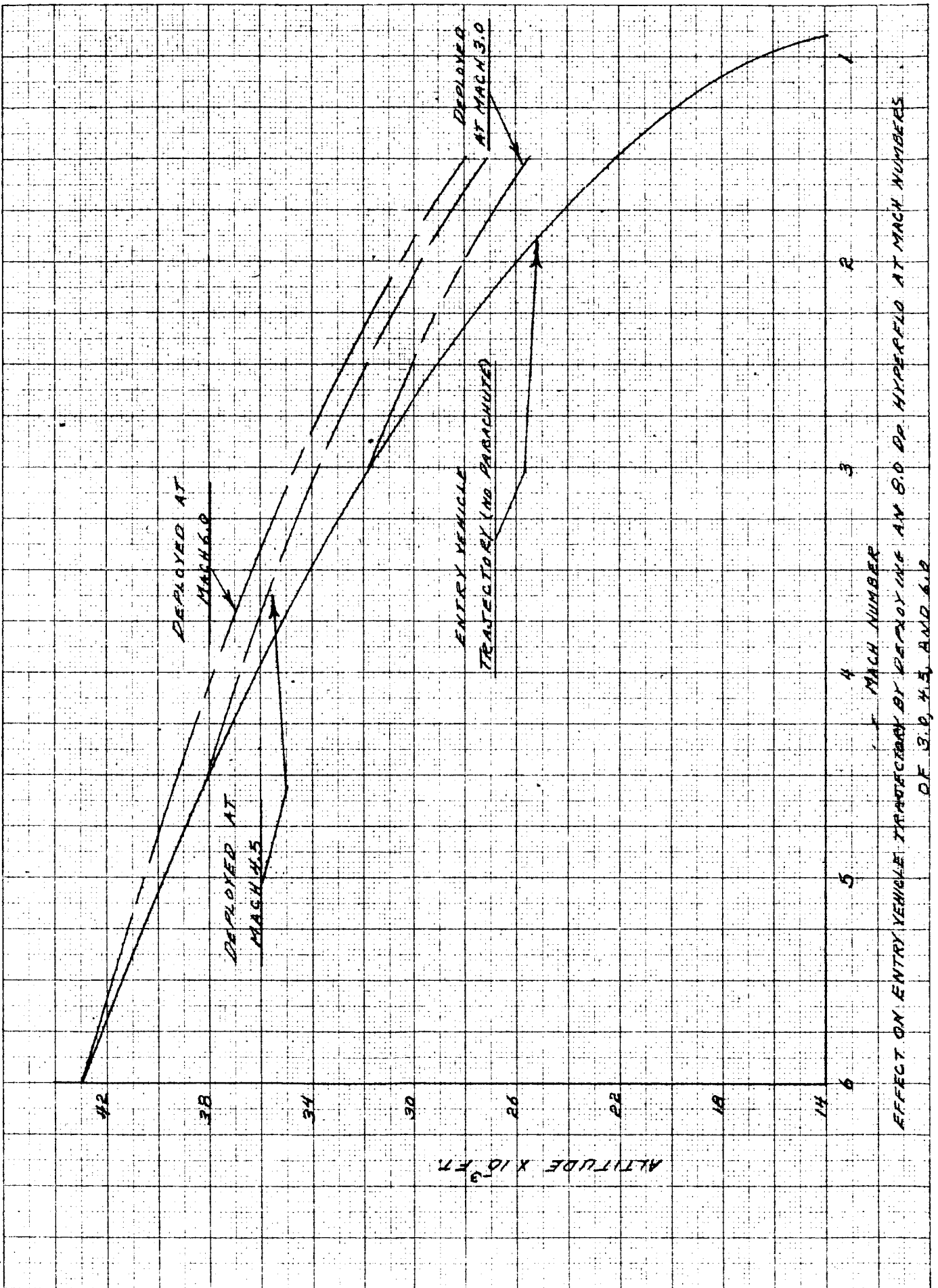
The choice of parachute design for the subsonic or terminal deceleration phase is mainly influenced by the degree of canopy oscillation permitted. Solid canopy shapes afford the largest drag coefficients; however, they are generally the least stable. The slotted canopy designs are the most stable configurations but afford lower drag coefficients (0.55 to 0.75) than do the solid textile canopies (0.65 to 0.90). Assuming that the same canopy material can be used in both slotted or solid canopies the solid canopies afford the most drag area per pound. Based on oscillation data obtained by this contractor for fully extended skirt designs, oscillation limits of ± 5 degrees can be maintained. For these designs the quick damping of any wind-shear-induced oscillations have also been shown (Reference 2). The drag coefficient which is realizable for this type of canopy design (0.9 for a $W/C_D A$ equal to 0.35) based on total geometric area is quite high and may be even better for lower $W/C_D A$'s. This conclusion is based on data given in Reference 3 which shows that in reducing the canopy loading W/S , where S is the total geometric area, an increase in drag coefficient is realized. The limit of this variation has not been experimentally verified and until data are available a maximum value of 0.9 has been chosen so as not to be optimistic.

In keeping with the design objectives of proving minimum weight and maximum time of descent a 14.3 percent fully extended skirt canopy has been chosen as the configuration which will provide the maximum drag area per pound of parachute plus stability for the terminal descent.

(B) Deployment Conditions

The range of candidate deployment conditions selected for this study was based on the maximum Mach number for which the Hyperflo parachute has demonstrated satisfactory wind tunnel performance and the maximum subsonic Mach number for which deployment of a reefed extended skirt canopy is considered practical. The maximum supersonic Mach number resulting from this criteria is 6.0. The maximum subsonic value is 0.9. This latter limit is based on the belief of this contractor that deployment of a large terminal descent parachute at a higher Mach number is not advisable independent of the magnitude of the free stream dynamic pressure.

Considering this Mach number span as possible deployment conditions, plotted in Figure 3 are the candidate deployment altitudes taken from the entry vehicle trajectory provided by JPL for G atmosphere 90 degree entry flight path angle. This figure shows that delaying the first stage deployment to a Mach number of 0.9 (required if a single subsonic parachute is chosen) reduces the deployment altitude to 32 percent of that attained by deployment at Mach 6. This reduction in deployment altitude was considered to be prohibitive and therefore further consideration to a single subsonic parachute was abandoned. It was also



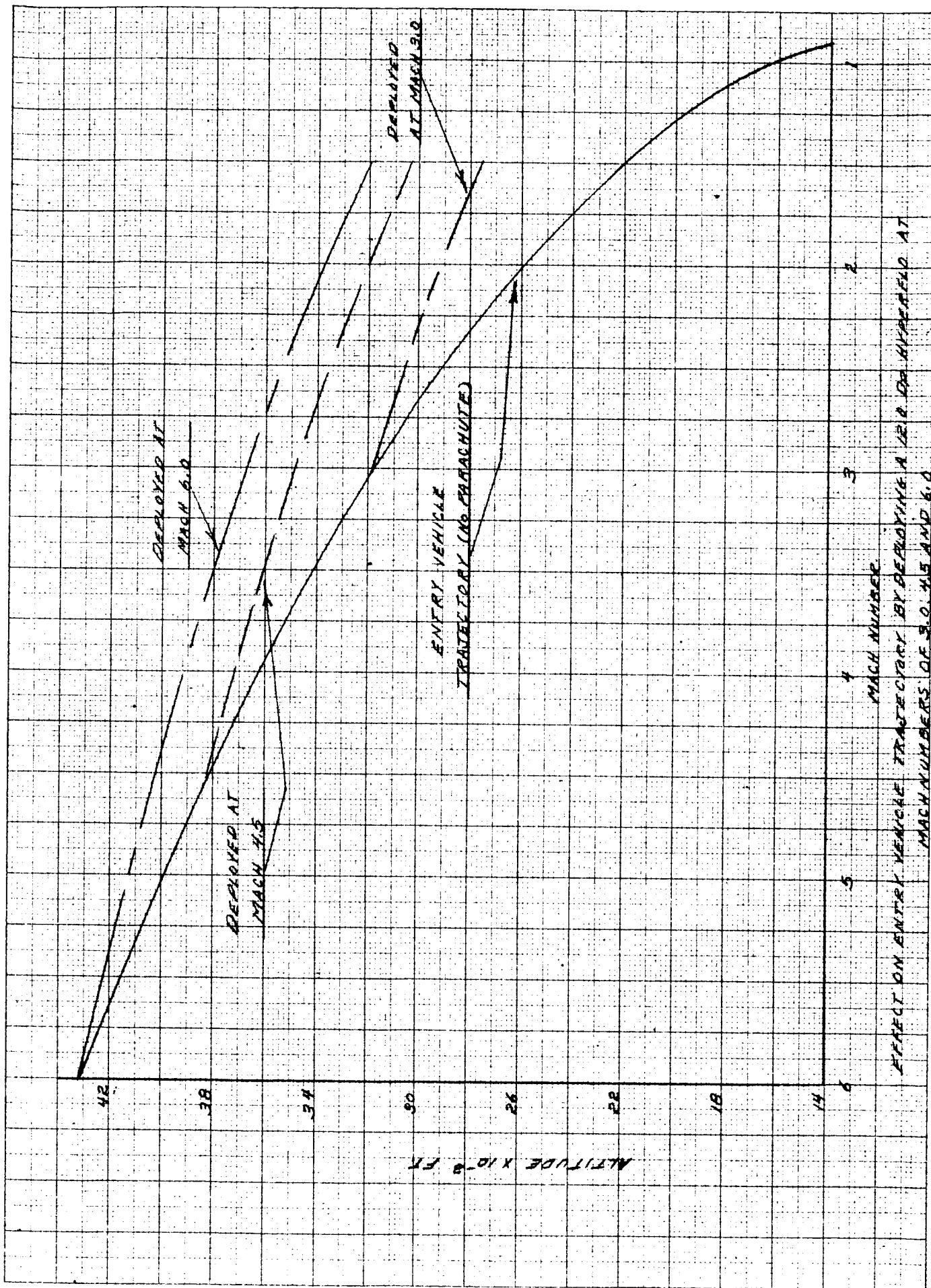
noted that the slope of the curves steepen appreciably as the deployment Mach number is reduced below 3. Based on these observations preliminary trajectories were calculated for an 8 and a 12 foot Hyperflo deployed at Mach numbers of 6, 4.5, and 3. These parachute sizes were chosen arbitrarily and the only requirement that they fulfilled was a design stipulation that the Hyperflo diameter not exceed three times the vehicle diameter (limit of successful Hyperflo test experience to date). For these cases (350 lb. entry vehicle) the entry vehicle diameter was assumed to be 7.44 feet. In the computation of these preliminary decelerator trajectories it was assumed that the parachute opened instantaneously. Figures 3 and 4 show the altitude history as a function of Mach number for the 8 foot and 12 foot D_p Hyperflo's, respectively.

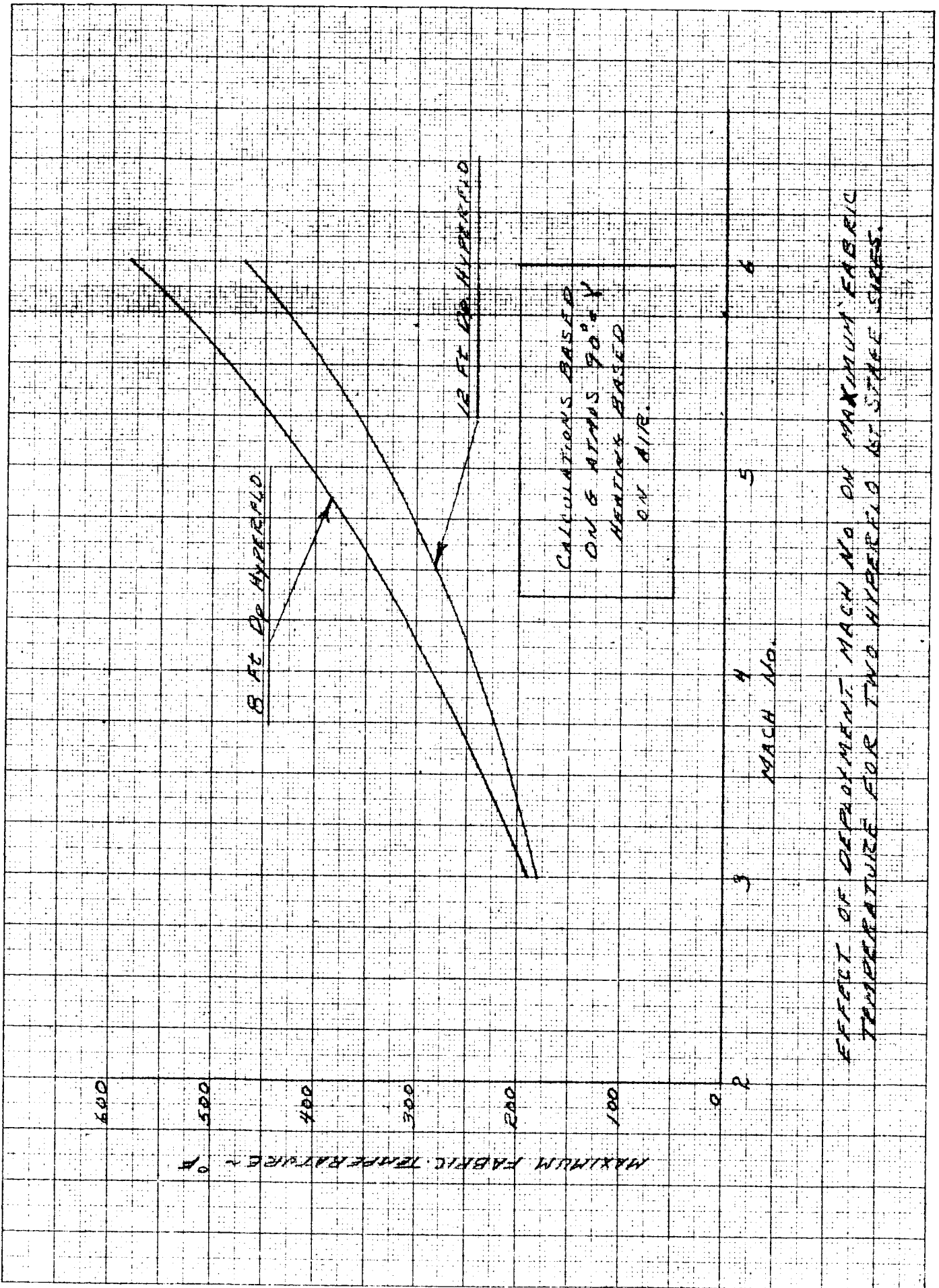
It is seen in Figure 3 that deploying an 8 foot Hyperflo at Mach 6, as compared to Mach 3, provides only 2,500 feet difference in altitude when Mach 1.5 is reached. The dynamic pressure and vehicle deceleration at Mach 6 are approximately 3 times larger than that at Mach 3. Therefore, a weight penalty must be paid for the increase in altitude.

The 12 foot diameter Hyperflo trajectories shown in Figure 4 indicate the Mach 6 case provides 5,000 feet more altitude to work with at Mach 1.5 than does the Mach 3 case. This altitude gain is approximately twice that provided by an 8 foot parachute.

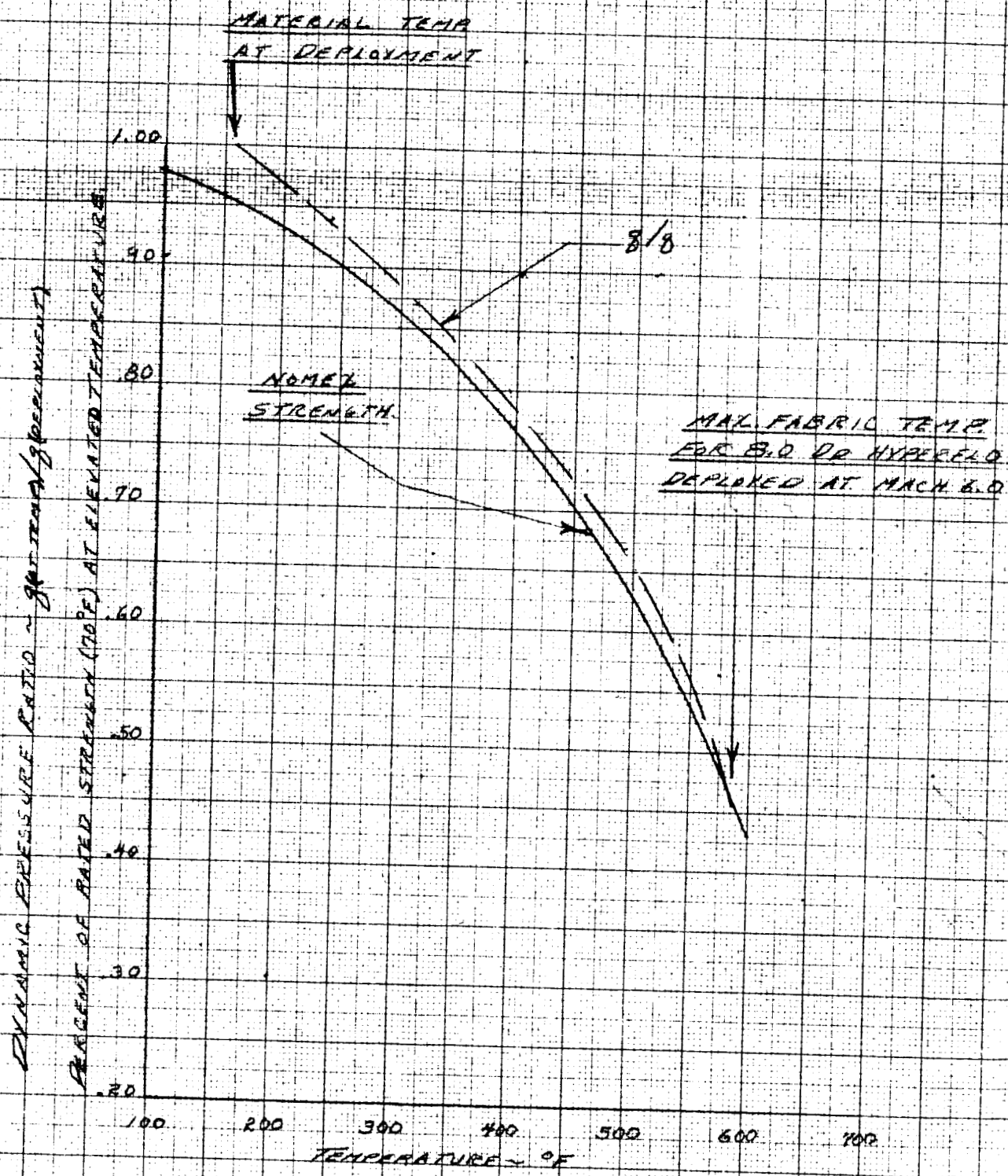
To obtain a cursory indication as to the magnitude of the aerodynamic heating, fabric temperatures based on air properties were calculated for the 8 and 12 foot Hyperflo's as a function of deployment Mach number. The procedure used for these analyses is given in Reference 4. For these computations a 60 lb. tensile strength Nomex 3/8 inch ribbon roof material was assumed as the critical member for this preliminary investigation. This width material was selected based on favorably stability characteristics demonstrated in flight tests given in Reference 4. The tensile strength chosen was based on estimated low opening loads.

The maximum fabric temperatures for the 8 and 12 foot Hyperflo's are shown in Figure 5 as a function of the deployment Mach number. The results of these computations indicate the 8 foot Hyperflo achieves a maximum fabric temperature of 580°F for a Mach 6 deployment. Based on data contained in Reference 5 which gives Nomex filament strength after a soak period of 5 minutes, it is anticipated that at 580°F the ribbons assumed in the canopy will have an ultimate strength of less than 50 percent of the room temperature value (70°F). Due to this high reduction in strength it was deemed advisable to determine in a preliminary fashion the rate at which the load reduced due to a reduction in flight velocity as a function of material temperature. To accomplish this it was assumed that the ratio of instantaneous dynamic pressure to deployment dynamic pressure would approximate the required strength of the material. Figure 6 shows the results of this calculation





EFFECT OF DEPLOYMENT MACH NO ON MAXIMUM FABRIC TEMPERATURE FOR TWO HYPERVELO STAGE SURFS.



DYNAMIC PRESSURE REDUCTION AND NOMEX MATERIAL STRENGTH REDUCTION VERSUS CALCULATED MATERIAL TEMPERATURE FOR PREDICTED TRAJECTORY OF ENTRY VEHICLE WITH B.O. DA HYPERFOLD DEPLOYED AT MACH 6.0

and also includes the predicted material strength decay as a function of temperature for the 8 foot diameter Hyperflo. It is noteworthy that based on the assumptions given above for this set of conditions, the material strength and load reduce at nearly the same rate. Based on these preliminary heating results (which do not account for the effects of an atmosphere which has CO₂ as a major constituent) it appeared that for a Mach 6 deployment an 8 foot parachute is near the minimum size. A smaller parachute producing less deceleration probably would incur material failure due to temperature degradation at conditions after maximum parachute load had been encountered.

In keeping with the design objective of maximizing the deployment altitude and based on the results obtained in the preliminary analysis, initial deployment Mach numbers of 6, 4.5 and 3 were selected for detailed investigation. It was noted that because of the high fabric temperatures encountered for the Mach 6 trajectories and the higher vehicle decelerations at time of deployment, a Mach 6 deployment would impose weight penalties. However, the magnitude of these penalties could not be assessed without detailed investigation.

(C) Parachute Filling Time Relationships

To determine accurately the trajectory of a body being decelerated by a parachute, a knowledge of the parachute's filling time is required. The problem of accurately predicting the filling time of conventional subsonic parachutes has in the past been quite nebulous. Predicting the filling time of parachutes which incorporate geometric porosity is much more difficult. A recent document (Reference 6) pertaining to filling time of high speed parachutes shows that deviations between design and performance curves vary over 200 percent. This discrepancy is somewhat understandable since supersonic parachute operation is relatively new and not fully explored from the analytical viewpoint. The data available pertain to a wide range of parachute designs and geometric configurations. Deployment methods for these tests varied and, in general, only a limited amount of reliable data are available for correlation purposes.

The classical factors which are known to influence significantly the opening characteristics of a parachute are the parachute geometry, the deployment velocity and, to some degree, the geometric porosity. To obtain some understanding of how the predicted constituents of the Mars atmosphere would affect the filling time of a parachute, the one obvious factor, porosity, was investigated. Porosity tests were conducted for two material samples, a 1.1 oz. nylon cloth and a 3.79 oz. Nomex cloth. The samples were first investigated in an air atmosphere and then tested in a CO₂ atmosphere. It was found that a 6.4 percent increase in permeability for CO₂ over that obtained for air was measured for the nylon sample, and a 11.1 percent increase over that for air was measured for the Nomex sample. Since the geometric porosity for the nylon cloth is approximately 3.5 percent, an increase of 6.4 percent in this value should have little effect on the opening characteristics. At least, it is beyond the present state-of-the-art to be able to accurately predict a deviation as a result of this change. These same conclusions

apply equally well for the Nomex material. The other factors mentioned above (geometry and velocity) are not directly related to gas molecular structure and hence the effect of a change in atmosphere should not be consequential.

1. Hyperflo Filling Time

To predict a filling time relationship for the Hyperflo at the high Mach numbers, data from Cree free-flight tests (Reference 4) and Tomahawk sled runs (Reference 7) were used to empirically develop an equation. These data spanned a velocity range of 1,200 to 4,000 feet per second. From these tests 12 were chosen as representative for the Hyperflo filling time. Even with this selection in tests, however, considerable scatter in the filling time occurs (Figure 7). Due to the few available data points and the apparent random variation with geometric porosity tested, (7.5 to 15 percent) it was decided that no attempt to incorporate a porosity term was justified. This decision was based on the fact that future Hyperflo designs are expected to be within this porosity range.

The parameter incorporated in the empirical filling time equation which does not appear in any of the classic filling time equations is the free stream dynamic pressure (q). This term was incorporated based on a limiting condition that if " q " goes to zero the filling time should be infinite. The Cree flight test points chosen span a dynamic pressure range of 345 to 55 psf and indicate that some correlation can be obtained by incorporating a dynamic pressure term. Based on this observation and the limiting condition at zero " q " the empirical equation arrived at is as follows:

$$\frac{t_f}{D_p} = \frac{380}{V q^{0.35}}$$

where

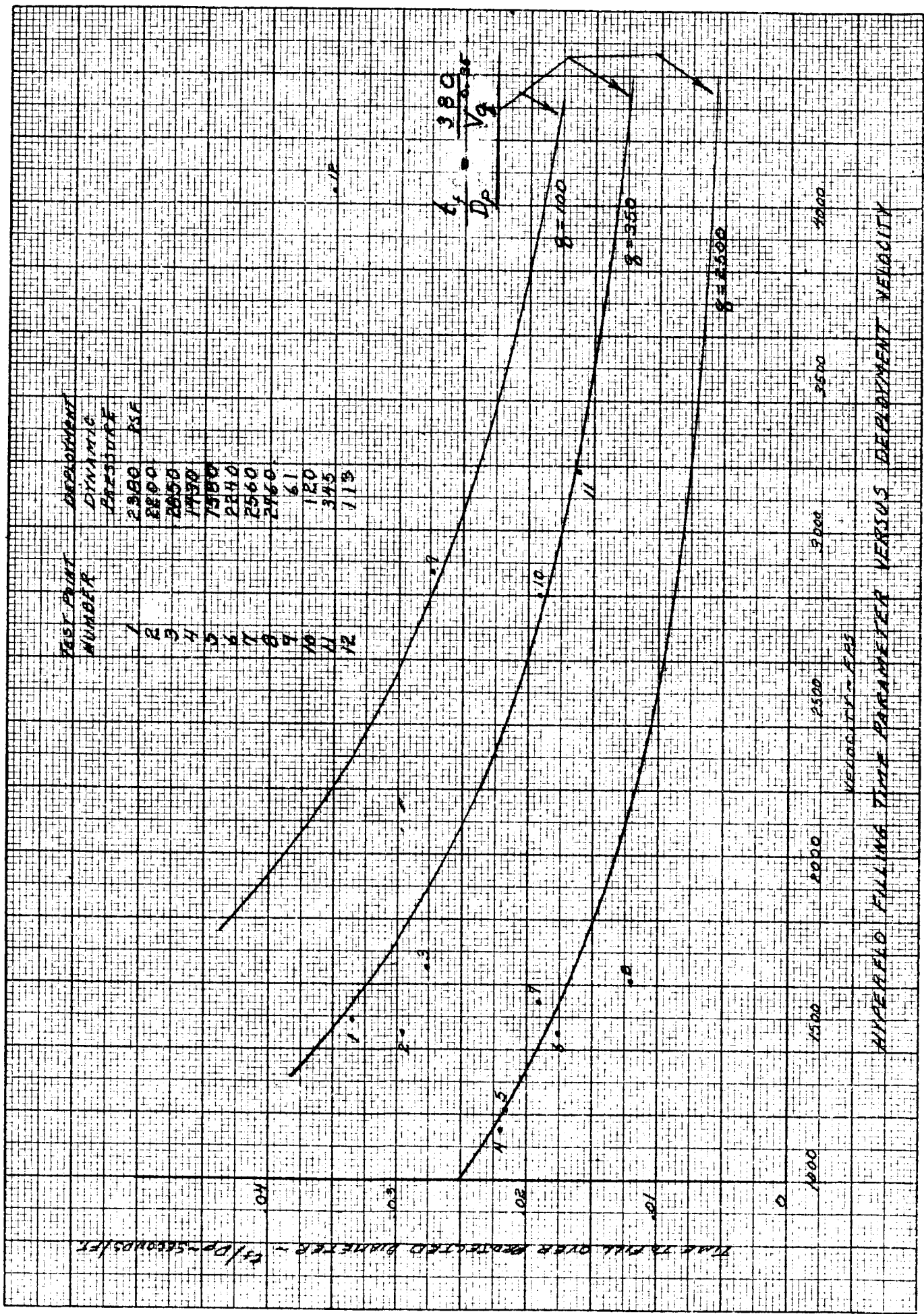
t_f = time to fill (seconds)

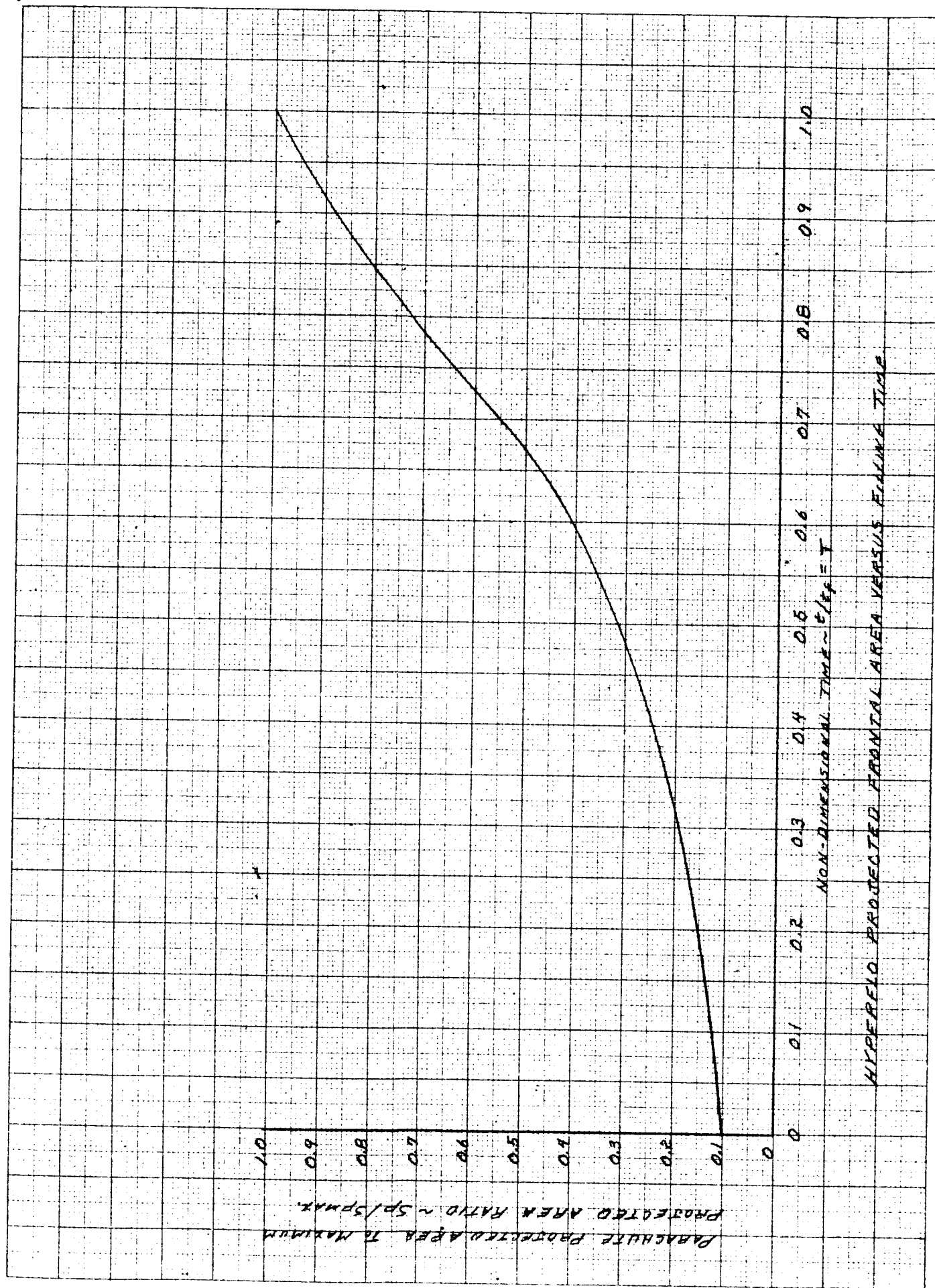
V = vehicle velocity at time of deployment (ft/sec)

D_p = maximum projected diameter of the Hyperflo (ft)

q = free stream dynamic pressure (lbs/ft²)

From the test data a projected area ratio ($S_p/S_p \text{ Max}$) was obtained as a function of non-dimensional time (t/t_f). This relation, which is shown in Figure 8, was obtained by measuring the projected area of the Hyperflo as it





inflated. The area ratio at $t = 0$ was found to vary between sled runs and the flight test data even when the same size parachute was used. This difference is in part due to the difference in deployment conditions. It is expected that for this study the free-flight data are more applicable since they more nearly represent typical free-flight and hence the curve was weighted in favor of these tests.

2. Reefed Extended Skirt Parachute Filling Time

The equation given below for the reefed extended skirt parachute was arrived at from review of past tests performed by these laboratories and results obtained from El Centro tests (Reference 8). The basic equation used to correlate the data was of the same form as that given in Reference 9.

$$\frac{t_f}{D_o} = \frac{n}{V_s 0.9} \left[\frac{C_{DA}}{C_{DA \text{ max}}} \right]^{1/2}$$

where

t_f = time to fill (seconds)

D_o = Parachute nominal diameter (ft)

n = empirically determined constant

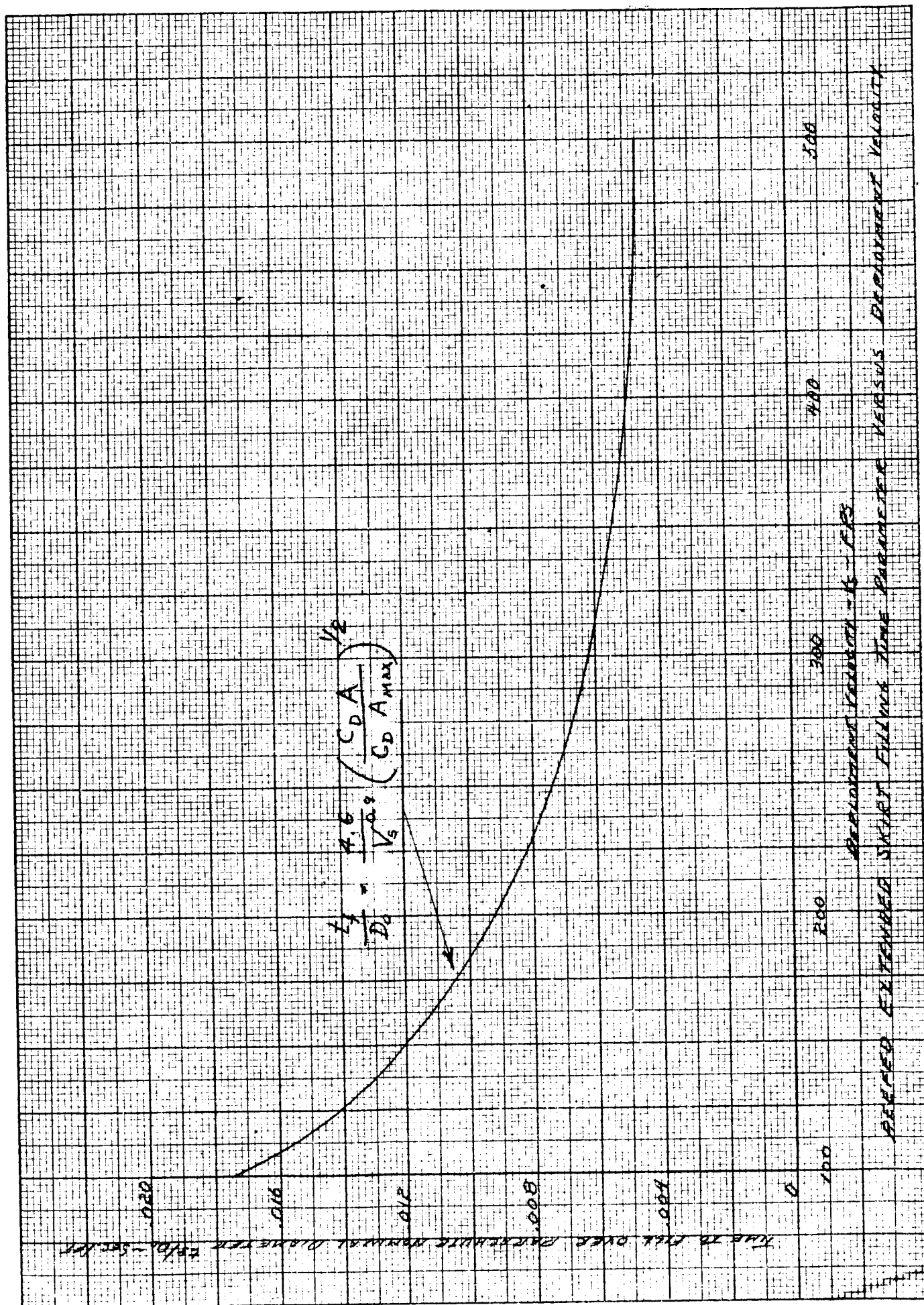
V_s = parachute velocity at line stretch (ft/sec)

C_{DA} = drag area of parachute in reefed configuration (ft²)

$C_{DA \text{ max}}$ = fully inflated drag area of parachute at deployment conditions.

The constant "n" which best fit the data was 4.6. It is noted that the test data used for determining the constant covered a velocity range of 200 to 500 feet per second. Reefed extended skirt data above this velocity range could not be found. Figure 9 shows the variation of t_f/D_o as a function of velocity as determined by the above equation.

The time variation of drag area during the inflation of reefed fully extended skirt parachutes was obtained from photograph measurements. These photographs were from tests of reefed 55 and 67 foot 14.3 percent fully extended skirt parachutes deployed over a velocity range of 220 to 475 feet per second and



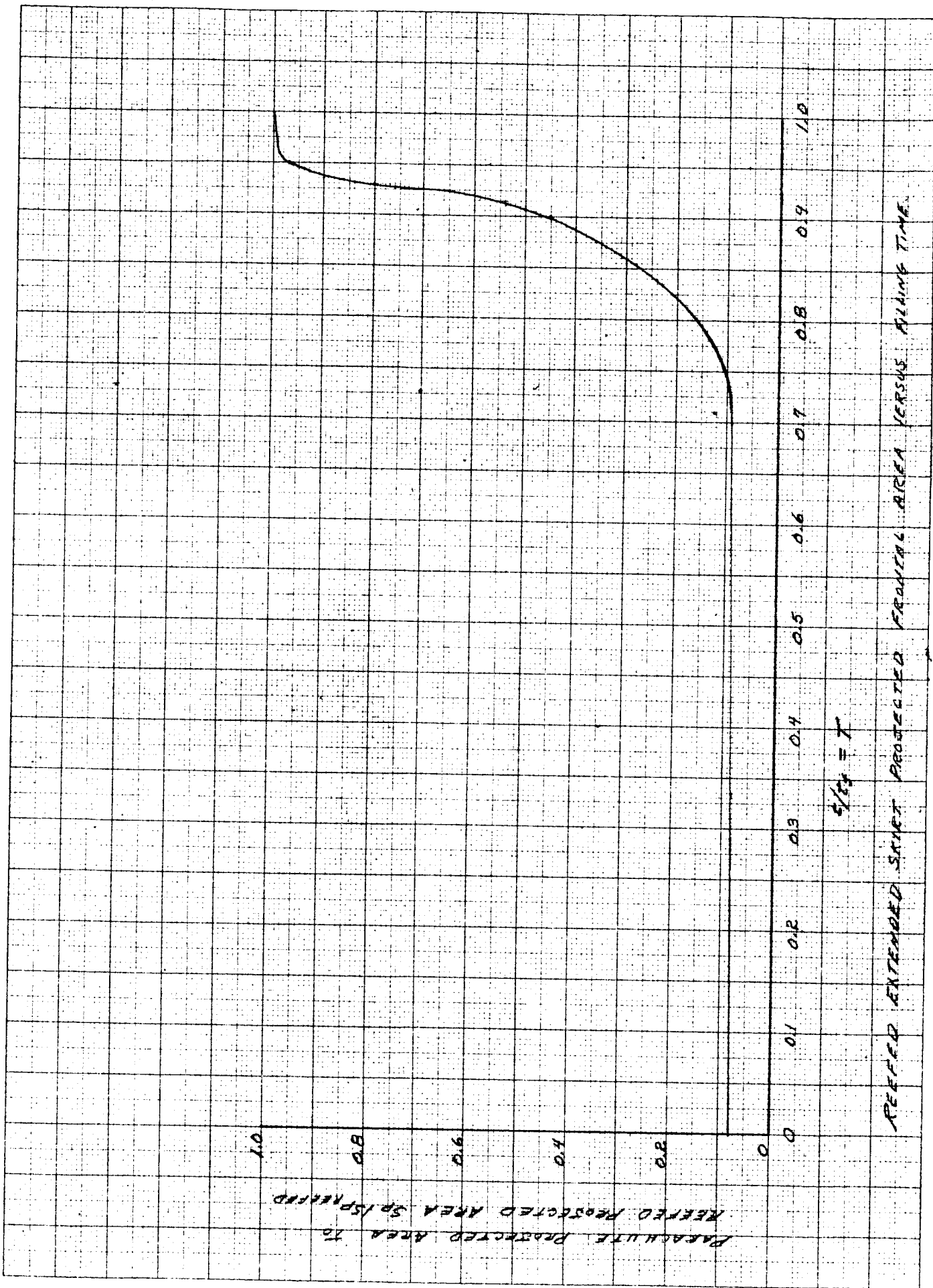
an altitude range of 3,000 to 20,000 feet. These data were obtained in a test programs reported in References 2 and 10. Figure 10 shows the faired time variation of the ratio of the instantaneous projected parachute area to the reefed fully inflated projected area. The characteristic low area ratio for the first 0.7 units of nondimensional time results from the time required for the initial air bubble to rise to the top of the canopy. For all computations performed, it has been assumed that the projected area ratio of the canopy is directly proportional to the drag area ratio. Hence, the curve given in Figure 10 represents the variation in drag area as a function of nondimensional time for a fully extended skirt canopy deployed in a reefed state.

3. Time to Fill From Reefed Condition for Extended Skirt Parachute

The filling time of the fully extended skirt canopy from the reefed to fully inflated condition has been approximated by using a modification to a formulation given in Reference 6 for a solid flat canopy. The modification included considerations of canopy projected area variations with time and inflow and vent outflow velocities with time. The latter two modifications were incorporated based on measurements obtained subsequent to Reference 6 being published. The results of these measurements were reported in Reference 11.

The concept used and discussed in detail in Appendix 1 is effectively a balancing of the volume of gas which must be encompassed in a canopy at full inflation with prescribed geometry considerations and inflow and outflow velocities as a function of filling time. The advantage of this approach, and one of the principal reasons for using it, was that it analytically accounts for a variation in filling time as a function of atmospheric density. Since the limited experimental tests conducted with CO₂ as discussed earlier did not significantly alter the effective porosity of the material it is anticipated that the most significant characteristic of the Mars atmosphere for parachute inflation is its low atmospheric density.

The effect of atmospheric density on the filling time of a parachute has been a topic of much discussion and considerable question in recent years. Due to the scatter of filling time data it has been impossible to determine empirically a filling time expression that covers the entire altitude (density) spectrum and is acceptable to all parachute authorities. In the various filling time equations which have been proposed, the density ratio appears with an exponent varying from 0.2 to 1.0. Attempts have also been made to compensate for Reynolds number and in turn describe the variations as functions of this parameter which includes density. In general, no approach has been completely satisfactory. Reference 12 shows the variation of drag coefficient as a function of Reynold's number for two high altitude (190,000 feet) parachute descents. In these tests the same parachute size was used for two different payload weights. While descending to lower altitudes (higher densities) the lighter of the two payloads exhibited a



significant drag coefficient increase at a specific Reynolds number (6.0). The heavier payload did not experience the same effect even though it encountered the same Reynolds number at an altitude of approximately 10,000 feet higher (120,000 versus 110,000 feet). The inability to determine empirically a reason for these variations has caused a great deal of consternation and the endeavors of parachute authorities to conduct test specifically for formulating analytical expressions for defining parachute characteristics meets with great approval.

SECTION III

PARAMETRIC INVESTIGATION TO DETERMINE OPTIMUM PARACHUTE SYSTEM

A. Parachute Sizing

In order to size the first stage parachute it was necessary to decide upon an atmosphere to evaluate the dynamic pressure at the established deployment Mach numbers of 3, 4.5 and 6. Because atmosphere G defines the lowest first deployment altitude it was considered mandatory to maximize the deployment altitude for this atmospheric profile. Thus the dynamic pressures associated with Mach numbers of 3, 4.5 and 6 in G atmosphere were designated as the design values.

It was realized that these deployment Mach numbers may result in dynamic pressures in other atmospheres which are higher than the design values. In these cases, in keeping with maintaining minimum recovery system weight, first stage deployment (in denser atmospheres) must be accomplished at lower than the established Mach numbers in order not to exceed design loads. This procedure results in an altitude loss for these cases; however, the deployment altitude will remain significantly higher than that in G atmosphere. The resulting design dynamic pressure values selected for first stage deployment were 61, 116 and 182 pounds per square foot.

The selection of the parachute weight allowances of 21, 35 and 45.5 (6, 10 and 13 percent of the entry vehicle weights) discussed in Section II A and the deployment conditions given above leave two variables remaining to be determined for defining the sizes of parachutes that could be used. These variables are the materials to be used in the parachute designs and the deployment conditions for the second stage parachute. Considering the second variable it was assumed, based on the results of the preliminary analysis discussed in Section II B, that the second stage deployment altitude (maximum dynamic pressure) for a Mach number of 0.9 would never be lower than 20,000 feet. This altitude was arrived at by considering the deceleration afforded by the vehicle and an 8 foot Hyperflo which is considered the smallest usable based on predicted aerodynamic heating and test data limitations. As a result of these assumptions the dynamic pressure associated with Mach 0.9 and an altitude of 20,000 feet (7.5 psf) was used for the design condition.

The selection of materials to be considered in this program were based on materials which were considered most likely to pass the required sterilization

environment of 297°F for 36 hours and capable of withstanding the aerodynamic heating environment. The first stage fabric temperatures predicted in the preliminary trajectories for deployment Mach numbers of 4.5 and 6 dictate the utilization of Nomex. For the Mach 3 deployment conditions conventional parachute fabrics could probably be utilized; however, for simplicity and to provide an additional safety margin for possible premature deployments Nomex was used for all first stage parachutes. The selection was influenced by the fact that although Nomex is a relatively new material for parachute application, this contractor's experience with this fabric in recent supersonic parachute tests have shown that it performs quite satisfactorily and poses no fabrication difficulties.

The selection of materials for the second stage was not quite as obvious as that of the first stage. The material which was considered most desirable was nylon. The factors which favored the use of nylon were its extensive use as a parachute material and its availability in various Government specification strengths for both cloth and lines. These factors are particularly important when it is considered that the fabrication and designing of parachutes relies largely on empirical formulations based mainly on experience with nylon parachutes. The predominant question with regard to the use of nylon was its ability to survive the sterilization and hard vacuum environment for a space flight. Due to this unknown, dacron, which has had limited parachute application, was also considered as a candidate. This material possesses better high temperature characteristics than does nylon and as a result was considered more likely to survive the sterilization environment. The use of Nomex was also considered. The chief disadvantage of Nomex is that the DuPont Company, supplier of Nomex yarn, presently produces only 100 and 200 denier yarn. This denier yarn if woven into a cloth would produce an excessive weight penalty for applications where low loads are to be encountered. To weave a light weight cloth which would be suitable from a strength and porosity standpoint for this parachute application, approximately 30 denier yarn would be required. Information obtained from Mr. Ross of the Materials Laboratory at Wright Field indicates that a cloth has been made with 30 denier yarn which was woven in accordance with the MIL-C-7020 Type 1 specification for 1.1 oz/yd² nylon cloth. The approximate strength of the Nomex cloth was 50 pounds per inch and it was not susceptible to shifting, which would produce an irregular porosity distribution. The most remarkable characteristic provided by this cloth was that it weighed 1 oz/yd². This lightweight and high strength is consistent with information obtained from Mr. Melvin of the DuPont Company who stated that for a given denier yarn Nomex has a better strength after weaving than either nylon or dacron. The disadvantages afforded by Nomex material are that at present the weaving of low denier Nomex yarn requires considerably more care than does nylon. Furthermore, the 30 denier yarn supplied to the Air Force was on a special basis and at present the DuPont Company does not have a market nor facilities which would justify the production of this light yarn. The understanding by this author is that the size of the present pilot plant and production requirement of high denier yarn prohibits the production of

low denier yarn. The conclusions drawn from the above are that a light weight Nomex cloth could be produced if yarn were available, and that the fabric weight would be approximately the same as dacron. Due to the non-availability of the required yarn, Nomex was not used for the terminal parachute.

Assessment of the unknowns with regard to strength degradation associated with the sterilization and vacuum environment resulted in the selection of both nylon and dacron as fabrics to be used in sizing the parachutes for the second stage. This choice proved to be a wise decision since a concurrent program (Reference 13) to determine experimentally the effects of sterilization and vacuum on dacron, nylon and Nomex showed that nylon fabrics are not capable of withstanding the sterilization environment without sustaining extremely large strength degradation. These results eliminate nylon as a possible candidate material under the present sterilization specifications and hence, only dacron (which showed little strength loss) has been considered acceptable. Although nylon parachutes were sized during the performance of this study (assuming negligible strength losses) the results were invalidated by the sterilization tests. Hence, they were not presented in this report and only the dacron parachutes are discussed.

Reefing was assumed for sizing the second stage parachute. This was based on practical experience which has shown that for large fully extended skirt canopies a more reliable deployment can be attained by reefing the parachute. The term reefing refers to restricting the inflation of the parachute to a drag area less than that obtained in a full open condition. The reefing ratio assumed for these analyses was ten percent. This ratio was selected based on providing at least a factor of 2 over minimum limits for reefing and thereby provide a high confidence level in the parachute's ability to open properly.

The actual sizing of the parachutes, once the above selections were made, was predicated on obtaining a range of five first stage sizes for each deployment Mach number and weight allowance. This variation in first stage sizes, holding other parameters constant, was designed to show the effect of first stage weight on deployment altitude of the second stage and descent time. The limiting constraint imposed for this sizing was that the first stage diameter be between 8 and 21 feet. The 21 foot limit arises from the fact that experimental data were not available for diameter ratios (parachute to forebody) larger than 3 and that data to date indicate some decrease in stability with increasingly diameter ratio.

The procedure used in sizing the parachutes was to first select a first stage parachute diameter and determine its weight. This weight comprises the weight of the parachute plus the weight of a riser which would put the canopy six vehicle diameters behind the entry vehicle. The six vehicle diameter requirement stems from Hyperflo test data which indicate this location to be near optimum in terms of stability and drag coefficient. The difference between the total weight

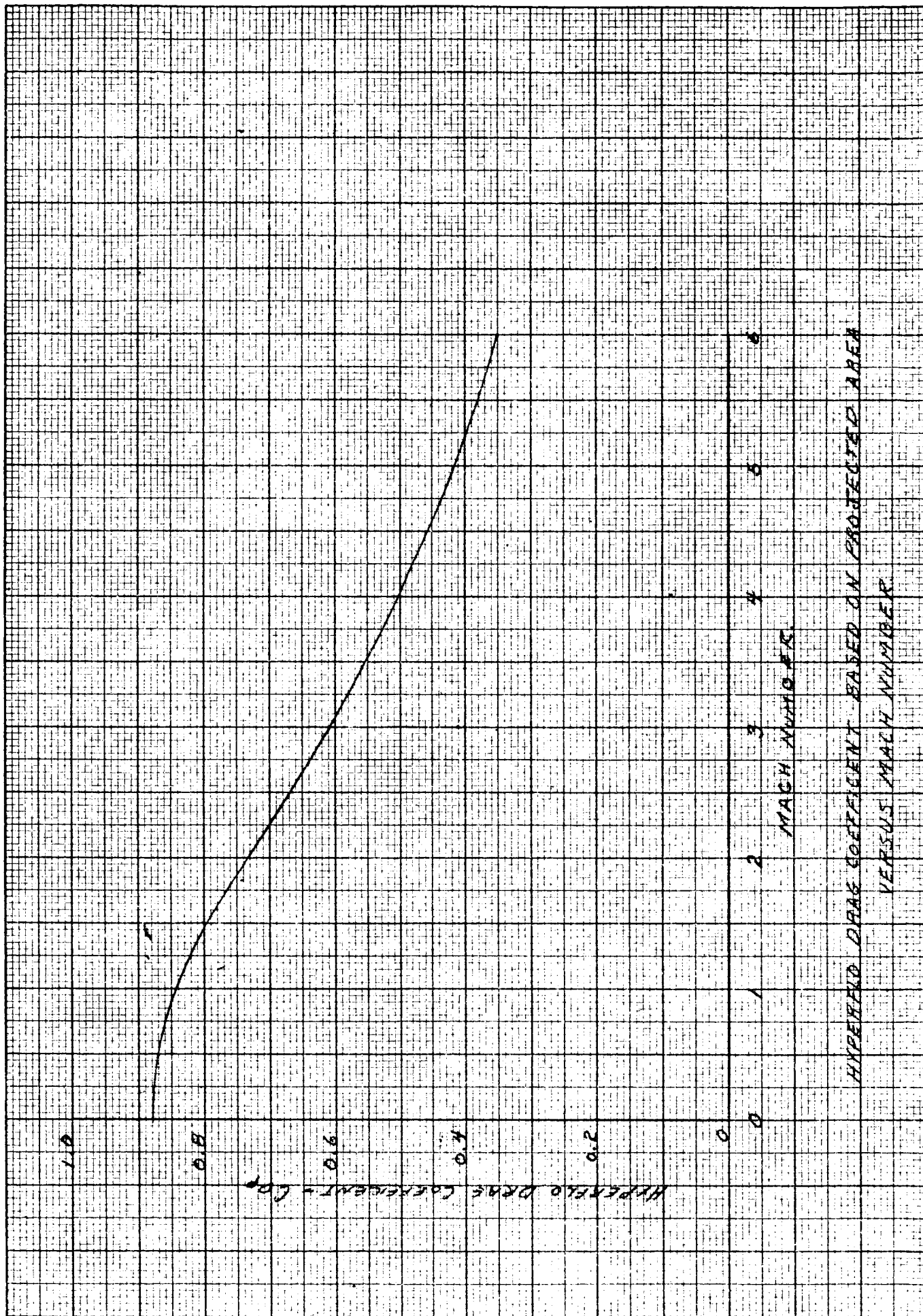
allowance and first stage weight was then used to determine the maximum second stage size. A factor which was considered in the determination of the second stage weight was the optimum number of gores for the parachute. Since there is, based on standard practice, a minimum limit defined by 3.14 feet between lines and a maximum value limited only by practical spacing of the lines on the skirt, a range in the number of gores was investigated to assure that a minimum weight parachute was obtained for a given nominal parachute diameter (D_0). The equations used in selecting the materials for both the first and second stage parachutes are given in Appendix II. These equations are contained in an IBM 1920 computer and the iterative calculations for determining the size of the second stage parachutes were performed by the computer. For expediency it was assumed that the proper second stage size was found when a diameter of parachute was determined whose weight was within 2 percent of the specified weight. An optimizing routine with respect to the number of gores was included in the program because of multiple solutions. For a given weight allowance it is possible to obtain more than one solution to the size of parachute and accordingly the number of gores. In these cases, the solution which rendered the largest diameter (maximum drag area) was selected. In other instances due to discontinuities in the selection of the number of gores a diameter parachute whose weight was less than the allowable was selected if it rendered the largest drag area of all the possible solutions.

The drag coefficients used in the sizing program for the various first stage deployment Mach numbers are shown in Figure 11. Due to the scatter associated with the first stage filling time data (Figure 7) the dynamic pressures used to determine material strengths were those at the assumed deployment conditions. No reduction in load due to deceleration during the filling time was incorporated. This assumption is considered mandatory since the amount of data available for supersonic parachutes are so limited and the force data available (Reference 4) indicate that little if any reduction in dynamic pressure occurs during filling.

The drag coefficient used for the second stage parachute in the reefed condition was 0.4. This low value was assumed based on reefed opening force data obtained from 55 and 67 foot nominal diameter extended skirt parachutes deployed at velocities of the order of 500 fps. Further substantiation for this value is Reference 14 which shows that small extended skirt canopies deployed in the Mach number range of 0.5 to 0.8 exhibited average drag coefficients of approximately 0.42.

Table II shows the results of the sizing computations. A significant factor shown in this table is the weight of the first stage riser. This riser weight stems from positioning the first stage canopy 6 vehicle diameters behind the entry vehicle as stated previously. This position was based on the optimum location for stability purposes as determined for pointed forebodies. Solid

10 INCH 39T
KEUFEL & ESSER CO. MADE IN U.S.A.
ALUMINUM



HYPERSONIC DRAG COEFFICIENT BASED ON PROTECTED AREA
VERSUS MACH NUMBER

TABLE II

Parachute Sizes And Weights For A First Stage Made With
Nomex Material And A Second Stage Made With Dacron Material

Case Number	Parachute		D _p -1st Lbs.	Wt-1st Lbs.	D _o -2nd Ft.	Wt-2nd Lbs.	M	Wt-Riser	Wt-1st
	Wt. Allowance	Lbs.							Wt-Allowance
1	45.5	8.0		5.72	78.7	39.7	3.0	1.42	12.7%
2	45.5	12.0		12.3	72.6	33.1	3.0	2.11	27.0
3	45.5	15.0		19.4	63.7	26.0	3.0	1.81	42.7
4	45.5	18.0		28.7	51.2	16.7	3.0	1.53	63.2
5	45.5	20.0		37.7	34.3	7.71	3.0	1.44	83.0
6	45.5	8.0		6.15	78.7	39.3	4.5	1.63	13.5
7	45.5	12.0		14.9	68.7	30.5	4.5	2.43	32.7
8	45.5	14.0		20.0	62.5	25.4	4.5	2.61	44.0
9	45.5	17.0		31.9	45.6	13.5	4.5	2.63	70.0
10	45.5	18.0		34.0	42.3	11.4	4.5	2.23	74.8
11	45.5	8.0		7.16	78.2	38.3	6.0	1.63	15.7
12	45.5	10.0		10.2	73.7	35.2	6.0	1.84	22.4
13	45.5	12.0		17.0	67.0	28.4	6.0	2.87	37.3
14	45.5	15.0		25.8	55.8	19.6	6.0	3.41	56.7
15	45.5	17.0		33.5	43.1	11.9	6.0	2.63	73.6
16	35.0	8.0		5.72	67.5	29.2	3	1.42	16.3
17	35.0	10.0		7.8	65.7	27.1	3	1.42	22.3
18	35.0	12.0		12.3	59.3	22.6	3	2.11	35.2
19	35.0	15.0		19.4	48.7	15.5	3	1.81	55.5
20	35.0	17.0		26.9	35.2	8.06	3	1.8	77
21	35.0	8.0		6.15	67.5	28.8	4.5	1.63	17.6
22	35.0	10.0		10.2	62.5	24.7	4.5	1.84	29.2
23	35.0	12.0		14.9	56.2	20.0	4.5	2.43	42.5
24	35.0	14.0		20.0	48.7	14.9	4.5	2.61	57.2
25	35.0	16.0		27.1	34.3	7.8	4.5	3.02	77.5
26	35.0	8.0		7.16	66.7	27.8	6.0	1.63	20.4
27	35.0	10.0		10.2	62.5	24.7	6.0	1.84	29.2
28	35.0	12.0		17.0	52.5	17.9	6.0	2.87	48.5
29	35.0	14.0		22.7	43.4	12.2	6.0	2.61	65
30	35.0	16.0		28.6	30.8	6.33	6.0	3.02	81.5

TABLE II - Cont'd.

Case Number	Parachute	D _p -1st Lbs.	Wt-1st Lbs.	D _o -2nd Ft.	Wt-2nd Lbs.	M	Wt-Riser	Wt-1st
	Wt. Allowance Lbs.							Wt-Allowance
31	21.0	8.0	5.72	48.7	15.2	3.0	1.42	27.1%
32	21.0	10.0	7.8	45.0	13.1	3.0	1.42	37.1
33	21.0	12.0	12.3	36.6	8.68	3.0	2.11	58.7
34	21.0	13.0	14.6	30.9	6.3	3.0	1.93	69.6
35	21.0	14.0	17.8	21.8	3.15	3.0	2.02	84.8
36	21.0	8.0	6.15	48.1	14.8	4.5	1.63	29.2
37	21.0	10.0	10.2	40.5	10.7	4.5	1.84	48.6
38	21.0	11.0	12.5	36.0	8.46	4.5	2.29	59.6
39	21.0	12.0	14.9	30.4	6.04	4.5	2.43	71
40	21.0	13.0	18.4	19.3	2.53	4.5	2.62	87.5
41	21.0	8.0	7.16	46.2	13.8	6.0	1.63	34.0
42	21.0	9.0	9.19	42.3	11.8	6.0	1.98	43.7
43	21.0	10.0	10.2	40.5	10.7	6.0	1.84	48.5
44	21.0*	11.0	13.7	33.5	7.24	6.0	2.64	65.4
45	21.0	12.0	17.0	24.3	3.93	6.0	2.87	81.0

*Sum of first and second stage weights lower than weight allowance.

(Note) First stage design dynamic pressure at deployment Mach numbers of 6.0, 4.5, and 3, were 182, 116 and 61 psf respectively. The design deployment Mach number for the reefed second stage was 0.9 at a dynamic pressure of 7.5 psf. Reef drag area was 0.10 percent of that at full inflation at 0.9 Mach number.

cone decelerators data (Reference 15) indicate that the cones minimum distance aft of the vehicle for drag purposes is approximately 3.2 calibers for the Mach numbers of interest. Since the shock wave shape associated with the Hyperflo design is similar to that of a 30 degree cone, it is possible that a significant portion of the riser weight, if not all of it, could be eliminated in some cases if wind tunnel data for a Hyperflo with shorter riser lengths were available.

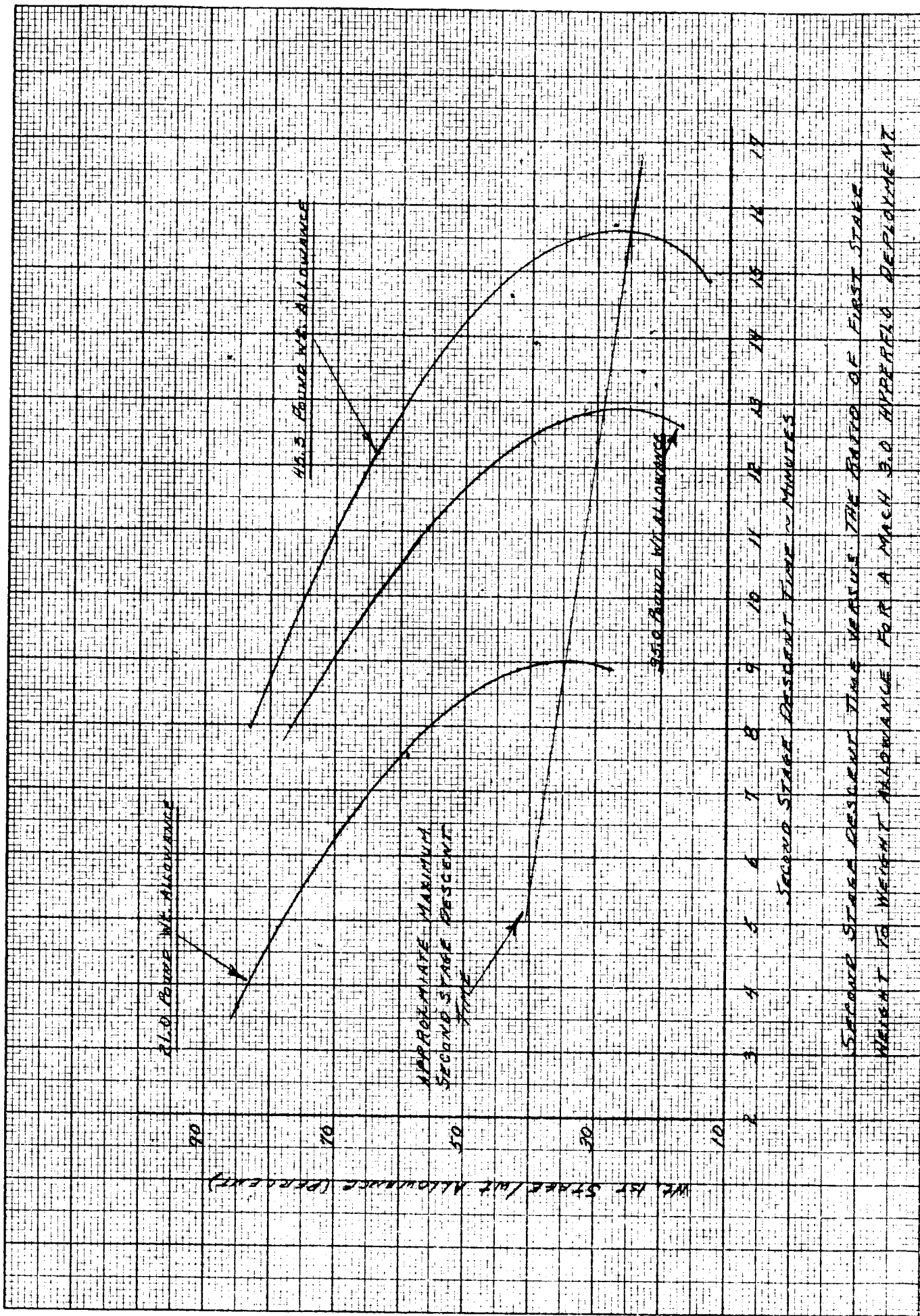
It should be noted that an asterisk precedes case number 44. This asterisk indicates that for this case the weight of the system is lower than the weight allowance given (21 pounds) due to the optimization of the second stage parachute size as discussed earlier.

B. Trajectory Computations

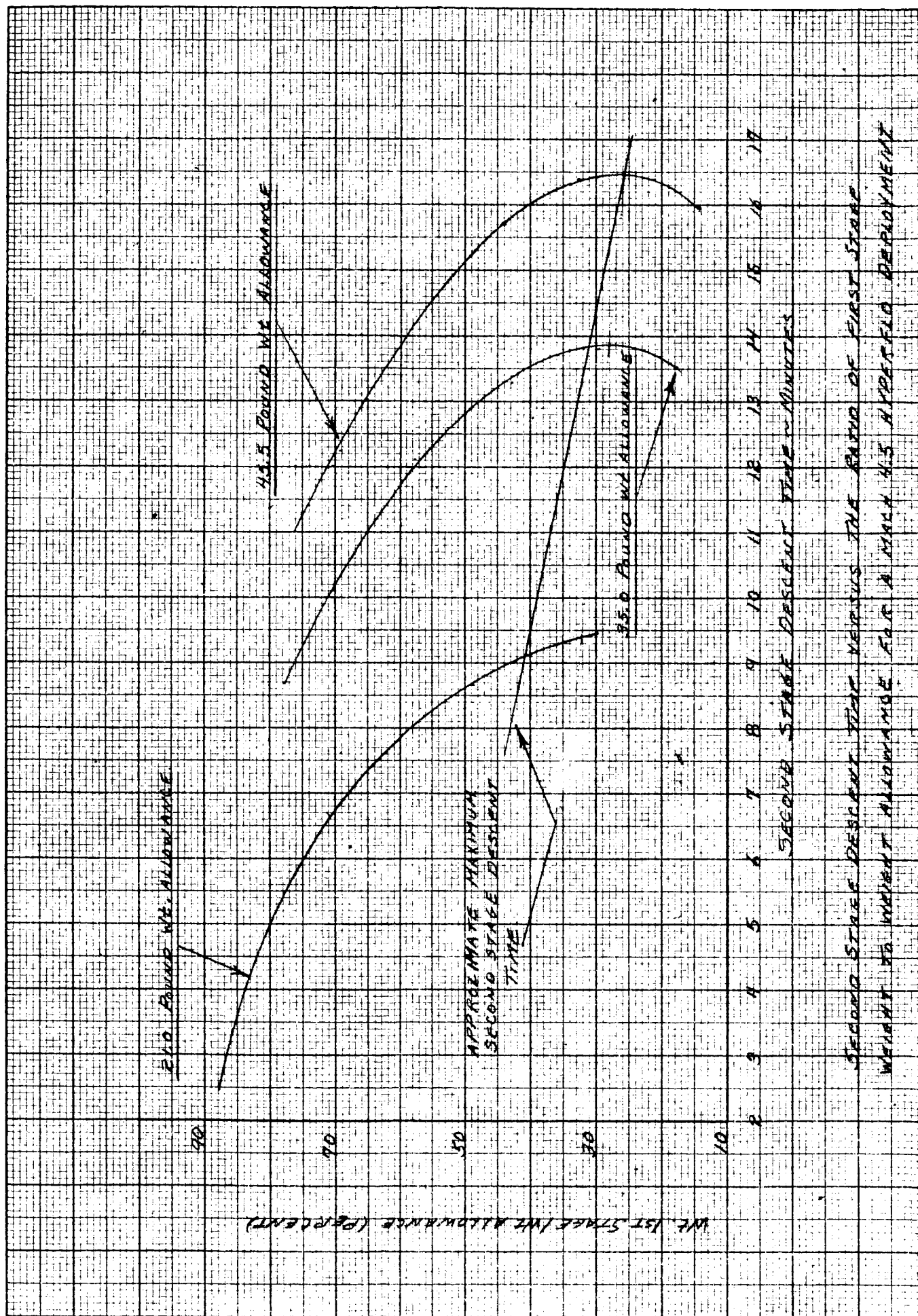
By means of trajectory computations the results of the parachute sizing calculations were used to determine the effects of variations of first stage deployment Mach number, parachute weight allowance and the ratio of first stage parachute weight to total parachute weight allowance. Atmosphere G, nominal entry velocity (26,000 fps) and 90 degree entry angle initial conditions were used in the trajectory computations. The assumptions used in the analysis were as follows. The first stage parachute was at line stretch and ready to open at the start of the computations. It was also assumed that a sensor on the entry vehicle could detect a Mach number of 0.9 and a dynamic pressure equal to, or less than 7.5 psf for the second stage reefed deployment. In these computations the second stage deployment time was not considered since at this stage of the study the deployment system was not determined and the altitude loss expected as a result of this deployment time is expected to be small. The disreef condition was initiated on a test which required that the dynamic pressure be equal to or less than 3.5 psf. The system weight for the calculations assumed 350 earth pounds during the first stage deceleration and 100 pounds during the second stage. This reduction in weight accounts for the separation of the heat shield and aft cover during the deployment of the second stage.

In computing the trajectories the drag area of the entry vehicle and Hyperflo (Figures 2 and 11) were added as functions of Mach number for the first stage operation. The drag area of the payload during the second stage reefed operation was assumed to be 2.4 square feet and was added to the extended skirt drag area in both the reefed and disreefed conditions.

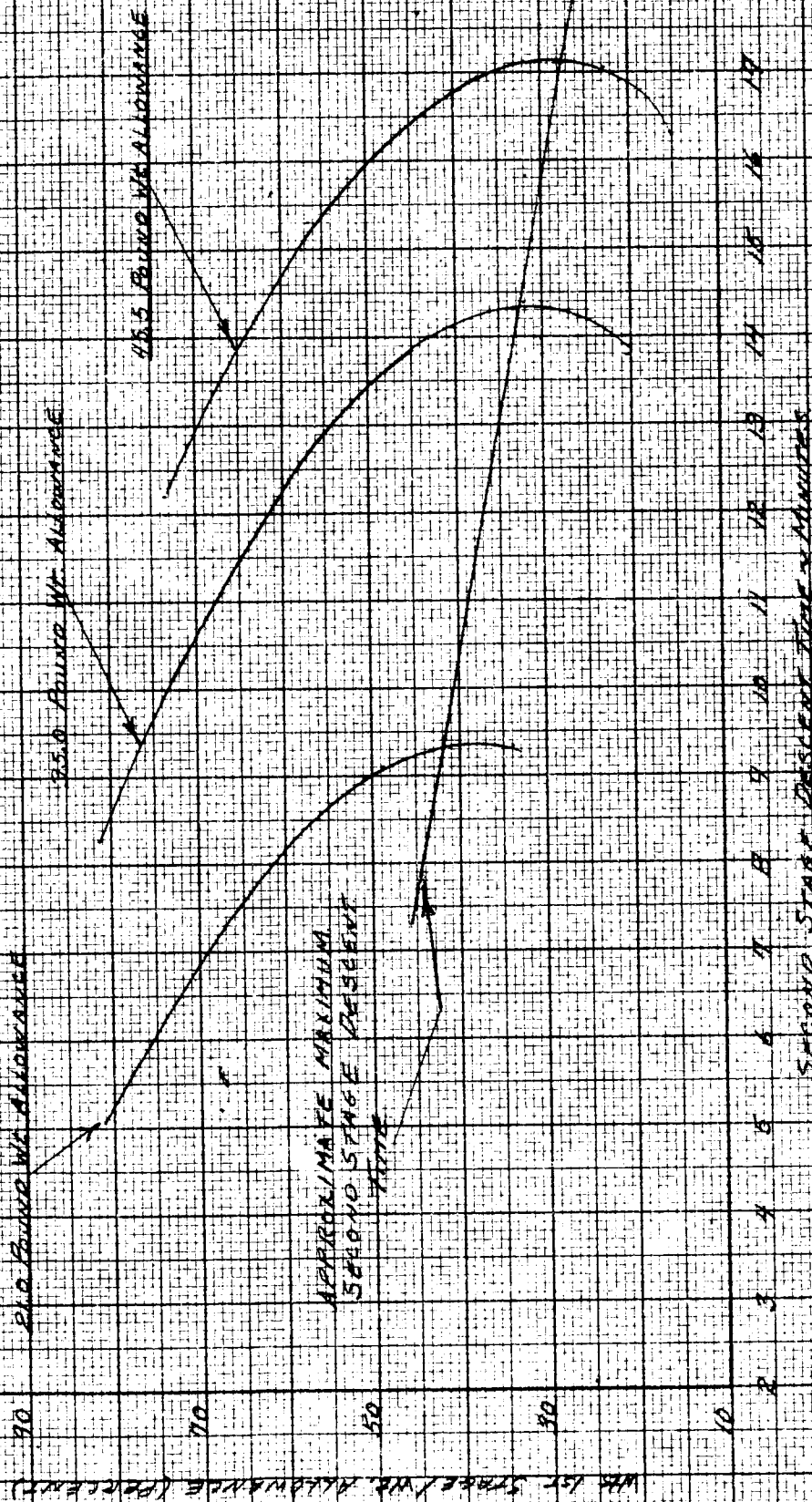
Figures 12 through 14 show the second stage descent time obtained by deploying the first stage Hyperflo at Mach numbers of 3, 4.5 and 6. In these figures the effect of the ratio of first stage parachute weight to parachute weight allowance on



SECOND STAGE DESCENT TIME VERSUS THE RATIO OF FIRST STAGE WEIGHT TO WEIGHT ALLOWANCE FOR A MACH 3.0 HYPERFLIGHT DEPLOYMENT



SECOND STAGE DESCENT TIME VERSUS THE RATIO OF FIRST STAGE WEIGHT TO WEIGHT ALLOWANCE FOR A MAXIMUM 4.5 HYPERFIELD DEPLETION



APPROXIMATE MAXIMUM
SECOND STAGE DESCENT
TIME

SECOND STAGE DESCENT TIME VERSUS THE RATIO OF FIRST STAGE
WEIGHT TO WEIGHT ALLOWANCE FOR A MARCH AND HYPERBARIC DEPLOYMENT

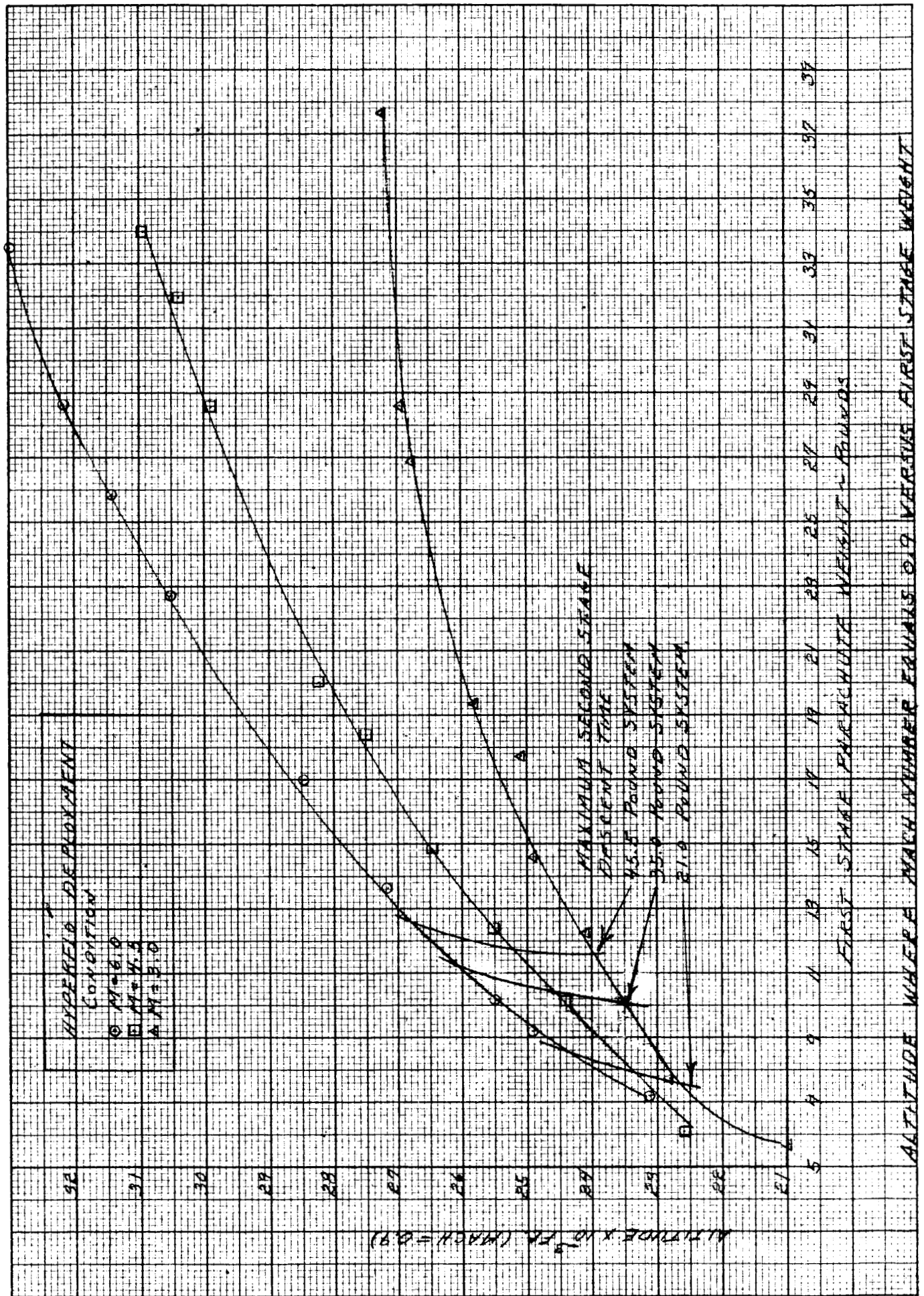
descent time is clearly shown.^{1/} The term "descent time" used throughout this report refers to the time between second stage deployment and ground impact. For these cases it is the time between a Mach number of 0.9 and ground impact. For all the trajectories calculated the optimum weight ratio for maximum second stage descent time varies between approximately 25 and 45 percent. The highest weight allowance for all first stage deployment Mach numbers cases requires the minimum weight ratio.

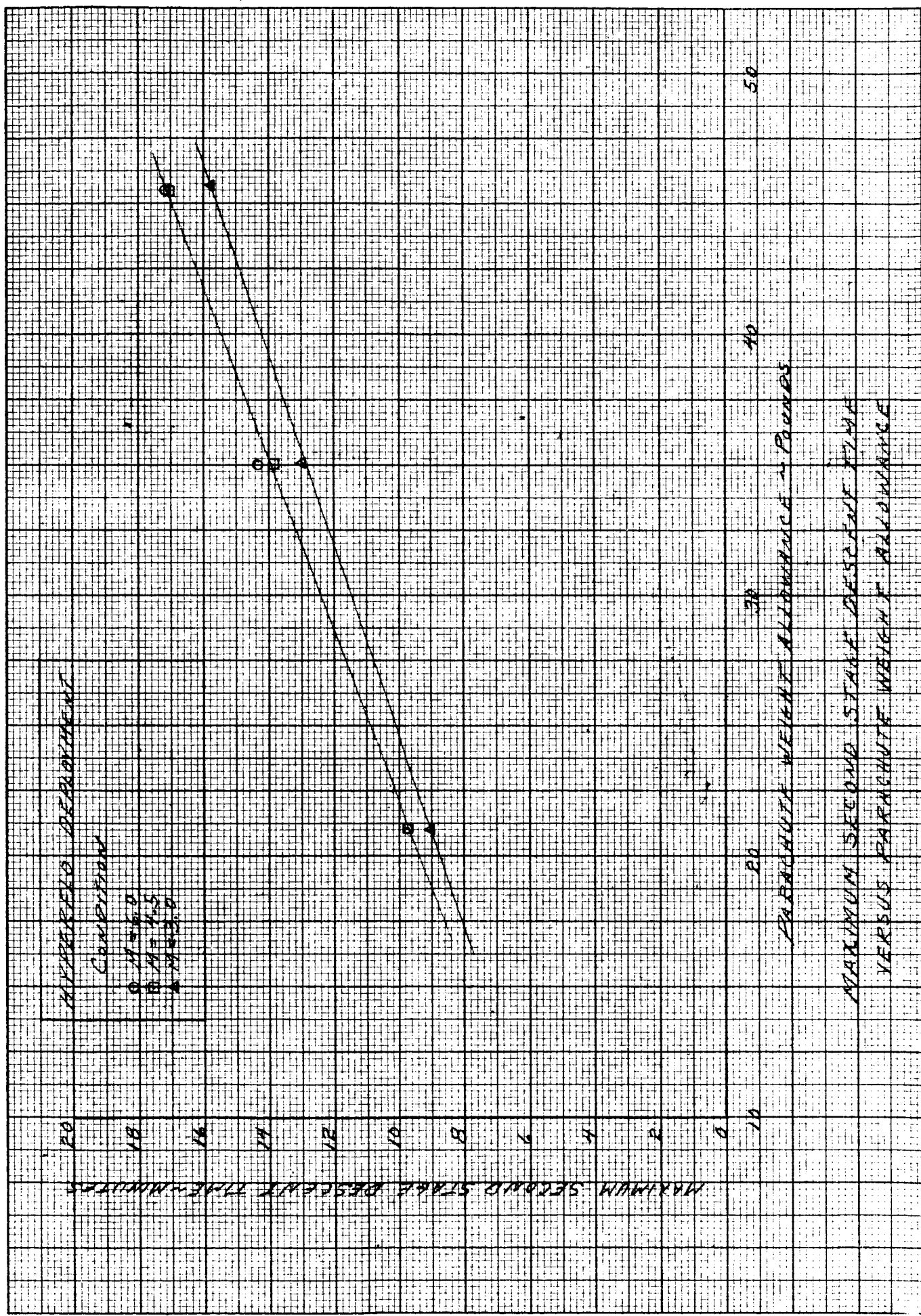
The altitude at which the second stage was deployed (Mach = 0.9) and the heat shield and aft cover were assumed removed for all the trajectories is shown in Figure 15 as a function of first stage parachute weight. Cross-plotted in this figure are the deployment altitudes where optimum descent time was achieved for all three parachute weight allowances. It is noted that above a first stage weight of approximately 15 pounds, for the Mach 3 deployment conditions, a reduction in the rate at which second stage deployment altitude increases occurs. For first stage parachute weights greater than 30 pounds there is a negligible increase in second stage deployment altitude. The Mach 4.5 and 6 first stage deployment curves do not exhibit the same magnitude of change with first stage weight as that obtained in the Mach 3 cases for the parachute weight ranges considered.

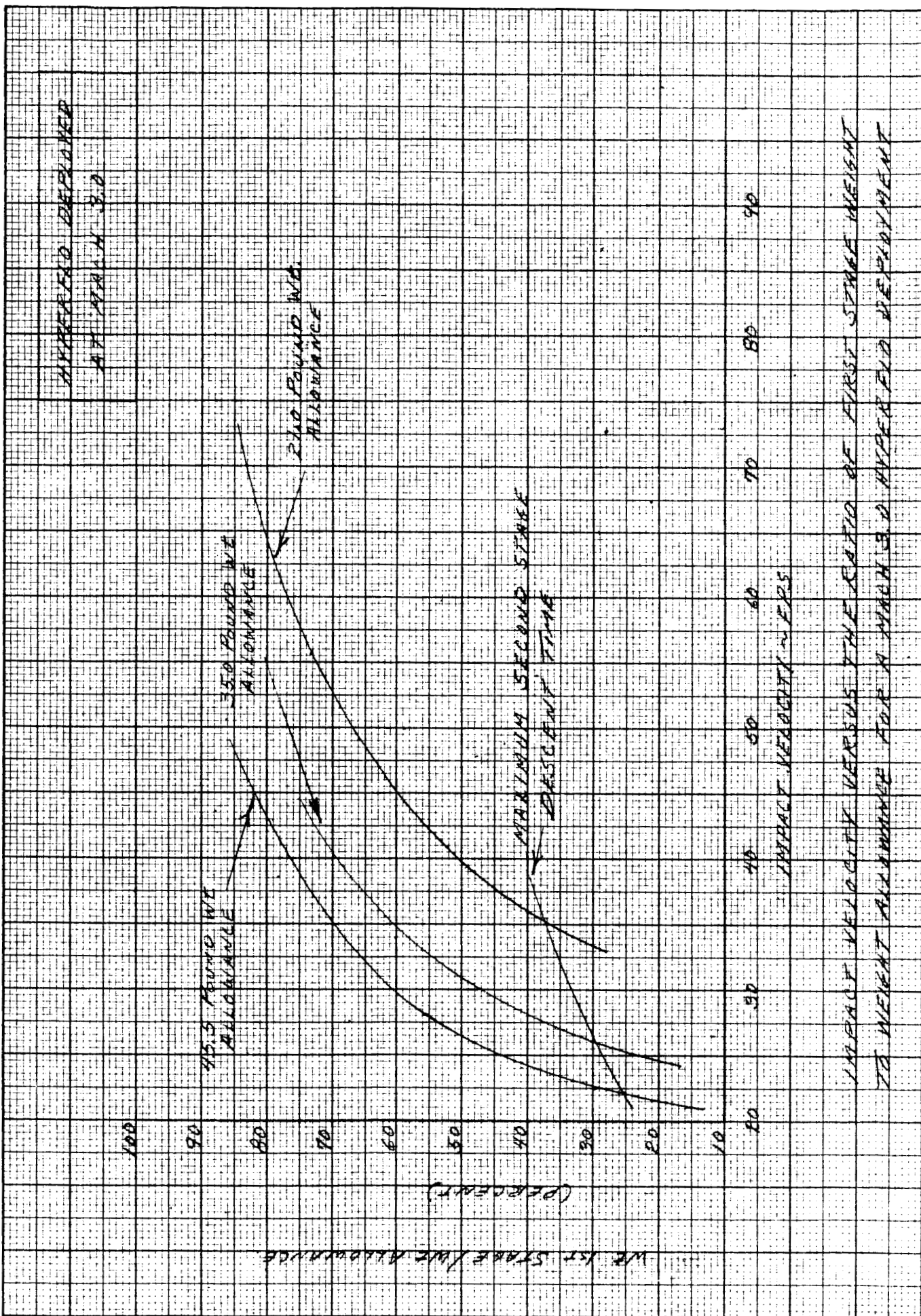
Figure 16 shows the optimum second stage descent time as a function of parachute weight allowance for all three first stage deployment Mach numbers considered. It is seen in this figure that no appreciable increase in descent time over that obtained by a Mach 4.5 deployment was achieved by deploying the first stage parachute at a Mach number of 6. The Mach 3 deployment shows approximately a 10 percent reduction in descent time from those obtained in both Mach 4.5 and 6.0 deployments.

The variation of impact velocity with first stage deployment Mach number and ratio of first stage weight to parachute weight allowance is shown in Figures 17 to 19. The weight ratios for maximum second stage descent time were cross plotted in all of these figures. Based on the trajectory computations the optimum descent time was obtained for impact velocities ranging from 22 to 37 fps for parachute weight allowances of 45.5 and 21 pounds respectively. For the same parachute weight allowances, and ratios of first stage weight to parachute weight allowance of twice that of the optimum values, the impact velocities ranged from 27 to 52 fps respectively. The average increase in impact velocity resulting from the factor of two increase in the weight ratio is 1.3. This represents approximately a 70 percent increase in kinetic energy at impact.

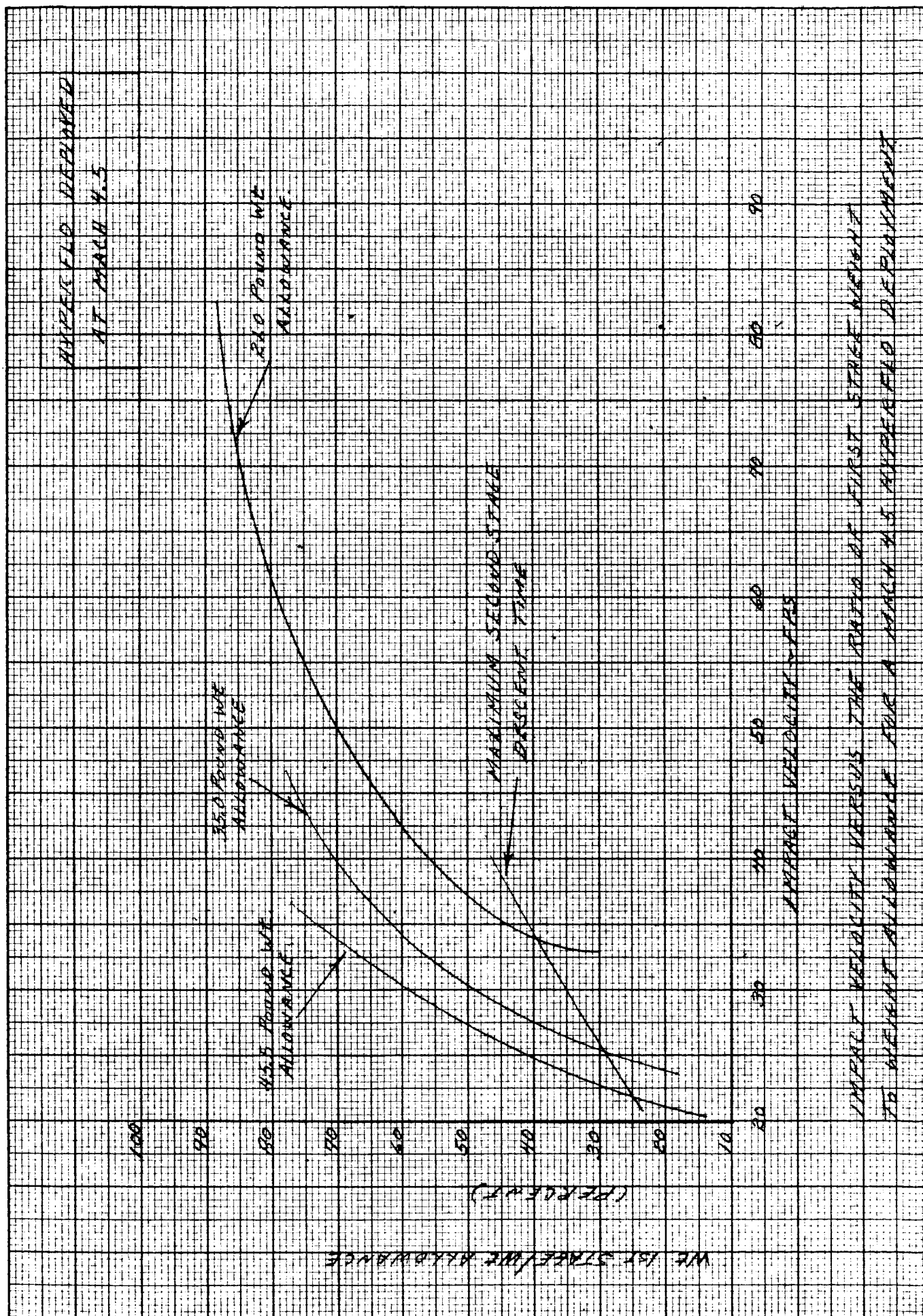
^{1/} A discussion pertaining to extending these curves to a ratio of 100 percent is given in Appendix IV.



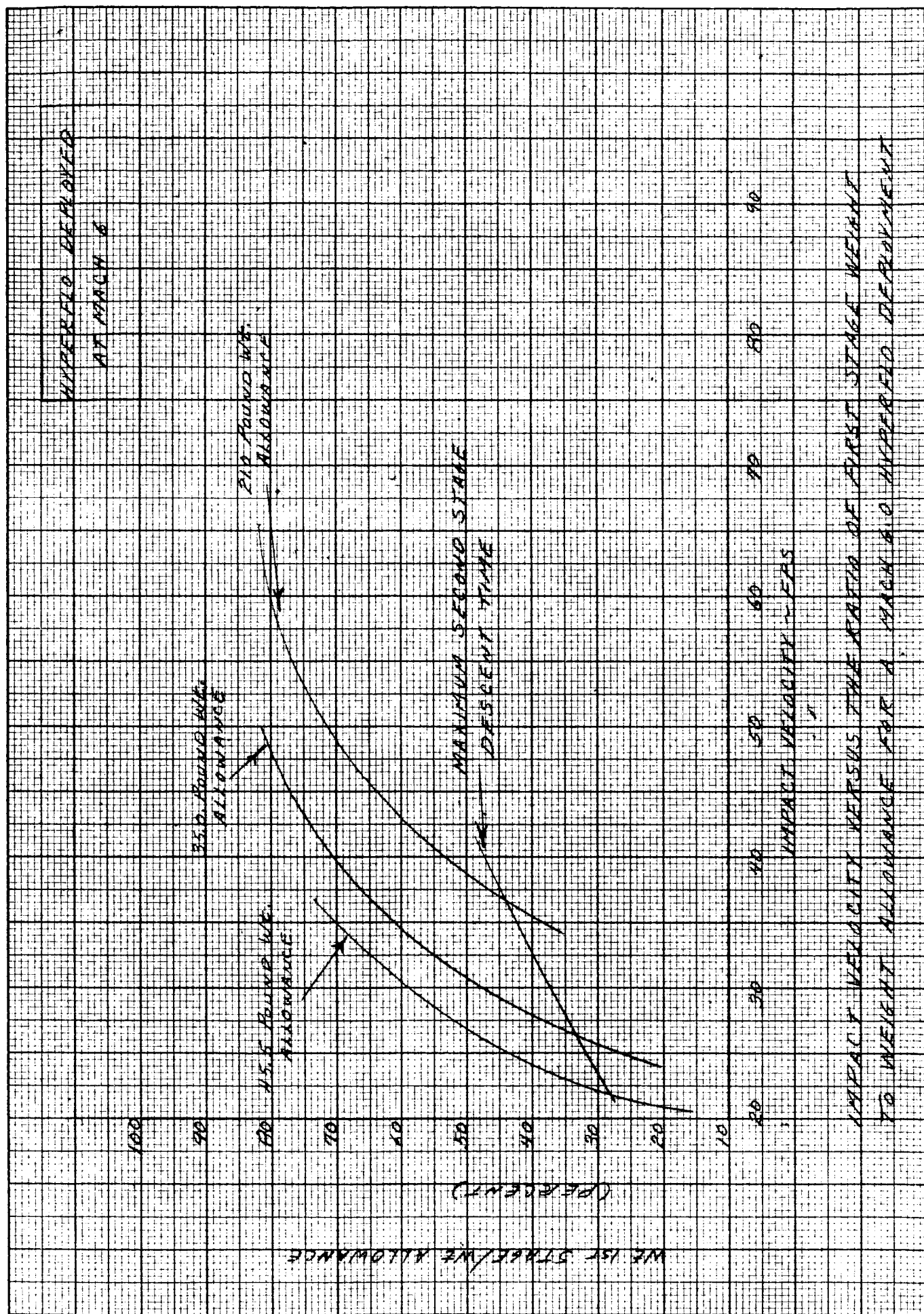




IMPACT VELOCITY VERSUS THE RATIO OF FIRST STAGE WEIGHT TO WEIGHT ALLOWANCE FOR A GRAIN 3.0 HYPERBOLIC DEPLOYMENT



IMPACT VELOCITY VERSUS THE RATIO OF FIRST STAGE WEIGHT TO WEIGHT ALLOWANCE FOR A 4.5 MPH IMPACT DEFLECTION



IMPACT VELOCITY DETERMINES THE RATIO OF FIRST STAGE WEIGHT TO WEIGHT ALLOWANCE FOR A MARCH 6.0 HYPERICID DEPLOYMENT

These results provide the trends and variations pertaining to the efficiency of the parachutes themselves; however, they do not reflect the total decelerator system weight variation with deployment conditions. Not considered in the above is the means by which the first stage decelerator attains line stretch, i. e. position where the parachute can function correctly. The weight of a system which would deploy the first stage is dependent on the type of ejection or extraction procedure used, vehicle geometry, decelerative loads at time of deployment, and first stage parachute weight. Some of the parameters which influence the ejector or extraction system have been used to evaluate the parachute's performance. Therefore, a true assessment of the total decelerator system weight cannot be made without evaluating these parameters.

The most common method of deploying a first stage decelerator is by mortaring the parachute to a region where the aerodynamic drag on the packed parachute will decelerate it relative to the vehicle. It is noted that it is assumed for any deployment procedure that the parachute is packaged in a bag during the extraction phase. Experience has shown that if a parachute is not deployed in an orderly fashion extremely high loads, commonly referred to as snatch forces, occur at line stretch. Aside from the problem of snatch force, the reliability of the parachute to function properly would be significantly reduced due to possible entanglement of lines, etc. if a bag were not used.

The mortar procedure utilizes a pyrotechnic charge to produce high pressures and thereby accelerate the parachute in a tube to ejection velocities compatible with the amount of deceleration the vehicle is undergoing and the distance the pack has to travel. This procedure has been used on all nose cone recoveries performed by the Cook Electric Company and is presently being employed on the Apollo and Gemini vehicles. Other methods, such as using the rear cover of a vehicle as a drag producing surface, have also been successfully demonstrated on other programs. The concept of using the rear cover to deploy the first stage in this program does not appear promising due to the unpredictable drag characteristics of the cone in the wake of the blunt forebody. Coupled with this problem is the question of stability of the aft cover and possible tumbling motions which may foul any bridle used to extract the parachute and thereby damage the deployment bag. Furthermore, to use this type of concept a multiple thruster arrangement must be used to provide the separation velocity. This scheme of attaining separation velocity is subject to the inherent problem of individual thruster timing errors. As a result of these problems, this technique was not considered applicable due to the amount of development testing which would have to be performed to assure a high degree of reliability.

A third alternative considered for obtaining first stage deployment is extraction by means of a lightweight pilot chute. The pilot chute would be deployed by

These results provide the trends and variations pertaining to the efficiency of the parachutes themselves; however, they do not reflect the total decelerator system weight variation with deployment conditions. Not considered in the above is the means by which the first stage decelerator attains line stretch, i.e. position where the parachute can function correctly. The weight of a system which would deploy the first stage is dependent on the type of ejection or extraction procedure used, vehicle geometry, decelerative loads at time of deployment, and first stage parachute weight. Some of the parameters which influence the ejector or extraction system have been used to evaluate the parachute's performance. Therefore, a true assessment of the total decelerator system weight cannot be made without evaluating these parameters.

The most common method of deploying a first stage decelerator is by mortaring the parachute to a region where the aerodynamic drag on the packed parachute will decelerate it relative to the vehicle. It is noted that it is assumed for any deployment procedure that the parachute is packaged in a bag during the extraction phase. Experience has shown that if a parachute is not deployed in an orderly fashion extremely high loads, commonly referred to as snatch forces, occur at line stretch. Aside from the problem of snatch force, the reliability of the parachute to function properly would be significantly reduced due to possible entanglement of lines, etc. if a bag were not used.

The mortar procedure utilizes a pyrotechnic charge to produce high pressures and thereby accelerate the parachute in a tube to ejection velocities compatible with the amount of deceleration the vehicle is undergoing and the distance the pack has to travel. This procedure has been used on all nose cone recoveries performed by the Cook Electric Company and is presently being employed on the Apollo and Gemini vehicles. Other methods, such as using the rear cover of a vehicle as a drag producing surface, have also been successfully demonstrated on other programs. The concept of using the rear cover to deploy the first stage in this program does not appear promising due to the unpredictable drag characteristics of the cone in the wake of the blunt forebody. Coupled with this problem is the question of stability of the aft cover and possible tumbling motions which may foul any bridle used to extract the parachute and thereby damage the deployment bag. Furthermore, to use this type of concept a multiple thruster arrangement must be used to provide the separation velocity. This scheme of attaining separation velocity is subject to the inherent problem of individual thruster timing errors. As a result of these problems, this technique was not considered applicable due to the amount of development testing which would have to be performed to assure a high degree of reliability.

A third alternative considered for obtaining first stage deployment is extraction by means of a lightweight pilot chute. The pilot chute would be deployed by

means of a mortared slug. This technique has been used successfully in programs where volume limitations prohibit the packing of a parachute in a shape amenable to mortaring and where low energy levels are required. Undesirable characteristics associated with this type of system are that for the pilot parachute to be significantly lighter than the first stage, it must be smaller in diameter than the vehicle. This requirement extends the current state of the art in supersonic parachute testing since it necessitates the prediction of a parachute's operation with a parachute-to-vehicle diameter ratio of less than one. For these conditions no experimental data are available. It also requires the inclusion of another event in the deployment sequence: the deployment of a pilot parachute. Due to these limitations it was decided that at least for the light-weight 350 pound entry vehicle it was advisable to retain proven concepts used in supersonic parachute programs and to use a mortar system.

To obtain a weight estimate of the mortars required to deploy the first stage parachutes sized previously (Table II) estimates of the required ejection velocity were made. In Reference 16 procedures for approximating the required ejection velocity are discussed. In this reference the wake flow field which influences the magnitude of the required ejection velocity is divided into two regions. The first region considered is that which has been named in the literature "dead air region". This region extends from the vehicle base to a location where the wake acquires a minimum thickness in supersonic flow. The second region extends from this minimum thickness location, referred to as the wake neck, to a point where the wake is no longer appreciable.

The effect of the first or close-in region on the ejection velocity is of an undesirable nature. For bodies ejected down the centerline of the wake the body must pass through a static pressure gradient, i.e., base pressure at the vehicle base and some pressure higher than static at the wake neck. Based on pointed forebody data in the Mach 3 to 6 region the magnitude of this peak positive pressure coefficient is approximately +.02. Coupled with this static pressure variation a subsonic reverse flow field exists. The magnitude of this reverse flow field has never been accurately measured for supersonic free stream Mach numbers due to the technical difficulties of aligning pitot static probes in a subsonic flow field with unknown stream tube directions and the complications associated with stings and side struts associated with wind tunnel tests. The evidence of such a flow field's existence, however, is unmistakable based on ejection tests performed in wind tunnels where metallic objects have been seen to float around in this region. For this application estimates of the effects of reverse flow indicate that they will not be significant. This stems from the fact that the static pressures are so low for the deployment conditions. An estimate of the maximum reverse flow force was established by assuming a reverse flow Mach number of 1 and free stream static pressure prevailing. Based on the

formulation given in Reference 16 these are the maximum possible values and are considerably greater than those predicted by the referenced formulation. For a Mach 3 deployment this assumption would provide a reverse flow dynamic pressure ratioed to the free stream value of 11.1 percent. For a Mach 6 deployment this ratio reduces to approximately 2.8 percent. Since for packed parachutes M/C_{DA} coefficients of the order of 2 are realistic and the dynamic pressures of 60 to 180 cover the Mach number range, it is apparent that in terms of earth g's peak deceleration values of approximately 0.1 g would be encountered for Mach 3 and 0.05 for Mach 6. Compared to vehicle decelerations at deployment conditions varying from 10 to 30 g's for Mach 3 and 6, respectively, the deceleration values are 1 percent or less of the vehicle values. A similar formulation for the horizontal pressure gradient shows that it is of a negligible force level compared to the deceleration of the vehicle. Refined estimates for these low force levels do not warrant further consideration.

In the spreading downstream wake (region two) computations were performed to determine the vehicle centerline wake conditions at a distance of six calibers or vehicle diameters (Reference 16). Centerline conditions were assumed since parachute pack diameters of approximately 6 inches are expected. The actual wake diameter for a blunt vehicle such as that being considered for this program is subject to some question. For pointed forebodies equivalent to the entry vehicles diameter at Mach 6 minimum wake diameters of 35 inches are expected; however, since the wake diameter in region two is a function of the vehicle base Mach number it is anticipated that the wake diameter will be significantly larger than 35 inches for the blunt shape. Assuming a vehicle base Mach number of 1.5 for the Mach 6 conditions would imply a minimum wake thickness of 60 inches based on Reference 17. Due to this unknown the centerline values which are more nearly representative of a 60 inch wake diameter are given below since they provide a conservative value if smaller wake thickness actually occur.

Mach Number	Wake centerline to free stream dynamic pressure ratio
3.0	0.35
4.5	0.23
6.0	0.15

Using the vehicle deceleration values obtained from trajectories for G atmosphere, vehicle decelerations (Mars) of approximately 30, 56 and 84 g_M's are experienced for deployment Mach numbers of 3, 4.5 and 6 respectively.

These g values are based on the predicted acceleration of gravity on Mars of 12.3 feet/sec². Considering a typical parachute pack to weigh 13 pounds (earth) and have a six inch diameter results in Mars pack deceleration values of 1.25, 1.56 and 1.64 g_M's for the above Mach numbers and centerline wake dynamic pressures at six calibers. The pack axial force coefficient used to determine these values was 1.5. Since the pack deceleration at locations closer to the vehicle base would be lower, the energy which must be imparted to the pack can be conservatively approximated by neglecting the pack deceleration and assuming the vehicle deceleration is a constant for the entire six caliber distance. By making these assumptions the energy which the mortar system must impart to the pack is directly proportional to the mass of the pack and the vehicle deceleration. The equations used to determine the weight of mortars for the 45 systems considered are given in Appendix III.

The first calculations performed using the equations given in Appendix III assumed a 20 to 1 peak-to-average pressure ratio for determining the thickness of aluminum required for the mortar. This large a pressure ratio arises from the fact that mortar systems commonly rely on a granular mixture of explosives which do not have controlled burning characteristics.

Experience gained with mortar systems shows that deviations in burning rates, surface area and other related parameters which control the pressure in a mortar tube force the designer to allow for these high values. Mortar system weights using the pressure ratio of 20 varied from 8 to 148 pounds. These values are highly restrictive and result in so high a weight penalty that only the lightest first stage parachutes can be considered practical with this type of system.

The problem of high peak-to-average pressure ratios in mortars was noted back in 1960. As a result of the large weight penalties associated with high-energy level mortar systems a study was undertaken to develop a controlled gas generator (Reference 16). The gas generator resulting from this study was essentially a small rocket motor with a grain size and mortar geometry such that the generated mass flow could be predicted and thereby control of the peak-to-average pressure ratio was possible.

In ejection tests performed with this system, peak-to-average pressure ratios of 2.1 to 1 were demonstrated for an ejection velocity of 91 fps. It is concluded that this reduction in pressure ratio over that obtained with conventional granular charge mortars warrants its use in this application where large energy levels are required. The required ejection velocities determined from the analysis given in Appendix III are as follows:

Deployment Mach No.

Pack Ejection Velocity

3	180
4.5	250
6.0	310

The mortar weights given in Table III column 2 were calculated using a peak-to-average pressure ratio of 3. This value has been arbitrarily chosen since the ejection velocities required are well above values which have been demonstrated. Tests must be performed to determine for this velocity range actual peak-to-average values. These tests were beyond the scope of the program and the assumed value of 3 was considered a representative value by which mortar weights could be estimated.

A problem area with the controlled gas generator which has never been analyzed thoroughly is the thermal protection requirements for the blast bag due to the high total temperature of the gases emanating from the gas generator. Several methods are open to the designer with respect to this problem. One method is to use a blast bag with sufficient thermal mass and insulative properties to prevent damage to the parachute at deployment. A second method, and the most efficient weightwise, is to use a propellant with a low flame temperature. This alternative requires an extensive study of possible propellents and their capabilities of withstanding the sterilization environment.

Once the mortar weights were determined based on the above assumptions, effort was exerted to determine an optimum system compatible with the design objectives of the program, i. e., descent time, deployment altitude, impact velocity and payload weight. The mortar weights discussed above have been included in this examination since this weight contribution is a variable depending on the particular weight of the first stage parachute. Other weights such as the sensing system and other hardware items which were not determined at this point in the study were not included since they represented fixed items and would not vary with the system chosen.

Table III gives merit numbers obtained based on parameters which were considered indicative of the system's performance. The first merit figure, given in column 8, relates the product of descent time and payload weight to the sum of the mortar weight and parachute weight allowance. The term "payload" used in this representation is the impact weight minus the second stage parachute weight or for these calculations 100 pounds minus the second stage weight. The systems which this merit number favored were the light weight parachute allowance

TABLE III

Determination of Merit Figures for the Parachutes Systems In Contention

Deployment Mach No.	Case No.	Mortar Wt. (Lbs.)	Parachute		2nd Stage Parachute Wt. (Lbs.)	Payload Wt. (Lbs.)	Descent Time (Minutes)	Merit		Altitude M=0.9	Merit		Terminal Velocity (fps)	Merit Figure No. 3 $\frac{10}{11}$
			System Wt. (Lbs.)	2+3 (Lbs.)				Figure No. 1 $\frac{6 \times 7}{4}$	Figure No. 2 $\frac{8 \times 9}{10,000}$					
M=3	1	1.35	45.5	46.85	39.7	60.30	14.85	19.1	20,842	39.6	20.4	1.94		
	2	2.85	45.5	48.35	33.1	66.90	15.7	21.7	24,061	52.3	22.1	2.36		
	3	4.46	45.5	49.96	26.0	74.00	14.6	21.6	25,782	55.7	25.1	2.22		
	4	6.58	45.5	52.08	16.7	83.30	12.12	19.4	26,903	52.2	31.3	1.66		
	5	8.62	45.5	54.12	7.71	92.29	7.95	14.1	27,520	38.8	46.7	0.83		
M=4.5	6	2.70	45.5	48.20	39.3	60.70	15.95	20.1	22,477	45.2	20.4	2.21		
	7	6.42	45.5	51.92	30.5	69.50	16.35	21.9	26,813	58.8	23.3	2.52		
	8	8.59	45.5	54.09	25.4	74.60	15.70	21.6	28,398	61.3	25.6	2.46		
	9	13.63	45.5	59.13	13.5	86.50	12.0	17.6	30,331	53.4	35.1	1.52		
	10	14.52	45.5	60.02	11.4	88.60	11.28	16.6	30,976	51.4	37.9	1.36		
M=6	11	4.86	45.5	50.36	38.3	61.70	16.25	19.9	23,073	46.0	20.5	2.24		
	12	6.88	45.5	52.38	35.2	64.80	17.05	21.1	25,952	54.7	21.7	2.52		
	13	11.36	45.5	56.86	28.4	71.60	16.90	21.3	28,644	61.1	23.9	2.56		
	14	17.16	45.5	62.66	19.6	80.40	15.25	19.6	31,392	61.5	28.7	2.14		
	15	22.2	45.5	67.70	11.9	88.10	12.2	15.9	32,954	52.2	37.2	1.40		
M=3	16	1.35	35.0	36.35	29.2	70.80	12.6	24.6	20,842	51.4	23.7	2.16		
	17	1.82	35.0	36.82	27.1	72.90	13.45	26.5	22,910	60.7	24.4	2.48		
	18	2.85	35.0	37.85	22.6	77.40	12.6	25.8	24,061	62.1	27.0	2.30		
	19	4.46	35.0	39.46	15.5	84.50	11.0	23.5	25,782	60.7	32.9	1.85		
	20	6.17	35.0	41.17	8.06	91.94	7.92	17.7	26,677	47.2	45.5	1.03		
M=4.5	21	2.70	35.0	37.70	28.8	71.20	13.55	25.6	22,477	57.7	23.7	2.43		
	22	4.43	35.0	39.43	24.7	75.30	13.78	26.2	24,715	64.8	25.6	2.53		
	23	6.42	35.0	41.42	20.0	80.00	13.25	25.6	26,813	71.4	28.5	2.50		
	24	8.59	35.0	43.59	14.9	85.10	12.1	23.7	28,398	67.4	32.9	2.05		
	25	11.59	35.0	46.59	7.8	92.20	8.65	17.1	29,842	51.0	46.7	1.09		
M=6.0	26	4.86	35.0	29.86	27.8	72.20	13.75	24.9	23,073	57.6	24.0	2.4		
	27	6.88	35.0	41.88	24.7	75.30	14.40	25.9	25,952	67.1	25.6	2.62		
	28	11.36	35.0	46.36	17.9	82.10	13.10	23.2	28,644	66.5	30.5	2.18		
	29	15.11	35.0	50.11	12.2	87.80	11.42	20.0	30,491	61.0	36.9	1.65		
	30	19.0	35.0	54.	6.33	93.67	8.23	14.3	32,227	46.0	51.9	0.89		

TABLE III - Cont'd.

Deployment Mach No.	Case No.	Mortar Wt. (Lbs.)	Parachute System Wt. (Lbs.)	2+3 (Lbs.)	2nd Stage Parachute Wt. (Lbs.)	Payload Wt. (Lbs.)	Descent Time (Minutes)	Merit Figure No. 1 $\frac{6 \times 7}{4}$	Altitude M=0.9	Merit Figure No. 2 $\frac{8 \times 9}{10,000}$	Terminal Velocity (fps)	Merit Figure No. 3 $\frac{10}{11}$
	1	2	3	4	5	6	7	8	9	10	11	12
M=3	31	1.35	21.0	22.35	15.2	84.80	8.87	33.7	20,842	70.4	32.9	2.14
	32	1.82	21.0	22.82	13.1	86.90	8.96	34.0	22,910	78.0	35.6	2.19
	33	2.85	21.0	23.85	8.68	91.32	7.56	28.7	24,061	69.1	32.7	1.58
	34	3.37	21.0	24.37	6.3	93.70	6.28	24.1	24,893	60.0	51.8	1.16
	35	4.10	21.0	25.10	3.15	96.85	3.62	13.9	25,213	35.0	73.3	0.478
M=4.5	36	2.70	21.0	23.70	14.8	85.20	9.44	33.9	22,477	76.2	33.3	2.24
	37	4.43	21.0	25.43	10.7	89.30	8.63	30.3	24,715	75.0	39.5	1.90
	38	5.40	21.0	26.40	8.46	91.54	7.88	27.8	25,979	72.4	44.5	1.62
	39	6.42	21.0	27.42	6.04	93.96	6.67	22.8	26,813	61.0	52.6	1.16
	40	7.91	21.0	28.91	2.53	97.47	2.42	8.16	27,845	22.7	82.7	.274
M=6.0	41	4.86	21.0	25.86	13.8	86.20	9.29	30.9	23,072	71.4	34.7	2.05
	42	6.21	21.0	27.21	11.8	88.20	9.05	29.3	24,827	72.7	37.9	1.92
	43	6.88	21.0	27.88	10.7	89.30	9.05	28.9	25,952	75.0	39.5	1.90
	44	9.19	21.0	30.19	7.24	92.76	7.6	23.4	27,210	63.7	47.8	1.33
	45	11.36	21.0	32.36	3.93	96.07	5.07	15.0	28,644	43.0	65.8	0.65

cases (21 pounds) and lower deployment Mach numbers (3 and 4.5). The least favorable cases in this comparison in general were the high Mach, high parachute weight allowance cases. In an attempt to demonstrate the advantages afforded by the high weight parachute allowance systems and high deployment Mach numbers merit figures number 2 and 3 were derived. Merit figure number 2 is the product of merit figure number 1 times the second stage deployment altitude or the altitude at which 0.9 Mach number was attained. For convenience merit figure number 2 was divided by 1 times 10 to the fourth. Although this merit figure did make the higher Mach number cases more favorable, the lightweight allowance cases still remained the most favorable.

The final merit figure investigated (number 3) is merit figure No. 2 divided by the system's impact velocity. The addition of impact velocity in the merit figure scheme completely inverted the previous results. For merit figure number 3 the Mach 6 deployment high weight allowance cases (45.5 pounds) became the optimum followed closely by the Mach 4.5 medium weight allowance case.

Upon review of the merit numbers considered, it became obvious that the optimum system depends on specific weighting factors assigned to the various design objectives. To aid in the selection of the desired system the aerodynamic heating of the parachutes was considered. The analytical expression used to predict the heat transfer coefficients is the method outlined in Reference 4 which assumes a stagnation point heating to a sphere with appropriate stagnation point velocity gradients. In this formulation the presence of the forebody is not considered. Based on this omission, it was expected that the formulation would produce conservative results for a decelerator with a forebody. Correlation of the predicted maximum fabric temperature with flight test data, however, gave fair agreement and in only one instance did it appear that the predicted value exceeded physically possible fabric temperatures. Due to the geometric dissimilarities between a sphere and a parachute the need for additional work in this area even though reasonable agreement was obtained is required.

The expression used to express the laminar heat transfer coefficient to the parachutes was the following:

$$h = K \frac{0.763}{Pr^{0.6}} \left(\frac{\beta D}{u_{\infty}} \right)^{1/2} \left(\frac{\mu_{\infty}}{\rho_{\infty} u_{\infty} D} \right)^{1/2} \left(\frac{\rho_{\delta}}{\rho_{\infty}} \right)^{1/2} \left(\frac{\mu_{\delta}}{\mu_{\infty}} \right)^{1/2} \rho_{\infty} u_{\infty} C_p$$

where

h = heat transfer coefficient, BTU/ft² sec °R.

Pr = Prandtl number

- u = velocity, ft/sec
 μ = coefficient of fluid viscosity
 ρ = fluid density, $\frac{\text{lb-sec}^2}{\text{ft}^4}$
 β = stagnation point velocity gradient, ft/sec-ft
 D = body diameter, ft
 C_p = fluid specific heat at constant pressure, $\frac{\text{BTU-ft}}{\text{lb-sec}^2\text{-}^\circ\text{R}}$
 K = 1.36 = factor accounting for the increased heat transfer rate due to a possible 100 percent carbon dioxide atmosphere, nondimensional.

The subscript ∞ refers to free stream conditions and the subscript δ refers to local conditions outside the boundary layer. The factor K arises from a 9 percent increase in heat transfer coefficient due to changes in thermodynamic and heat transport properties (Reference 18) and a 25 percent increase in this value recommended by JPL due to experimental scatter.

The temperature histories of the materials were obtained by using an assumption of infinite material conductivity and the heat sink capability of the lightest component in the parachute design independent of its physical location. This assumption is based on a uniform heat transfer rate over the inner surface of the canopy equal to the stagnation heating to a sphere whose diameter is the projected parachute diameter. Due to the lack of applicable experimental data to predict accurately the base heating of the canopy, a value of 50 percent of the heating rate on the inside of the canopy has been used. The resultant total heat flux to the canopy is then 1.5 times that predicted for the inner surface of the parachute. For all calculations performed, a turbulent flow recovery factor of 0.9 was assumed on both the inner and outer surfaces of the canopy. Radiation shape factors of 1.0 and 0.5 were used for the front and rear of the canopy, respectively, assuming an inflated hemispherical canopy contour. The radiation sink temperature assumed for both space and planet surface was the predicted surface temperature for the specific atmosphere used.

$$\Delta T_w = \frac{1.5}{C_p} \left[h(T_r - T_w) - \epsilon \sigma (T_w^4 - T_a^4) \right] \Delta t$$

where

$$T_w = \text{wall surface temperature, } ^\circ\text{R}$$

$$\begin{aligned}
\sigma &= \text{Stefan - Boltzman constant, } \frac{\text{BTU}}{\text{ft}^2 \text{sec } ^\circ\text{R}^4} \\
\epsilon &= \text{wall emissivity, (0.8 used for Nomex)} \\
T_a &= \text{radiation sink temperature, } ^\circ\text{R} \\
h &= \text{heat transfer coefficient, } \text{BTU}/\text{ft}^2 \text{ sec } ^\circ\text{R} \\
\rho &= \text{material density, } \text{lb}/\text{ft}^3 \\
C_p &= \text{material specific heat } \frac{\text{BTU}}{\text{lb } ^\circ\text{R}} \quad (0.30 \text{ used for Nomex}) \\
t &= \text{time (sec.)} \\
T_r &= \text{recovery temperature, } ^\circ\text{R}
\end{aligned}$$

Using the above formulation, maximum material temperatures were obtained for all the potential parachute configurations and these values are given in Table IV. For these computations the maximum predicted material temperature at deployment was assumed (160°F). The Nomex fabric which was used as the critical item for these computations was a 150 pound per inch cloth with a weight per square foot of 0.0202 pounds.

The maximum fabric temperature for the Mach 3 cases was 215°F or a 55 degree rise. The maximum fabric temperature for the Mach 4.5 systems was computed to be 423 degrees F. At this temperature the strength of Nomex is approximately 75 percent of room temperature strength. For the materials which had to be used for the parachute canopy designs due to materials available, this strength degradation will not reduce the material strength below that acceptable for initial deployment. Accounting for the fact that at the time the material achieves this maximum temperature the load on the canopy is approximately 80 percent of that at opening provides an additional safety factor.

The Mach 6 parachute designs did not exhibit as favorable peak temperatures as those given above. The peak temperature computed for the 8 foot D_p parachutes was 752 degrees F. At this temperature Nomex material possesses less than 25 percent of its room temperature strength. From the trajectory computations this temperature occurs while the canopy is loaded to 83 percent of the opening load. As a result of this temperature, load history case numbers 11, 26 and 41 (Table IV) are unacceptable and were not considered further. Performing the same type of analysis given above for the remaining Mach 6 systems and accounting for the material strengths used in the canopy revealed that all first stage parachutes with a 10 foot projected diameter or less (cases 12, 27, 42 and 43) were unacceptable based on a material temperature-load history. First stage parachutes with a projected diameter equal to or less than 12 feet (cases 13, 28, 44 and 45) all

TABLE IV

Aerodynamic Heating Results

<u>Deployment Mach No.</u>	<u>Case No.</u>	<u>Maximum Fabric Temperature Degrees Fahrenheit</u>	<u>Deployment Mach No.</u>	<u>Case No.</u>	<u>Maximum Fabric Temperature Degrees Fahrenheit</u>
3	1	2 15	6.0	26	752
	2	200		27	681
	3	193		28	623
	4	188		29	574
	5	185		30	534
4.5	6	423	3	31	215
	7	357		32	206
	8	334		33	200
	9	307		34	197
	10	300		35	195
6.0	11	752	4.5	36	423
	12	681		37	386
	13	623		38	371
	14	554		39	358
	15	517		40	345
3.0	16	215	6.0	41	752
	17	206		42	716
	18	200		43	681
	19	193		44	650
	20	190		45	623
4.5	21	423			
	22	387			
	23	357			
	24	334			
	25	315			

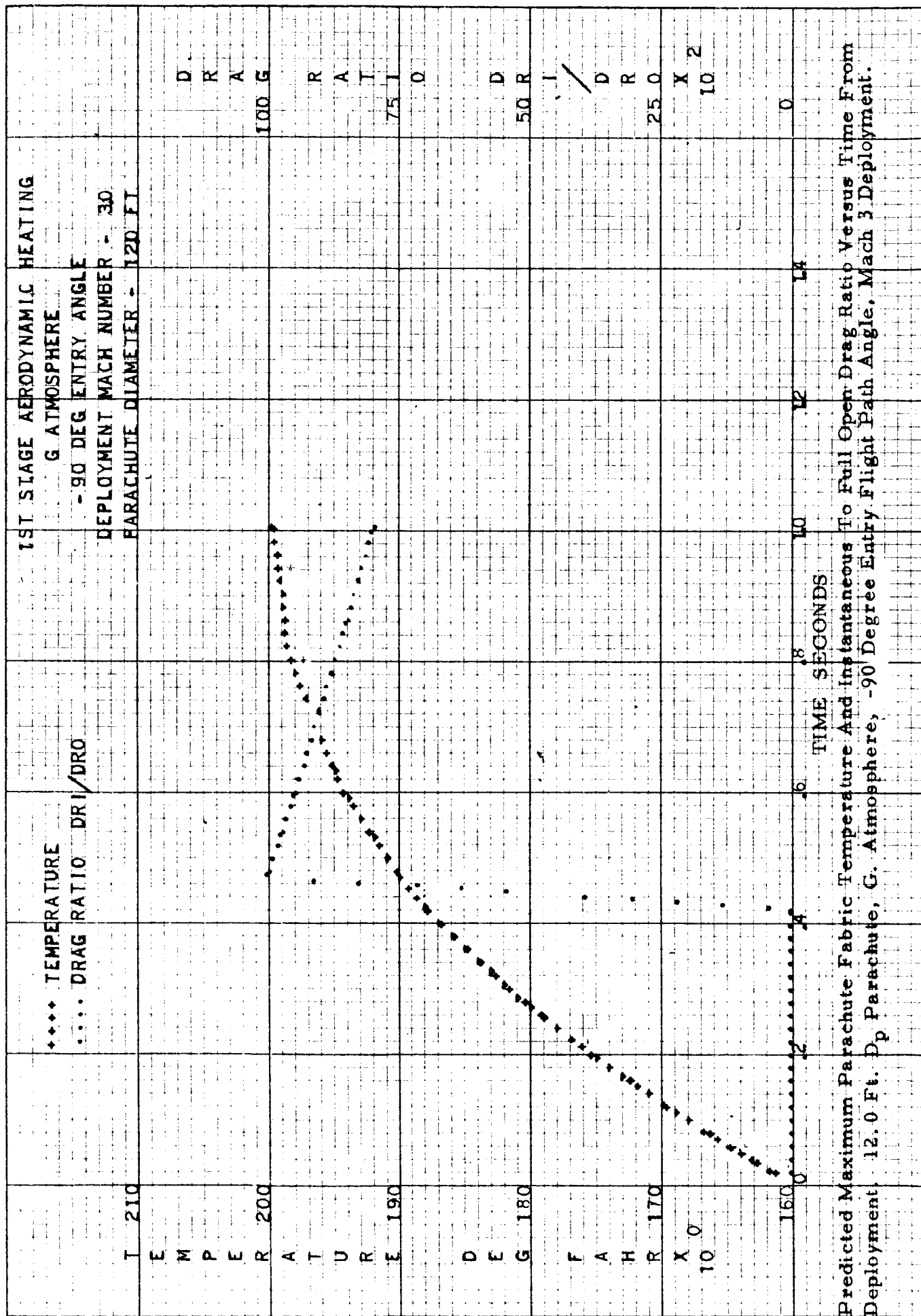
exceed the temperature for which the material strength is reduced to fifty percent of room temperature strength. It was felt that these cases were somewhat questionable due to the limited knowledge of Nomex characteristics as a parachute material even though theoretically they are acceptable. A factor which ultimately eliminated these system was the consideration that possible sensing errors would increase the magnitude of these temperatures thereby making them unacceptable. Cases 14, 15, 29 and 30 were the only Mach 6 deployment designs considered as possible candidates. These designs all have peak temperatures lower than 575 degrees F and have projected diameters of 14 feet or greater.

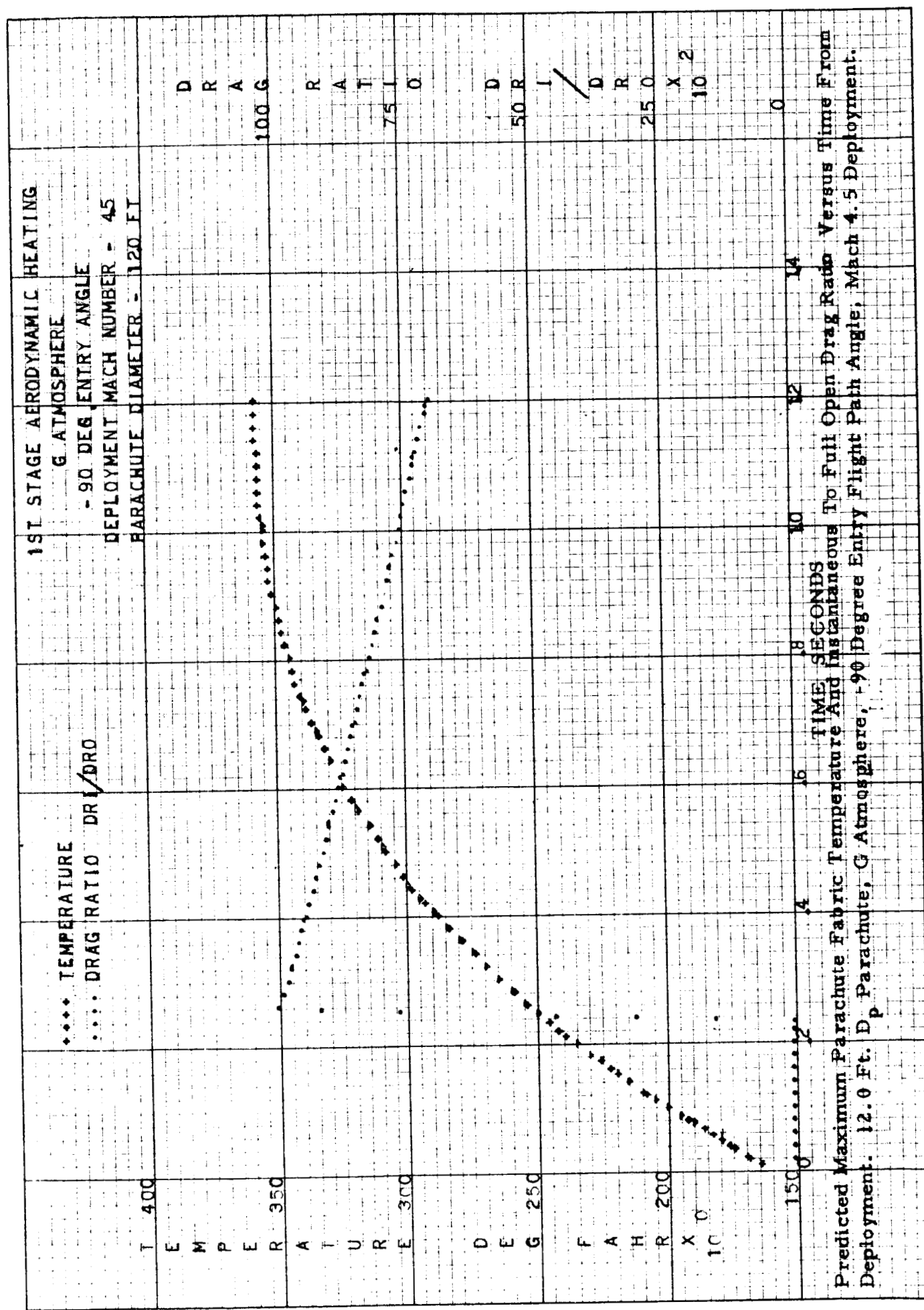
The results of the heating analysis show that all Mach 3 and 4.5 designs are acceptable candidates and that the Mach 3 systems sustain negligible material strength degradation (approximately 7 percent) as a result of aerodynamic heating. Figures 20 through 22 show the temperature-time histories for a 12 foot diameter Hyperflo deployed at Mach numbers of 3, 4.5, and 6. The ratio of DRI to DRO given in these figures is the ratio of the instantaneous parachute drag to the full open parachute drag. This ratio was calculated only after full inflation and has no meaning prior to achieving a value of one. The case numbers (Table II) for these representative calculations are 7, 18 and 28 respectively. For all these calculations the conical inlet material was the same independent of the deployment conditions and this component possessed the critical thermal mass. The weight per square foot of this material was 0.0202 lbs/ft².

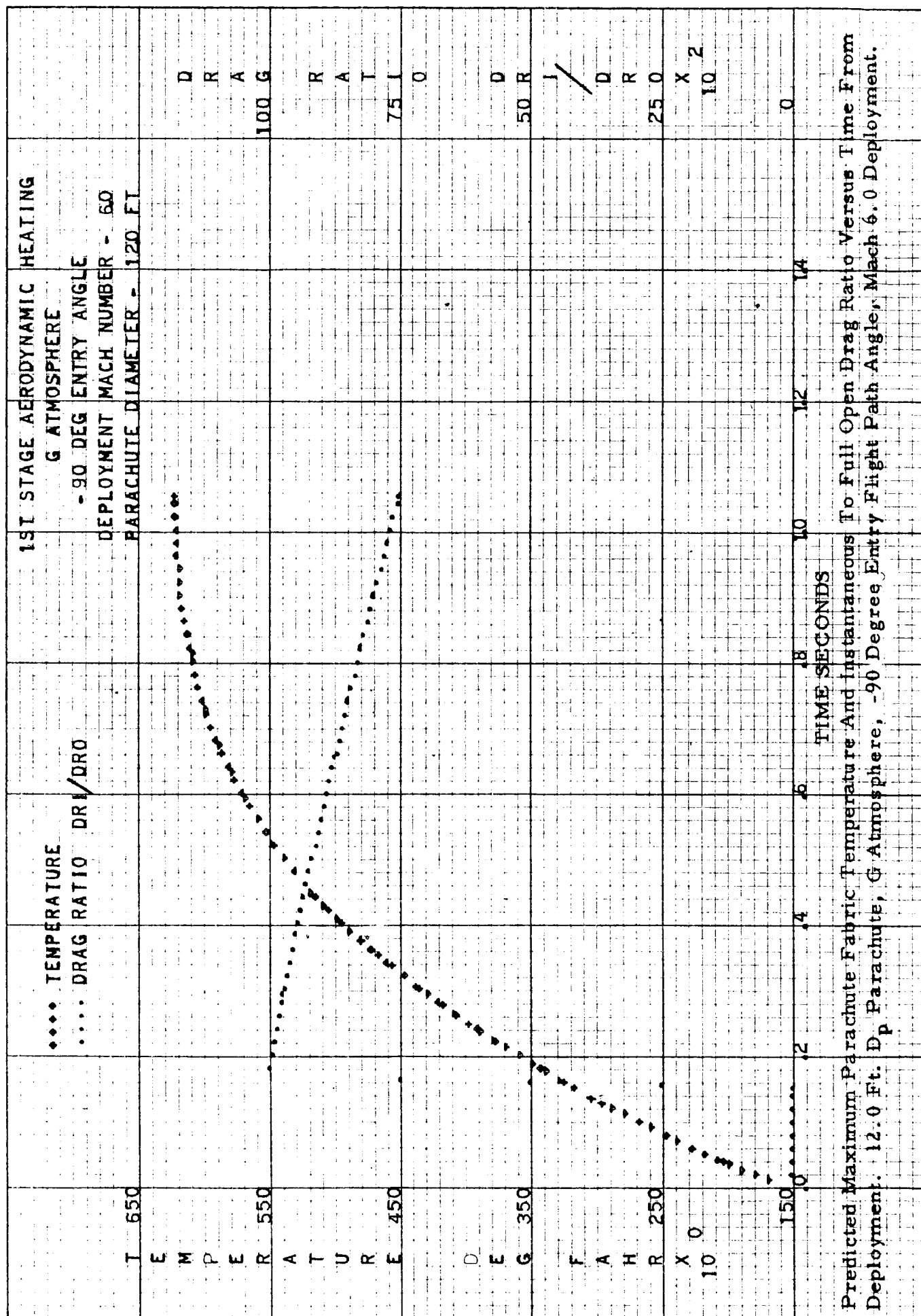
The selection of an optimum decelerator system was not yet obvious after the heating analysis was performed. The factors which are influenced by tradeoffs of deployment altitude, system weight and terminal velocity could not be totally assessed by this contractor with regard to mission requirements and, therefore, the selection was referred to JPL. The selection made was case number 18. This system is comprised of a 35 pound parachute weight allowance and a ratio of first stage weight to weight allowance of 35 percent. The deployment Mach number for this case is 3.0. The parachutes are a 12 foot first stage Hyperflo and a 59.3 foot fully extended skirt second stage.

C. Sensing System Requirements and Description

The parameters which are critical with regard to the optimum parachute system selected are the deployment dynamic pressure-Mach number combination and the maximum fabric temperature. The first combination is critical since it determines the opening loads the parachute will be subjected to and is equally important for both first and second stage deployments. The second parameter is of consequence for the first stage only.







Considering the heating factor first, the two parameters which directly influence the rate of aerodynamic heating are the atmospheric density and the aerodynamic velocity. The convective heat flux can be approximated by assuming it proportional to velocity cubed and density to the one half power. For a given peak heat flux the first stage deployment can take place at a higher velocity for a shallow entry than for a 90 degree entry since for a given ratio of instantaneous velocity to entry velocity the atmospheric density at deployment will be lowest for the shallowest entry angle. This conclusion must be tempered somewhat since for a given peak heat flux the dynamic pressure for a shallow entry must be lower than that obtained for a 90 degree entry. The reduction in dynamic pressure results from the fact that dynamic pressure is directly proportional to density and to velocity squared and it can be shown by equating the peak heat flux for two different densities to be approximately proportional to the density ratio to the two-thirds power. This reduction in dynamic pressure increases the time at the high heat fluxes due to a reduction in the aerodynamic load. Therefore, given a specific peak heat flux a higher peak fabric temperature would be expected for a deployment at a lower atmospheric density (shallower entry angle) and a given fabric thermal mass.

Based on the above discussion it appears that what is required for the first stage sensing system is a means by which Mach number or aerodynamic velocity plus dynamic pressure can be obtained. The second stage requires the same type of information. To obtain a measure of the dynamic pressure for the first stage deployment it is recommended that the vehicle deceleration be measured. This stems from the fact that for the Mach number range of interest the drag area remains almost constant thereby providing a reliable indication of the dynamic pressure. To obtain a measurement of Mach number several techniques may be feasible. One means is to determine from experimental pressure distributions whether a unique function of Mach number can be obtained by using the pressure ratio of two pressure ports located at different physical locations on the entry vehicle. A second means is to determine if there exists any location on the entry vehicle over the Mach number range of interest where a static pressure port would measure a reasonably accurate or constant fraction of the free stream static pressure. If such a location exists it appears feasible by electrical circuitry to correlate the static pressure with the dynamic pressure resulting from the vehicle deceleration to provide a Mach number history. To perform this determination of Mach number based on knowing the static and dynamic pressure an assumption for the ratio of specific heats must be made. Using the nominal value of γ for the atmospheres considered reduces the error due to this term to approximately 7 percent which is within tolerance.

For both of the above approaches a thorough knowledge of the surface pressure distribution on the entry vehicle is required. If this information is not presently

available extensive wind tunnel tests would be required. Problem areas foreseen with regard to these schemes, aside from those mentioned, are the possible blocking of ports due to the flow of ablation material, vehicle dynamics which would alter the surface pressures, and the low absolute magnitude of the pressures. To determine accurately these effects and perform the pressure distribution survey was beyond the scope of this program but is suggested as a possible approach which should be investigated.

Due to the above-mentioned problem areas associated with pressure measurement devices or any other known means of measuring the atmospheric environment a third alternate of predicting the entry vehicle velocity history was considered. This alternative eliminates the requirement of physically measuring the atmospheric environment but poses a requirement that the entry vehicle trajectory be approximated at the time it is ejected from the primary vehicle. The mechanical means considered for predicting the entry vehicles velocity is an integrating accelerometer. This technique has the disadvantage that during the time the vehicle is free falling in space the accelerometer would not sense the acceleration of gravity. Even if this acceleration were compensated for, the accelerometer would not be able to predict the angular component of the acceleration vector relative to the flight path. Once the capsule enters the measurable atmosphere the accelerometer can measure the vehicle deceleration due to aerodynamic loads, and thereby compensate for different atmospheric densities. The effect of gravity, however, would have to be accounted for specifically on shallow entry angles where aerodynamic forces are low and the component of gravity is at a large angle relative to the flight path.

The advantages afforded by such a system, if proven feasible, are that it would not require the measuring of atmospheric constituents to enable the prediction of the aerodynamic velocity or Mach number. This advantage is very significant since the above considerations indicate that the only alternative means of obtaining a measure of the required parameters is by measuring pressures and as stated earlier significant technical problems are associated with that scheme.

The determination of the feasibility of predicting the vehicle velocity based on compensating for the effect of gravity for the range of entry flight path angles was beyond the scope of this program. The task has been undertaken by the Jet Propulsion Laboratory. However, due to timing limitations the results of this study are not available at the time of writing of this report. The approach recommended is the determination of the feasibility of adding a velocity increment to the inertial velocity of the entry vehicle at the time of separation. The magnitude of this increment would depend on the predicted entry angle of the vehicle after final velocity corrections had been made to the primary vehicle and the location relative to the planet where the entry vehicle would be separated. The incremented

velocity added in the actual operation would be radio commanded based on calculations performed using ground tracking information of the primary vehicle. If this technique is found feasible, the direction of entry, opposing or with the planet rotation, can be compensated for in the setting of the decelerator deployment sensor. This effect of entering with, or opposing the direction of planet rotation is significant since the aerodynamic velocity, which is the critical item, for a given inertial velocity is dependent on this parameter. Hence, the velocity increment which must be added to the entry vehicles inertial velocity at time of separation from the primary vehicle is dependent on both the acceleration of gravity term and the direction of entry into the planets atmosphere. It is believed that for steep entry angle cases this technique will be acceptable due to the high decelerations which will be experienced during entry and the direct addition of the intergal of the acceleration of gravity to the entry vehicles inertial velocity at separation. The magnitude of the errors associated with shallow entry analysis and variable atmospheric profiles are expected to be the most severe and will probably determine the feasibility of the system.

For the purposes of defining initial conditions for trajectory calculations for various entry angles and atmospheric profiles the computed inertial velocity of the entry vehicle obtained from trajectories supplied by JPL was utilized. The inertial velocity (2420 fps) relative to the center of the planet Mars obtained at a Mach number of 3 in G atmosphere for the ballistic trajectories provided by JPL was used as the first stage deployment condition. Using this inertial velocity the deployment Mach number for atmospheric profile H, 90 degree entry was 2.82. For atmosphere J, 90 degree entry the dynamic pressure at an inertial velocity of 2420 was above the design limit of 61 psf. As a result of this restriction the inertial velocity at deployment was reduced to a value of 2151 fps which was compatible with the design dynamic pressure limit. In an actual flight this reduction in inertial velocity would be accomplished by having in a series circuit the velocity sensor and "g switch" which would prohibit deployment until an acceptable dynamic pressure was encountered. The deployment Mach number for this condition was 2.8.

The first stage deployment Mach numbers for atmosphere G, entry angles of 51, 34 and 20 for an inertial velocity of 2420 fps were 2.76, 2.77 and 3.12 respectively. For all these conditions the free stream dynamic pressure was below the design limit. Only in atmosphere H, 20 degree entry angle, was the first stage deployment Mach number (2.4) significantly lower than that used as the design value (3.0). Therefore, it is noted that except for the atmosphere H, 20 degree entry, all trajectories had first stage deployment Mach numbers within 8 percent of the design deployment Mach number. This factor is significant in that, based on first stage deployment conditions and aerodynamic heating conditions, all the trajectories except for H, 20 degree entry may be considered

representative of either a Mach number or predicted velocity sensing scheme.

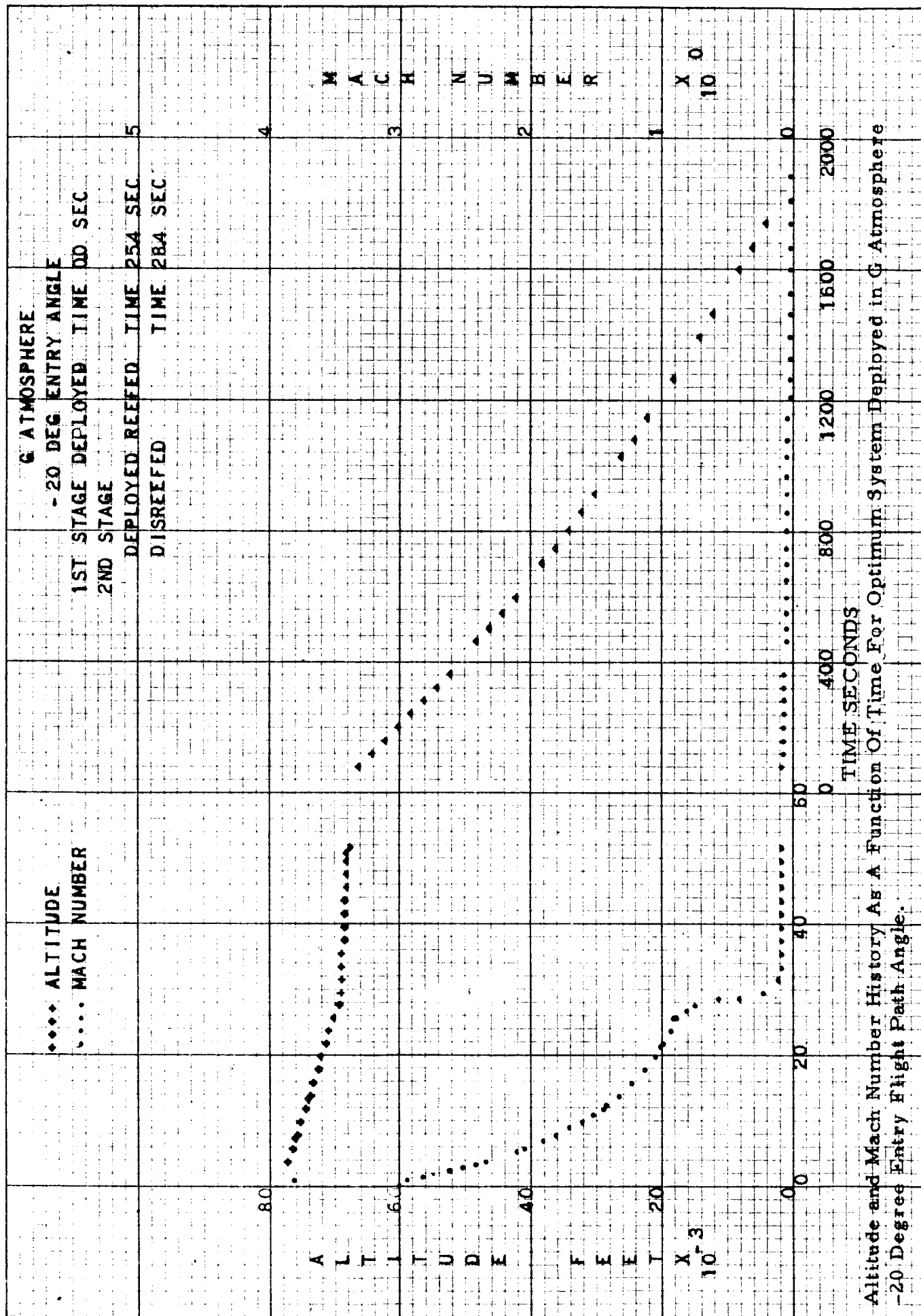
The computed inertial velocity based on trajectory computations used for the second stage deployment condition was 1045 fps. This velocity was obtained by using the value which was coincident with a Mach number of 0.9 on the 90 degree, G atmosphere trajectory. Using this velocity all second stage reefed deployment conditions were below 0.9 Mach number and a dynamic pressure of 7.5 psf. The disreef operation was performed on a 3 second time delay measured from the beginning of reefed inflation. Table V gives a listing of the pertinent sequencing events.

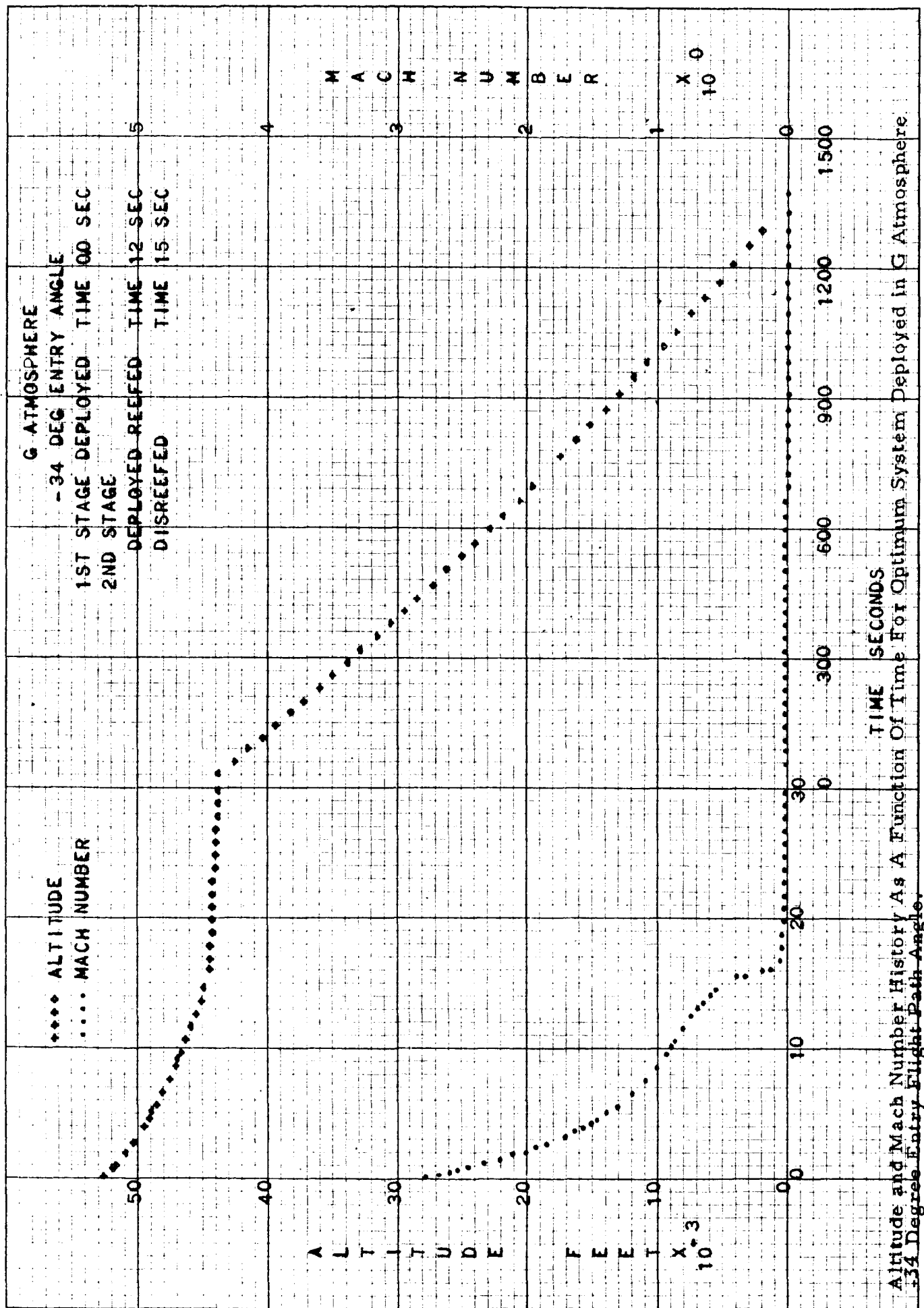
Figures 23 through 28 show the altitude and Mach number variation as a function of time from start of first stage inflation for all the decelerator trajectories calculated for G and J atmosphere profiles. Atmosphere H trajectories are not shown since they are very similar to those obtained for atmosphere G. On the graphs the times at which sequencing was performed are noted for reference purposes.

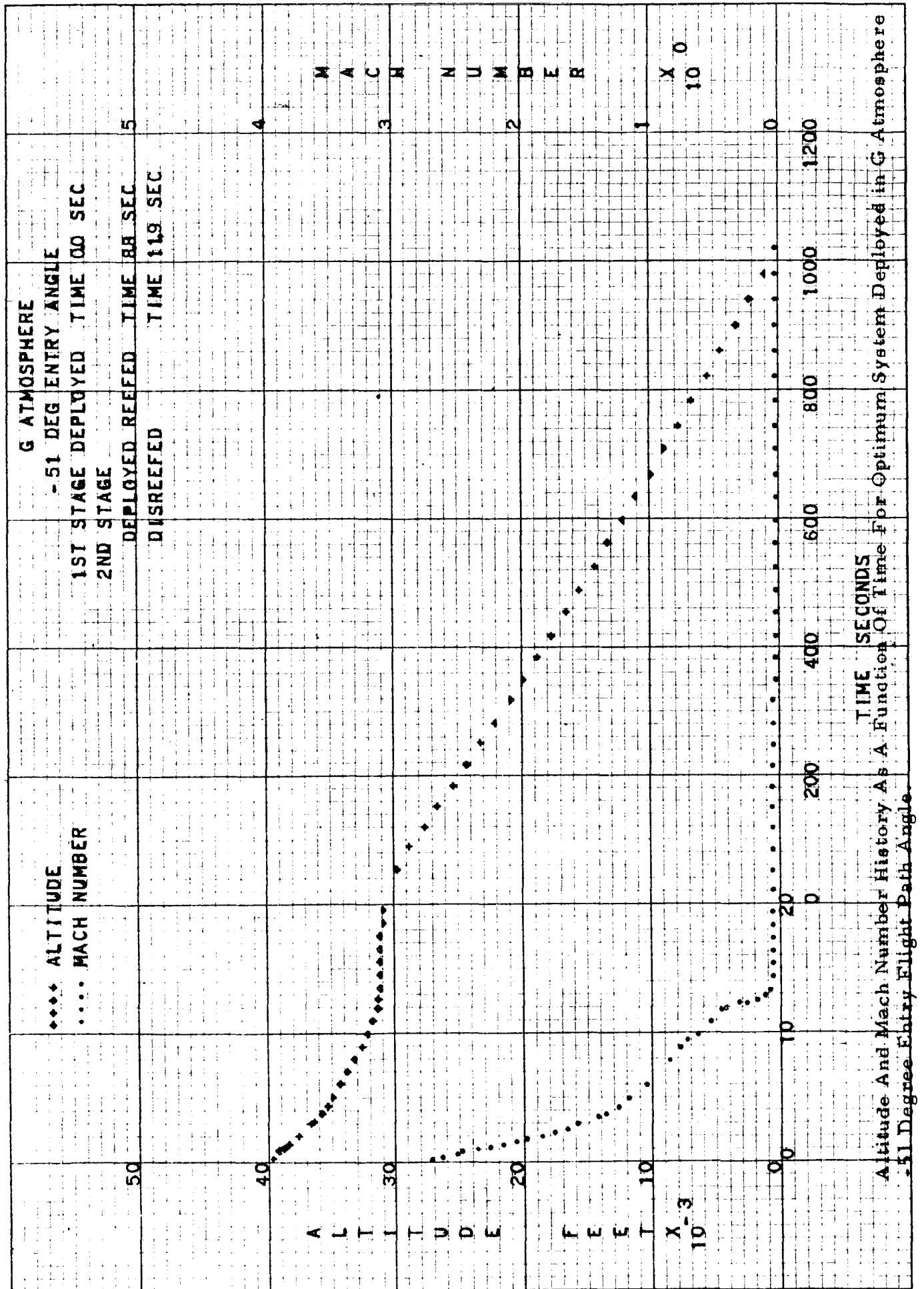
Decelerator temperature-time histories for entry angles of 90 and 51 degrees for G atmosphere are shown in Figures 20 and 29 respectively. The ratio of the instantaneous parachute drag load (DRI) to the full open drag load (DRO) after full inflation is also shown in these figures to enable a correlation between strength degradation due to temperature and reduction in parachute load with time. Due to the low peak temperatures (200°F) associated with these cases and the reduced peak load at peak temperature (80 percent) it is apparent that no problem exists for Nomex materials. Temperature histories for the 34 and 20 degree entry angle trajectories are not presented since at the time of deployment the radiation heat flux based on a 160 degree F. initial temperature was approximately the same or less than the convective heat flux. The peak temperature for the 34 degree entry angle trajectory was only 4 degrees higher than its initial deployment value and the 20 degree trajectory resulted in immediate cooling. The heating calculations for both the 20 and 90 degree entry angle trajectories for J atmosphere predicted immediate cooling also. The peak temperature for the H atmosphere profiles (20 and 90 degree entry angles) resulted in values which are very similar to the G, 51 degree entry trajectory and the G, 90 case respectively.

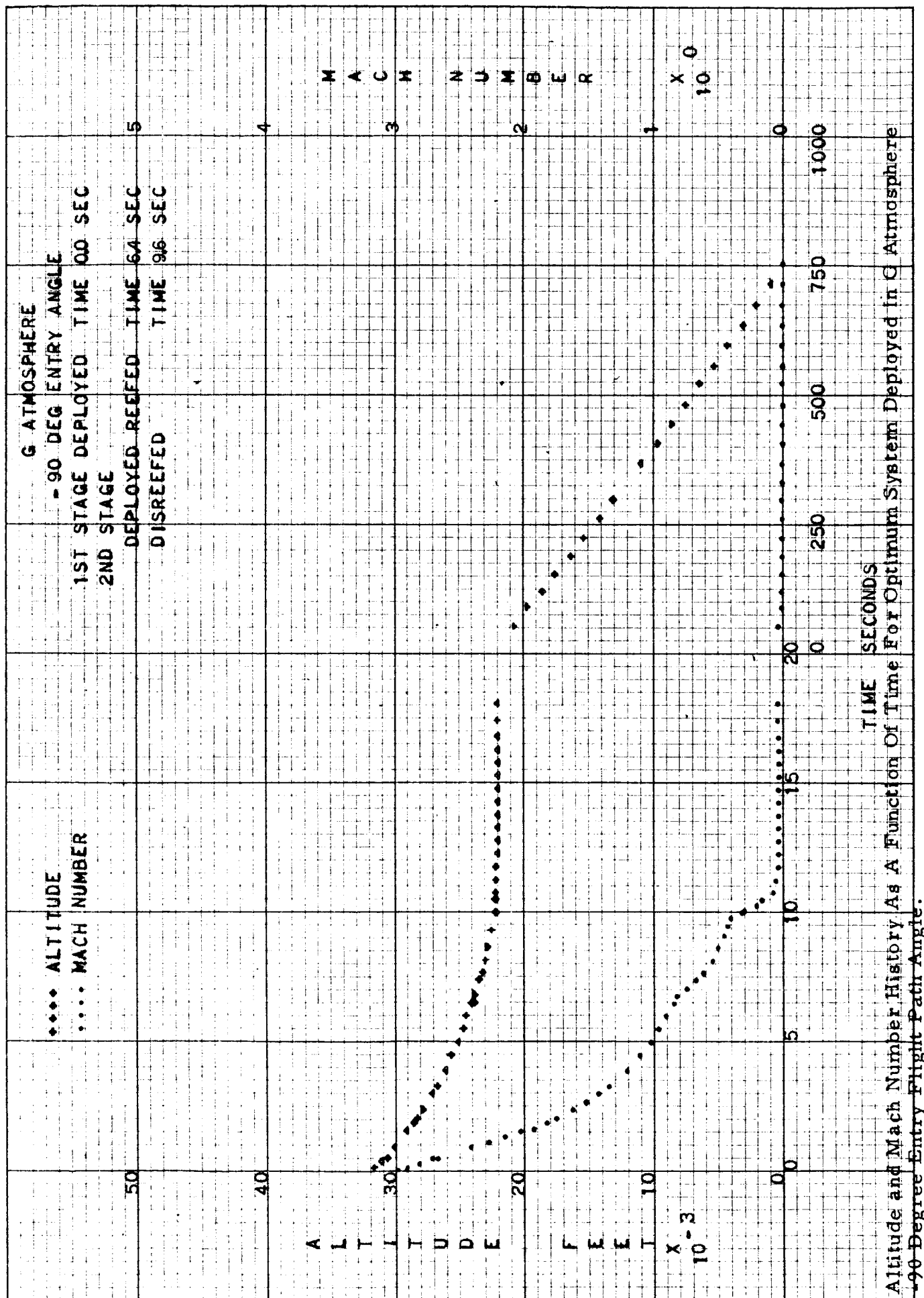
The parachute force-time histories for the G atmosphere 90 and 20 degree entry angle trajectories and the J atmosphere 90 degree entry angle trajectory are shown in Figures 30 through 32. These trajectories were selected since they depict the peak first stage parachute load, approximately the peak disreef load and the peak reefed load, respectively. These force histories also show the wide time variation as a function of entry angle.

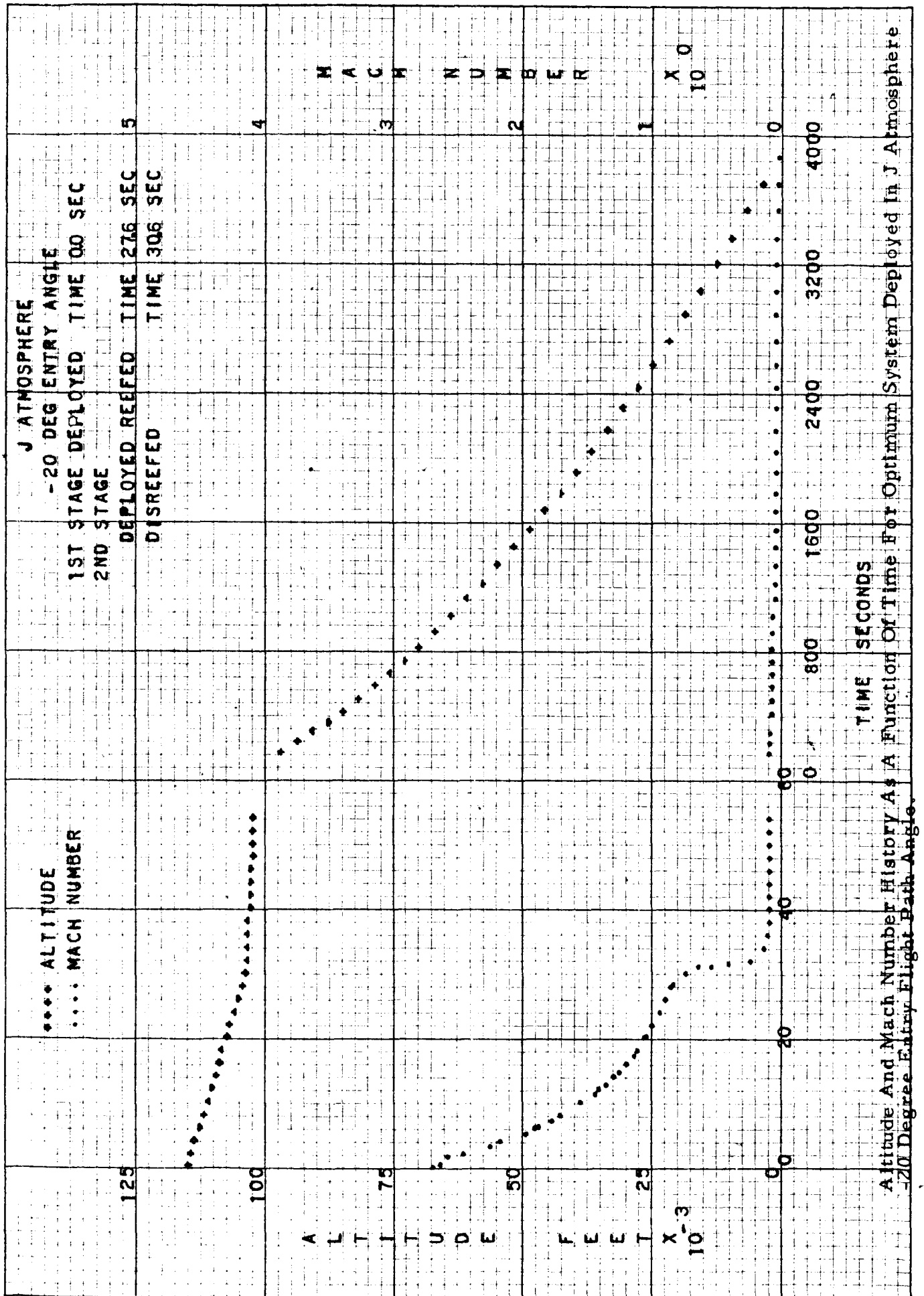
A comparison of the effects of second stage reefed deployment altitude and second stage descent time for atmospheres G, H and J as a function of entry angle

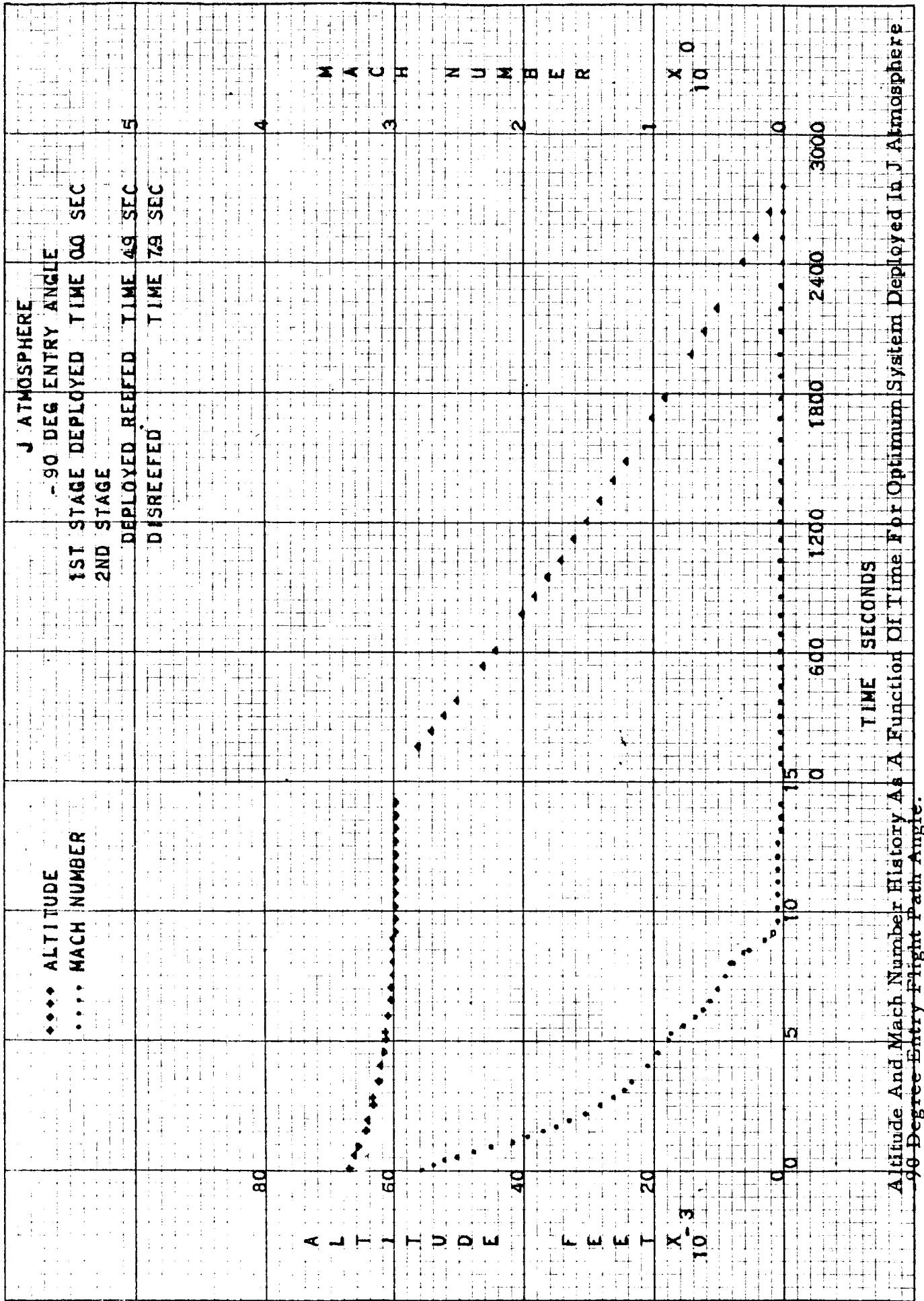




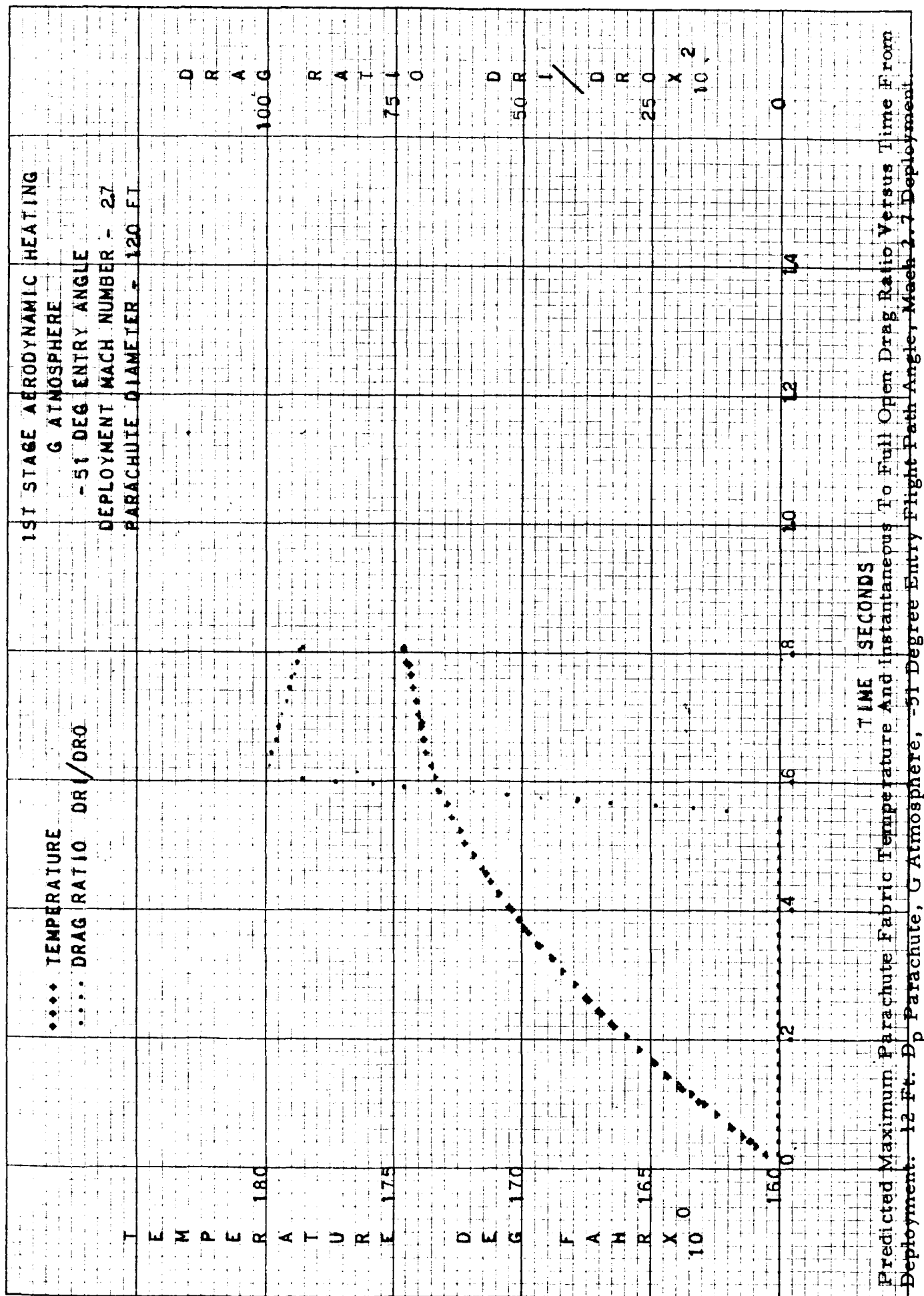


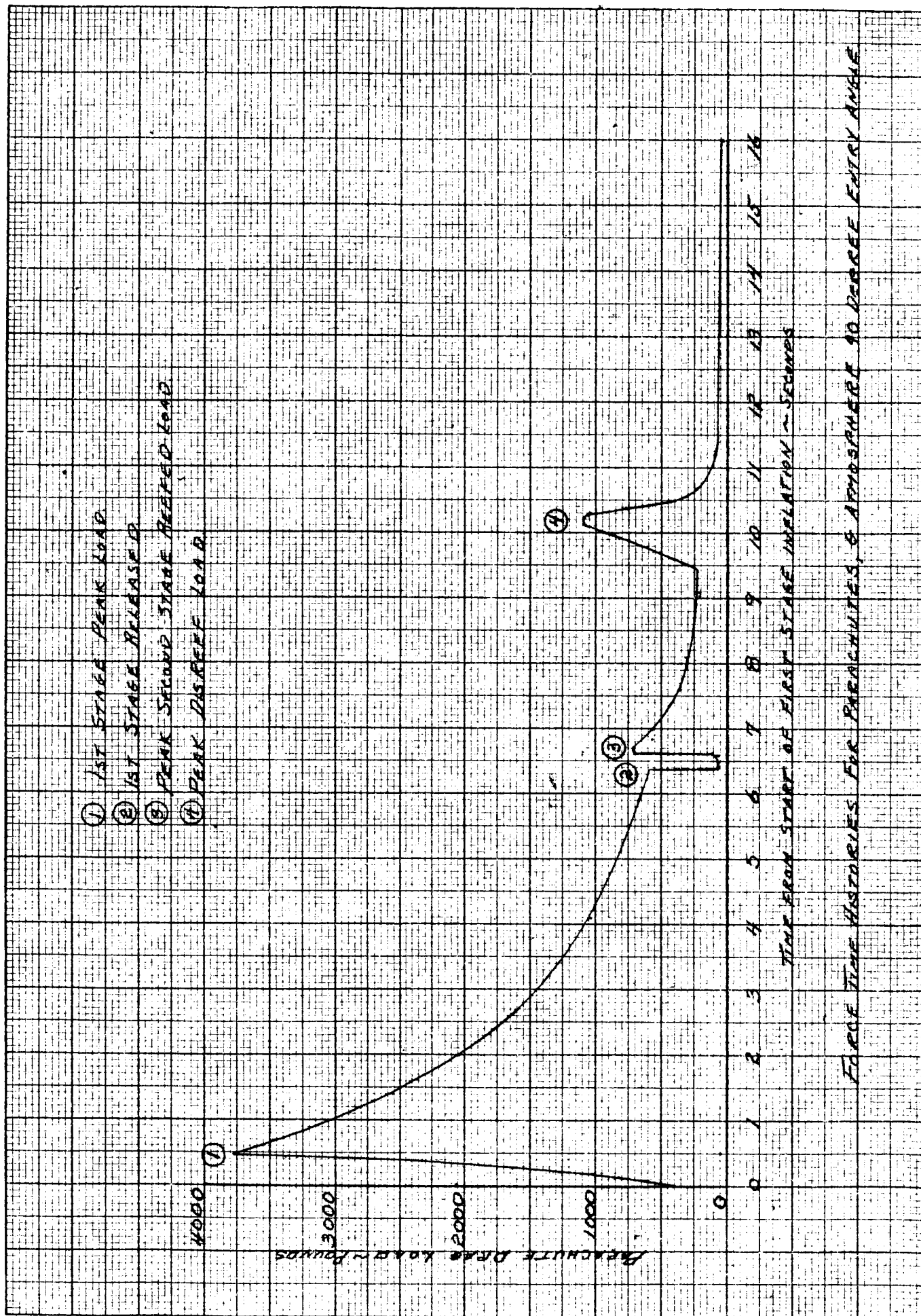




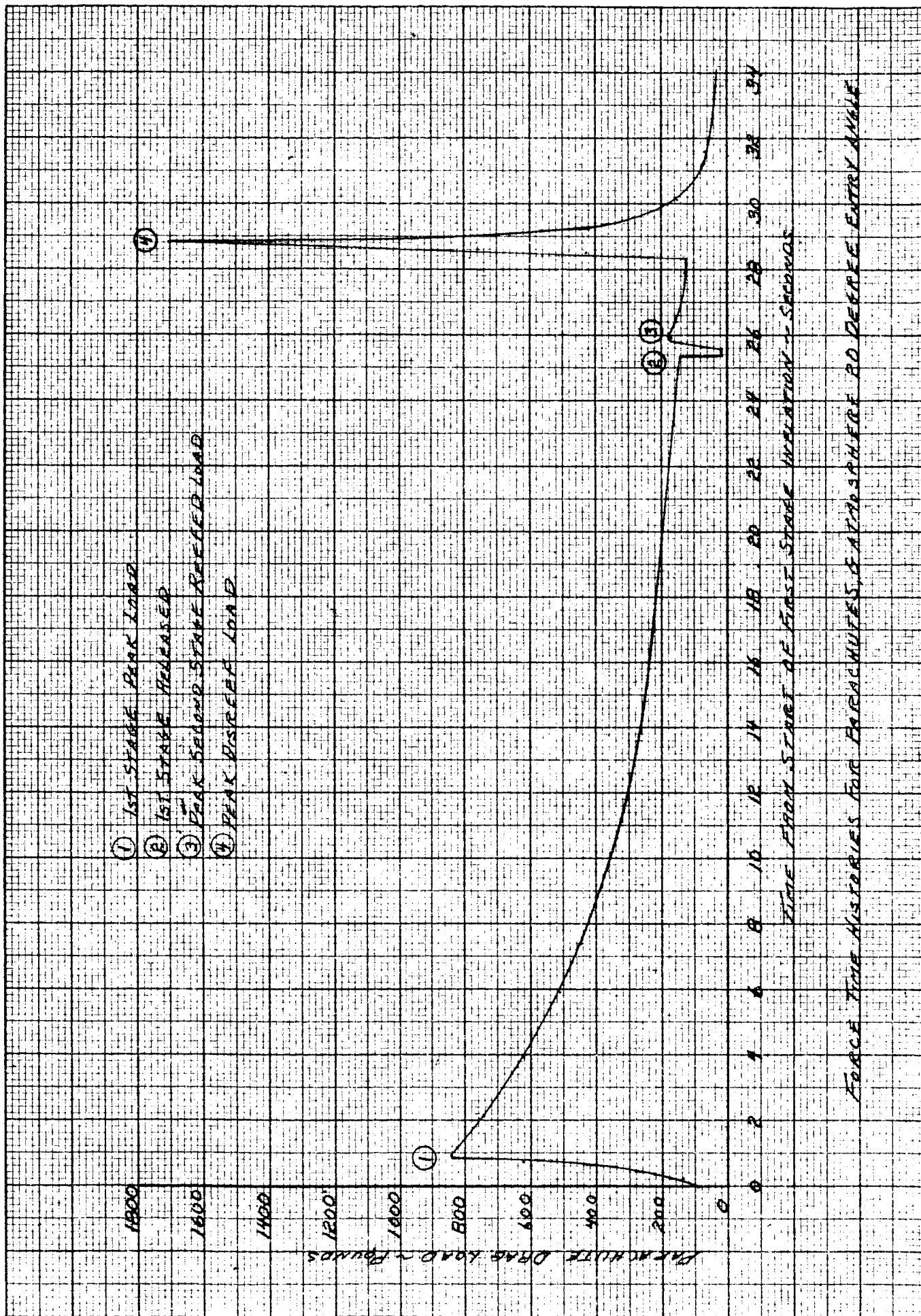


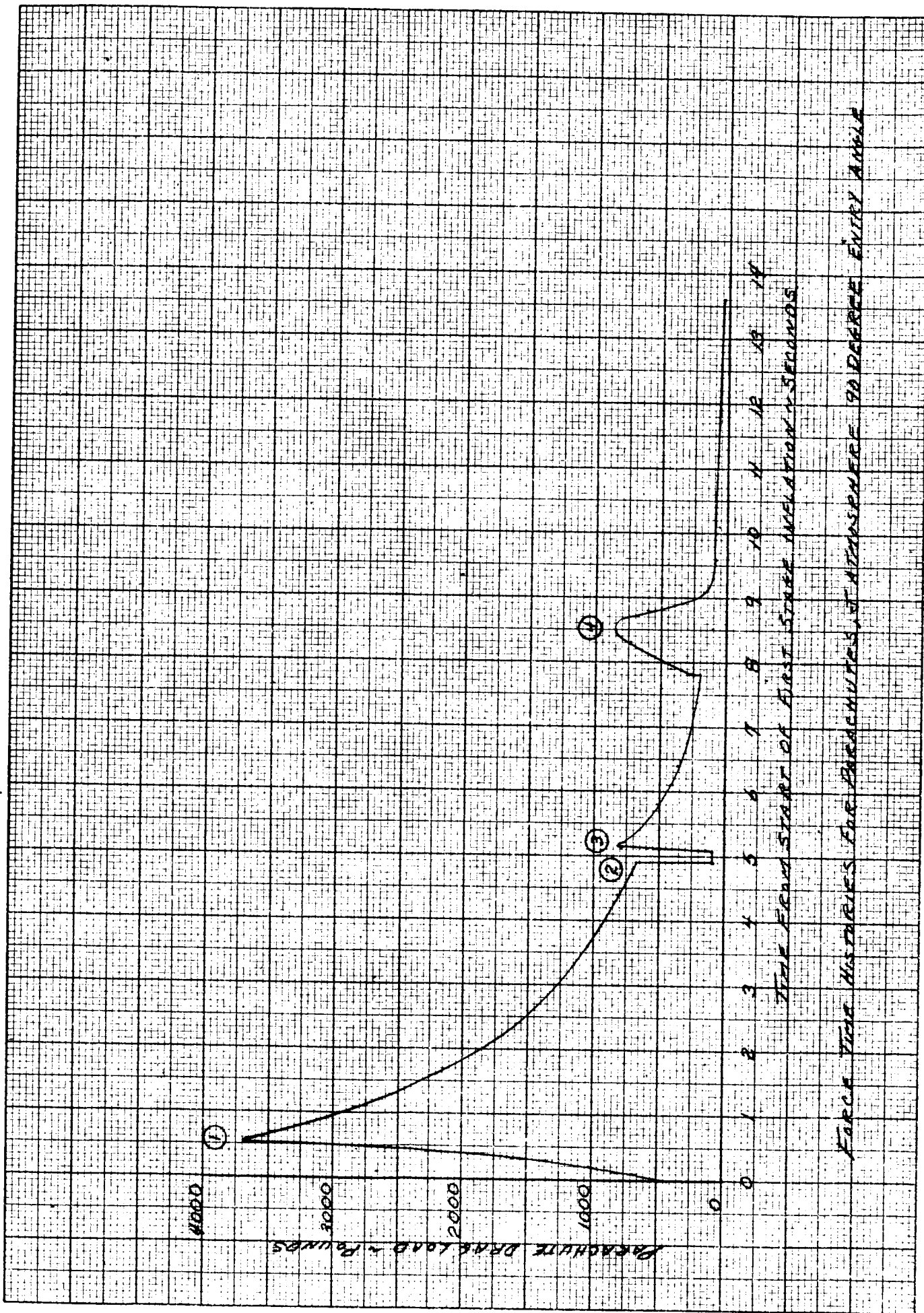
Altitude And Mach Number History As A Function Of Time For Optimum System Deployed In J Atmosphere
 90 Degree Entry Flight Path Angle.





FORCE TIME HISTORIES FOR PARACHUTES, 8 APPROXIMATE 90 DEGREE ENTRY ANGLE





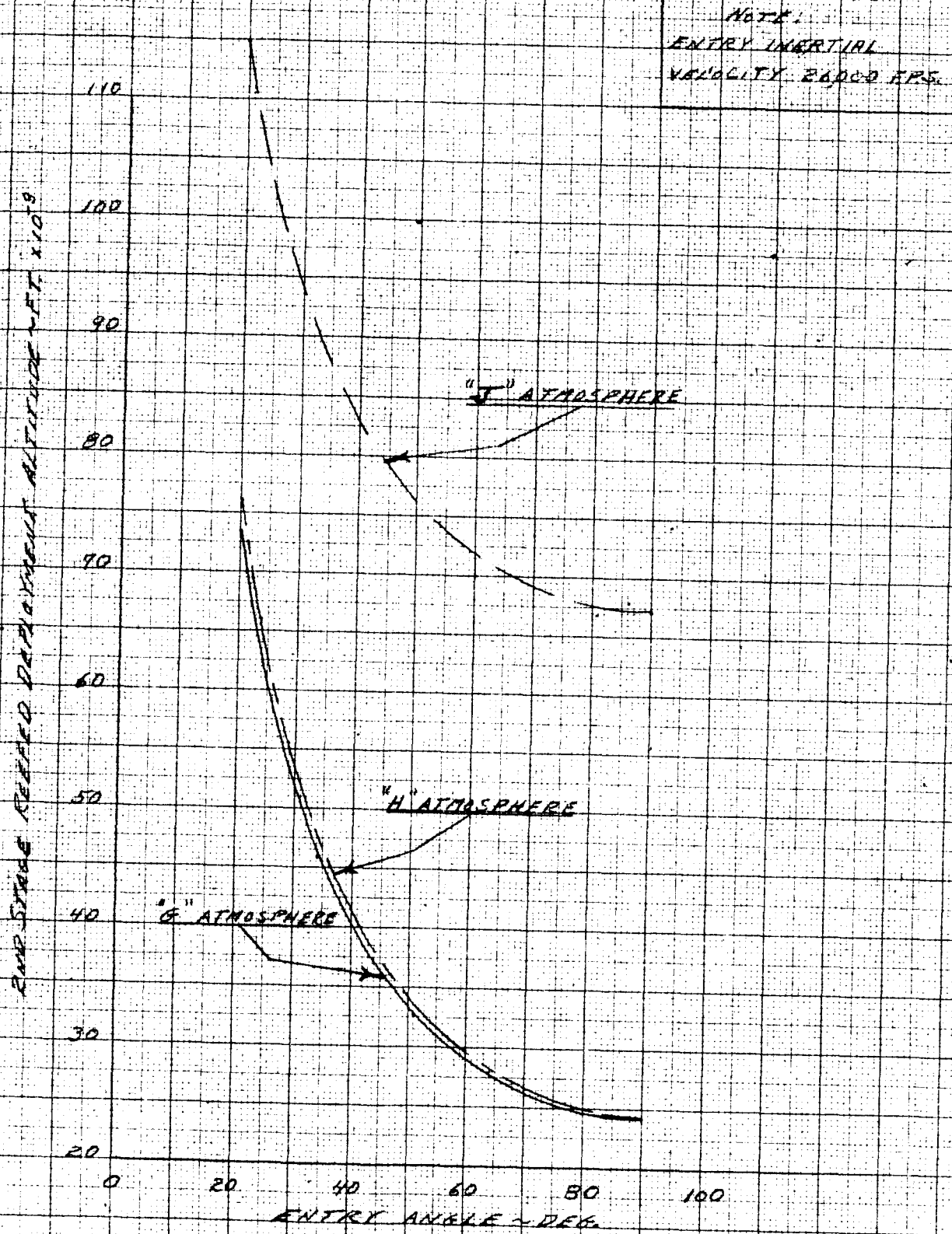
can be made from reference to the curves shown in Figures 33 and 34. In these figures the shape of the curve exhibited by the four known points in G atmosphere was used to fair between the known end points of H and J atmosphere (20 and 90 degree entry angles).

To determine the effect of entry velocity JPL computed ballistic trajectories for inertial entry velocities of 20,000, 23,000 and 30,000 feet per second at 800,000 feet. The atmosphere and entry angle used in these computations were G and 90 degrees respectively. Using initial deployment conditions taken from these trajectories the variation of second stage deployment altitude and the second stage descent time with entry velocity are shown in Figures 35 and 36 respectively. The variation in descent time was found to be linear with entry velocity and the effect of varying the entry velocity over the entire range results in a maximum variation of approximately 25 percent considering both variables. The sequencing procedure used for the trajectory computations was deployment of the first stage at a Mach number of 3 and reefed deployment at a Mach number of 0.9. The disreef operation was performed three seconds after the start of reefed inflation. The pertinent trajectory characteristics and parachute loads obtained from this analysis are shown in Table V.

The parachute loads resulting from the deployment sequencing procedure used are all within the prescribed safety factors dictated in Appendix II when the strength of the actual materials used are considered. The results of these analyses indicate that the concept of using either a Mach number sensing or predicted velocity technique coupled with a deceleration measuring device (that is, dynamic pressure indicator) for first stage deployment will limit the first stage loads to tolerable values if an accurate means of sensing these parameters can be obtained. The magnitude of tolerable errors has not been assessed since an error analysis of the sensing system must first be performed to determine practical limits. The sensing components required for the reefed second stage deployment are the same as for the first stage. Consequently, the feasibility of both the first and second stage reefed deployments are predicated on the accuracy of the velocity or Mach number sensing system used. The use of a 3 second time delay between the start of reefed inflation and the disreef operation proved to be satisfactory to control opening loads for all the trajectories calculated.

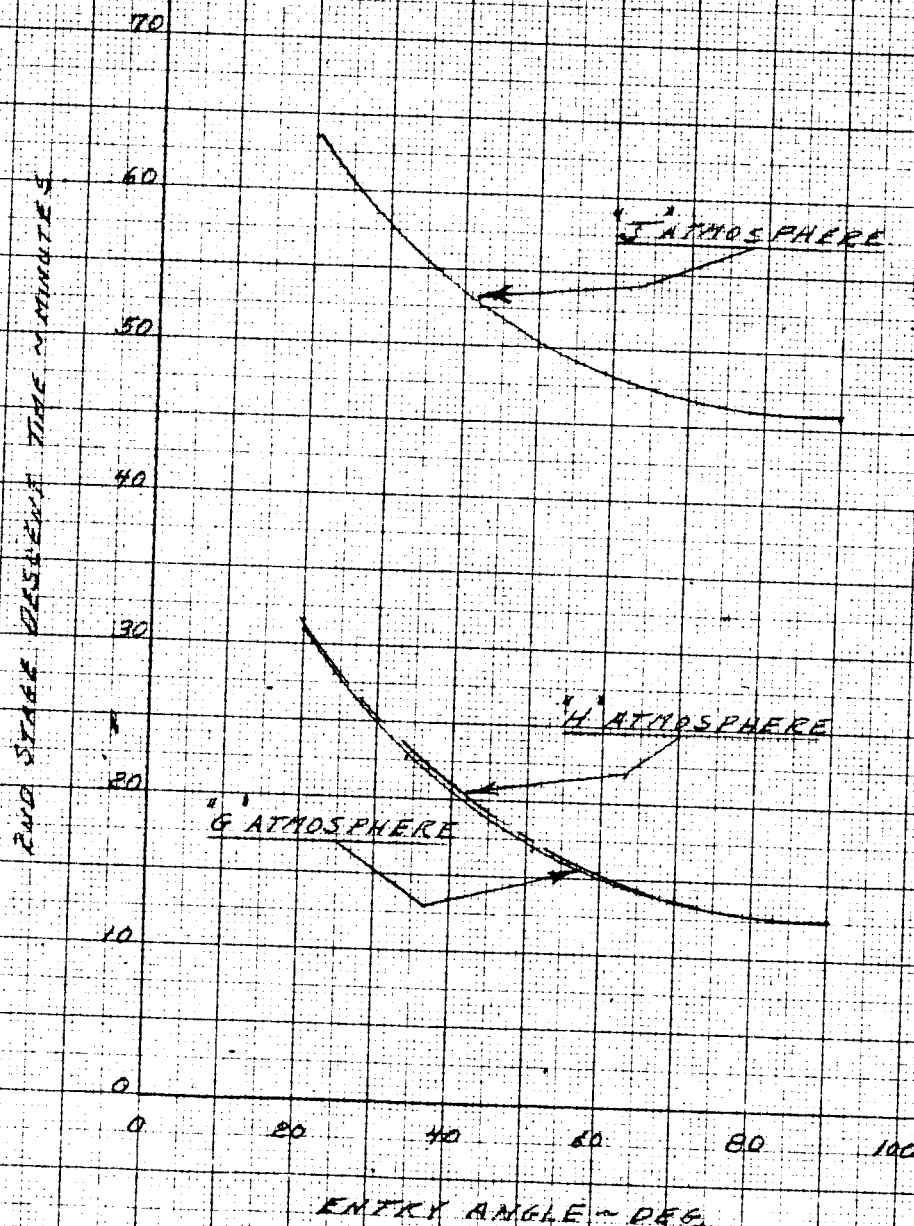
Due to the limited number of atmospheric profiles investigated, a preliminary study was conducted to determine the feasibility of scaling the results obtained to enable predictions for deployment conditions for other atmospheric profiles. To perform this investigation a study was made of the loss in altitude during the filling operation associated with each of the parachute staging operations. The values given in Table V were used for these calculations. It was found that for all the 90 degree entry trajectories considered, the altitude consumed during the first stage filling deviated from an average value of 1,040 feet by less than 6 percent.

10 TO THE
KE
-14
ALBANESE

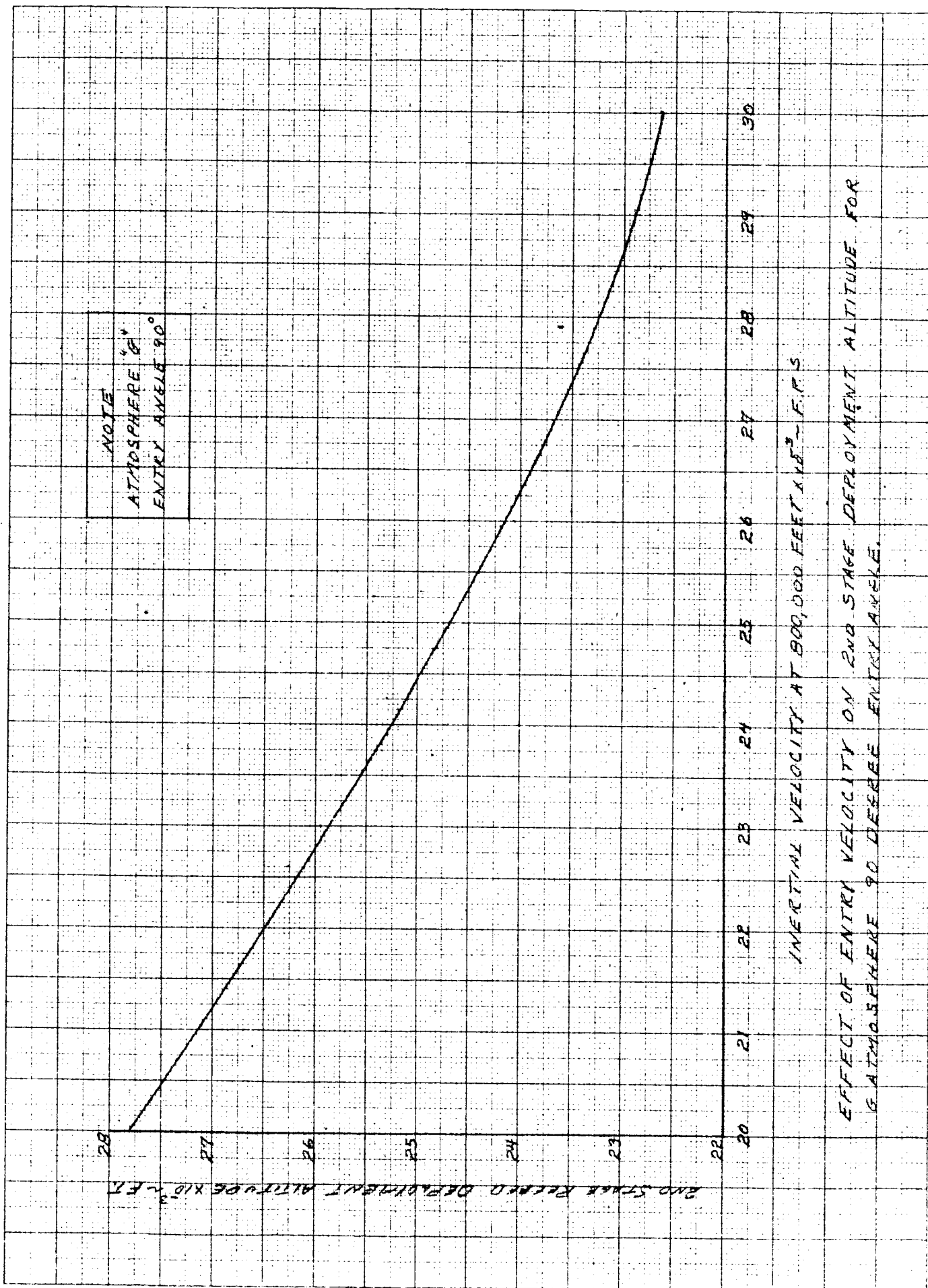


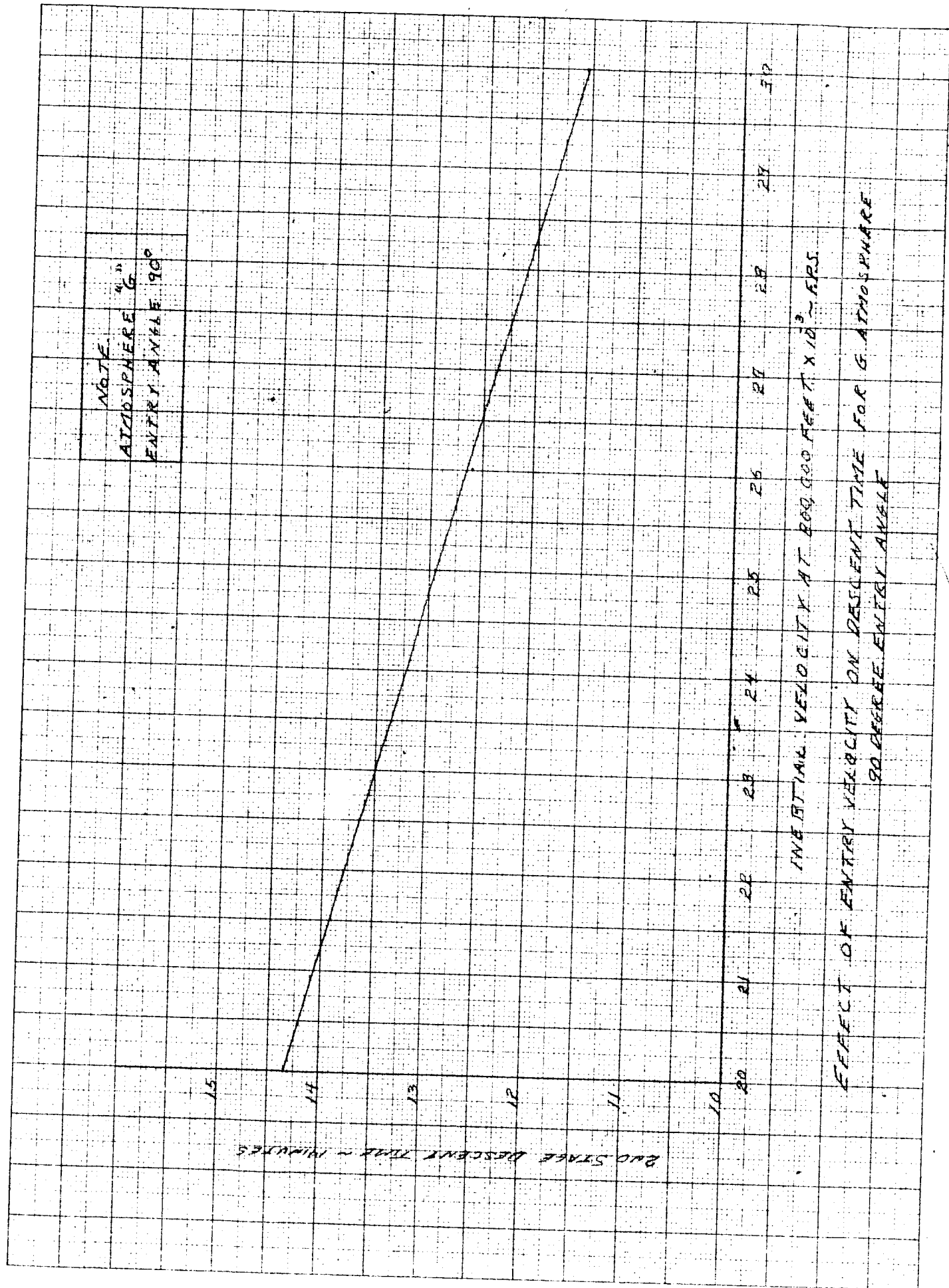
EFFECT OF ENTRY ANGLE ON 2ND STAGE
DEPLOYMENT ALTITUDE FOR THREE ATMOSPHERE
PROFILES.

NOTE:
ENTRY INERTIAL
VELOCITY 26,000 FPS



EFFECT OF ENTRY ANGLE ON 2ND STAGE DESCENT
TIME FOR THREE ATMOSPHERE PROFILES





Results of Computer Analysis For The Optimum Parachute System

(First Stage)

Inertial

Entry Angle and Atmospheric Profile	Inertial Entry Velocity at 800,000 feet (fps)	First Stage Deployment Altitude (Ft) and Mach No.	First Stage Filling Time (Seconds)	Altitude at Full Open (Feet)	Maximum Parachute Load (Pounds)	First Stage Maximum Fabric Temperature of
90° - G	26,000	31,830 2.96	0.47	30,800	3770	200
51° - G		39,960 2.74	0.54	39,050	2370	175
34° - G		52,860 2.77	0.72	52,130	1810	164
20° - G		79,240 3.11	0.95	78,780	840	160
90° - H		32,700 2.82	0.49	31,630	3570	208
20° - H		92,110 2.40	0.98	91,520	650	174
90° - J		67,110 2.79	0.54	66,090	3700	160
20° - J		114,900 2.70	0.99	114,360	880	160
90° - G	20,000	36,050 3.00	0.48	34,990	3510	200
90° - G	23,000	34,070 3.00	0.47	33,030	3690	201
90° - G	30,000	30,080 3.00	0.46	29,070	3850	202

TABLE V - Cont'd.

Results of Computer Analysis For the Optimum Parachute System (Second Stage)

Entry Angle and Atmospheric Profile	Second Stage Reefed Deployment Altitude (Ft) and Mach No.	Reefed Filling Time (Seconds)	Altitude at Full Reefed Inflation (Feet)	Maximum Load (Pounds)	Altitude (Ft) and Dynamic Pressure at Disreef (PSF)	Disreef Filling Time (Seconds)	Maximum Load (Pounds)	Altitude at Full Open (Feet)	Time from Second Stage Reefed Deployment To Impact (Minutes)	Impact Velocity (fps)
90° - G	24,060 0.85	0.24	23,900	700	22,510 1.64	0.70	1100	22,320	12.6	27
51° - G	32,600 0.78	0.27	32,470	460	31,410 1.48	0.65	1170	31,250	16.8	
34° - G	45,840 0.81	0.27	45,740	340	44,870 1.40	0.51	1510	44,750	22.6	
20° - G	70,340 0.90	0.28	70,250	180	69,450 1.05	0.40	1700	69,340	31.0	
90° - H	24,200 0.80	0.25	24,040	630	22,690 1.59	0.70	1080	22,500	12.6	
20° - H	76,010 0.76	0.26	75,900	150	74,850 1.00	0.35	1810	74,730	31.6	
90° - J	61,560 0.89	0.25	61,400	820	60,210 1.65	0.86	850	60,020	45.8	17.2
20° - J	104,080 0.83	0.27	103,980	180	103,110 1.06	0.38	1760	103,000	63.5	
90° - G	27,730 0.90	0.24	27,570	690	26,120 1.69	0.64	1230	25,930	14.3	27
90° - G	25,940 0.90	0.24	25,740	690	24,361 1.66	0.65	1180	24,180	13.5	
90° - G	22,630 0.90	0.24	22,470	750	21,080 1.64	0.71	1080	20,890	11.8	

For the 20 degree entry values the maximum deviation from the average value (530 feet) was approximately 13 percent. The values of 910 feet and 730 feet obtained in G atmosphere for entry angles of 51 and 34 degrees respectively appear to indicate a smooth trend of altitude loss with entry angle. Considering the loss in altitude with the reefed inflation for the 90 and 20 degree entry trajectories shows that values of 160 and 100 feet respectively are quite representative. For the single trajectories computed for entry angles of 51 and 34 degrees, values of 130 and 100 feet were obtained. The altitude loss during the disreef operation is extremely consistent as a function of entry angle and values of 190, 160, 120 and 110 feet were obtained for entry angles of 90, 51, 34 and 20 degrees irrespective of the deployment dynamic pressure or atmosphere considered.

The above trends indicate that reasonable estimates can be made of the loss in altitude for the filling time for the individual parachutes; however, when comparing the loss in altitude over the entire sequencing of the parachute system variations of the order of 60 percent occur for the 20 degree entry angle cases. A comparison of the total loss in altitude during the entire sequencing operation and that lost during the filling time indicates the filling time operation consumes less than 15 percent of the total altitude loss. A study of the results given in Table V shows that the major altitude loss during the sequencing operation occurs during the time between first stage fully open and second stage deployment. For correlation purposes it has been assumed that the loss in altitude is proportional to the density at the altitude of first stage deployment, since for the computations performed the aerodynamic velocity at first stage deployment is not radically different for the atmospheres considered for a given entry angle. Based on these assumptions, which are subject to further investigation, the following equation was used to correlate the loss in altitude during the sequencing operation.

$$\Delta h = \frac{(\text{Altitude loss in G atmosphere } \rho_2 \text{ for a given entry angle})}{\rho_1}$$

where ρ_2 is the first stage deployment atmospheric density for a given entry angle atmosphere and ρ_1 is the atmospheric density of G atmosphere for the same entry angle.

The accuracy obtained using the above procedure for the trajectories computed is given below.

ATMOSPHERE AND ENTRY ANGLE	COMPUTED LOSS IN ALTITUDE (TABLE V)	PREDICTED LOSS IN ALTITUDE	PERCENT ERROR
90-J	7,900	7,170	1.1
90-H	10,200	10,500	2.9
20-J	11,900	12,700	6.7
20-H	17,380	16,300	6.2

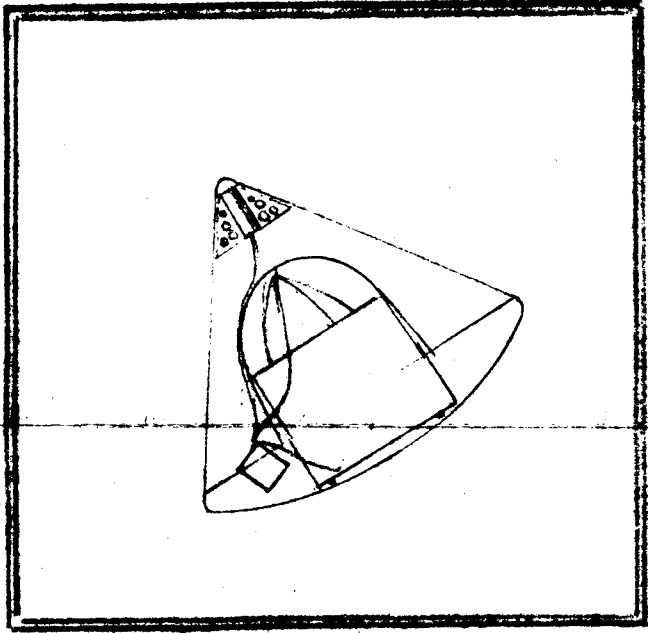
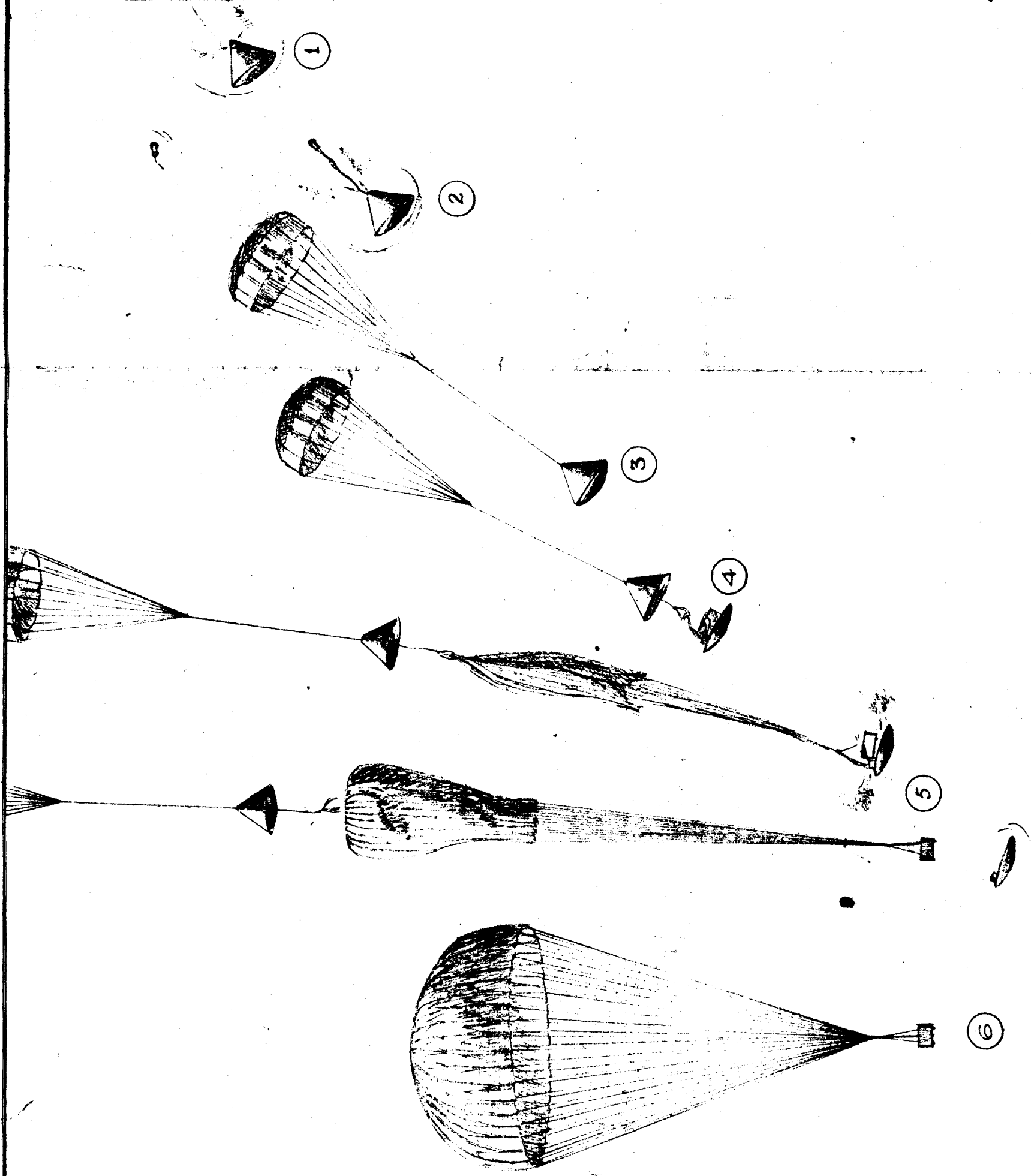
For the above calculations the first stage deployment altitude was known based on the trajectory calculations performed. To determine the deployment altitude for other atmospheres either trajectory computations must be performed or the method of Allen and Eggers (Reference 19) can be used to define the altitude where the vehicle will attain the design dynamic pressure of 61 psf. It is noted that when using the Allen and Eggers method the first stage deployment Mach number must be determined to assure that it is below 3.0 at the design dynamic pressure. In cases where the Mach number is above 3.0 a trial-and-error procedure must be performed to determine the deployment altitude that will satisfy both the Mach number and dynamic pressure requirement ($M \leq 3.0$, $q \leq 61$ psf). The performance of these analyses are recommended to assure that deployment conditions in other atmospheres will not violate any parachute design conditions.

D. System Sequencing and Weight Breakdown for the Decelerator System

The system deployment sequencing proposed for this program is based on using principles which have been shown to provide the highest degree of reliability in recovery operations. The sequencing is comprised of 6 operations which are given below and shown pictorially in Figure 37.

1. Release of rear cover over first stage mortar.
2. Mortar the first stage and rear cover to 6 vehicle diameters behind the entry vehicle.
3. Decelerate the entry vehicle to below 0.9 Mach number and a dynamic pressure less than 7.5 psf.
4. Release the aft heat shield and extract, by means of the first stage parachute, the heat shield and second stage parachute in the reefed state. At line stretch of the reefed parachute the front heat shield is separated from the payload.
5. Decelerate the payload by means of a reefed 59.3 foot fully extended skirt parachute.
6. Disreef the second stage parachute after 3 seconds of reefed inflation time and decelerate the payload to its impact velocity.

The suggested means by which each of the above operations would be performed are as follows. The release of the rear cover would be most efficiently and reliably performed by a dual ring of flexible linear shaped charge (FLSC) which would be ignited by separate circuits. This redundancy in circuits coupled with dual charges affords the highest degree of assurance of separation. Explosive bolts while possessing a high degree of reliability when combined with dual



SYSTEM SEQUENCING

1. Release of cover over mortar
2. Mortar first stage parachute plus rear cover
3. First stage deceleration
4. Release aft heat shield and extract second stage parachute
5. Release payload and inflation of reefed second stage
6. Full inflation of second stage parachute

electrical circuits, do not afford the advantage of allowing the complete sealing off of the compartment from the hot gases associated with entry. Another disadvantage is that in the event of one bolt failure no redundancy in separation can be achieved.

The mortaring of the rear cover and first stage 12 foot projected diameter Hyperflo back to a distance of 6 calibers will be performed by a controlled burning pyrotechnic gas generator as opposed to using a standard granular power charge. The system proposed is comprised of an aluminum tube measuring 17.4 inches in length and 7.7 inches in diameter. The energy level which will eject the parachute to a minimum velocity of 182 feet per second is 6300 foot pounds. Feasibility tests have been performed with a gas generator of this type having approximately this energy level, and a pack weight of 50 pounds (Section IIIB). However, the ejection velocity obtained in these tests was one-half that needed for this program. The advantage afforded by this system is the low average-to-peak pressure ratios which has been demonstrated (2.1). In the calculations performed for this mortar an average-to-peak value of 3 was assumed. The computed peak pressure based on this ratio was 330 pounds per square inch. This pressure produces a peak load of 15,500 pounds. It is proposed that the ignitor system for the gas generator be a dual electrical circuit with a single detonator with dual bridge wires.

The proposed scheme for the release of the aft heat shield is the same as that recommended for the mortar cover. The same fundamental requirements exist for both functions and therefore require the same method of approach. The extraction of the main parachute would be performed by a Nomex line extending from the bottom of the mortar and attached to the top of the second stage deployment bag. Computations based on the maximum dynamic pressure (7.5 psf) at time of deployment indicate that the maximum snatch force attainable by this scheme of deployment is 2,200 pounds. This force level is 50 percent of the total rated line strength. The time required for this extraction process has been calculated to be 0.6 seconds or a loss in altitude of approximately 300 feet for the 90 degree trajectories. The separation of the heat shield from the payload would be initiated by a pin pulled by a lanyard connected to the main parachute suspension lines. The force required to extract the pin would be based on minimum snatch force levels and thereby would prevent separation of the heat shield until sufficient force were exerted on the payload to stabilize it. The proposed means by which the payload is separated from the heat shield is again by the use of shaped charge explosives due to their ability to provide a redundant capability. Use of this type of charge also reduces the number of types of pyrotechnic items needed to be qualified for the sterilization and vacuum environment.

The disreef operation will be performed by two lanyard-activated 3 second time delay reefing cutters capable of cutting 100 pound dacron cord. This method of initiating the time delays for the reefing cutters is standard and has been shown to be reliable on hundreds of cargo deliveries.

The physical design descriptions of the first and second stage parachutes selected for this system are given in Table VI.

The estimated weight of the decelerator system is given below. Factors which could not be assessed in the assigning of weights to these components are the effects of the sterilization environment on items such as pyrotechnic charges and electrical components. The unknowns associated with the type of sensing system also preclude accurate weight estimates. For the calculation of the weight of the shaped charge explosives TACOT has been assumed as the type of explosive charge used. RDX and PETN, while possessing a lower weight core load for a given required cutting thickness, do not appear capable of sustaining the high temperature 36 hour exposure associated with sterilization. This information obtained from DuPont literature is approximate due to the many variables which affect the thermostability of explosives. Further investigation must be performed prior to the final selection of the explosive charge to be used.

The estimated weight breakdown for the decelerator system is:

First Stage Parachute	12.3 lbs.
Deployment Bag	0.4 lbs.
First Stage Mortar Tube Plus Charge	3.2 lbs.
Second Stage Parachute	22.6 lbs.
Skirt and Sleeve Bags	1.5 lbs.
Structure and Explosive Weight	9.0 lbs.
Sensing System	<u>5.0 lbs.</u>
	54.0 lbs.

The volume requirements for the proposed recovery system are mainly determined by the packing densities of the first and second stage parachutes.

Table VI

Parachute Design Characteristics

1st Stage Parachute

12 Foot Projected Diameter. Hyperflo

	Design Values	Material Used	Factor over Design Value	Max. Load From Traj.	Max. Temp. From Traj.	Strength Degradation Percent	Weight of Components Lbs.
Opening Load	6300			(1) 3700			
Roof Material	18 Lbs.	Nomex 3/8" Ribbon 60 Lbs.	3.3				2.8
Cone Inlet Material	28 Lbs./in.	Nomex Cloth 150 Lbs./in.	5.4		(2) 208	7	3.6
Lines	16 gores 590 Lbs.	Nomex 750 Lbs. Cord	1.3				2.4
Riser	4 - 2400 Lb. Lines 23' Long	Nomex 2" Wide 3000 Lbs. Ribbons	1.3				2.1
Radial Reinforcement	295 Lbs.	Nomex 1" Wide 300 Lb. Tape	1.0				.9

- (1) Obtained in Atmosphere G, 90 Degree Entry
(2) Critical Material - Lowest Weight Per Square Foot

Roof Material: Low Twist Pattern 689 Weave Pattern MIL-T-5608 Class C Type II
Cone Inlet: Stern and Stern Pattern HT-5-35
Line: 750 Lb. Cord Weave Pattern MIL-C-7515B Type III Valrayco Pattern 8796
Riser: 2 x 3000 Lb. Weave Pattern MIL-T-5608E Class E Type V
Radial Reinforcement: 1" x 300 Lb. Weave Pattern MIL-T-6134B Type II

2nd Stage Parachute

59.3 Nominal Diameter 14.3 Percent Fully Extended Skirt

	Design Values		Materials Used	Factor over Design Value	Max. Load From Traj.		Weight of Components Lbs.
	Reefer	Disreef			Reefer	Disreef	
Opening Loads	1240	2480			(1) 820	(2) 1810	
Canopy Material	17 Lbs./in.		Dacron Cloth 30 Lbs./in.	1.8			18.6
Line Material	44 gores 56 Lbs.		Dacron 100 Lb. Cord	1.8			3.6

- (1) Obtained in Atmosphere J, 90 Degree Entry
(2) Obtained in Atmosphere H, 20 Degree Entry

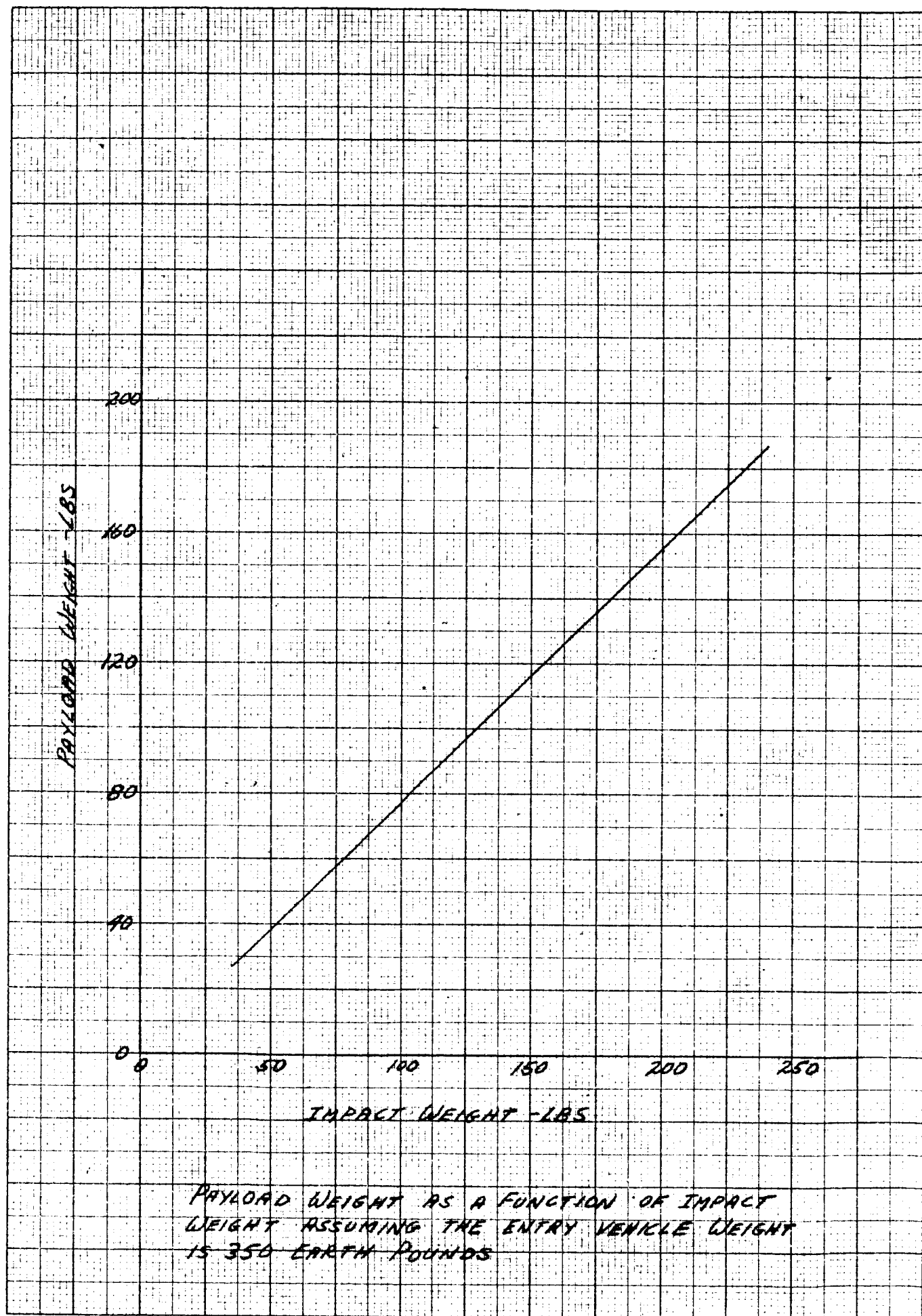
Canopy: Dacron Cloth Stern and Stern Pattern 15, 285
Line: Dacron Cord Spec. MIL-C-5040B Type 1A Valrayco Pattern 7528

For this system a packing density of 30 pounds per cubic foot is recommended since (1) volume requirements do not appear to be critical for the vehicle configuration chosen (2) packing densities of over 30 pounds per cubic foot may cause damage to reefing cutters and (3) deployment bag weights can be minimized. Further justification for the use of the low packing density is the fact that the stored volume (1.23 cubic feet) can be reduced only by approximately 7 percent if a packing density of 40 pounds per cubic foot (near maximum) is used for the first stage. The volume occupied by electrical equipment in the sensing system is expected to be less than 10 percent of the stored volume.

Due to the preliminary nature of the vehicle design at this time, consideration has been given to the effect on the deceleration system weight if the impact weight varies from its nominal value of 100 pounds. To determine the deceleration system weight various second stage parachutes were sized to provide the same ratio of second stage drag area to impact weight as used on the nominal case since it was desired to keep the impact velocity a constant. The parachutes sized for various impact weights maintaining the same ballistic coefficient ($\frac{W}{C_{DA}}$) or terminal dynamic pressure are listed below.

<u>Impact Weight, Lbs.</u>	<u>Second Stage Parachute D₀, Feet</u>
35	35.1
50	41.9
75	51.2
100	59.3
125	66.2
150	72.6
175	78.3
200	83.8
225	89.0
240	92.0

Figure 38 shows the variation in payload weight (impact weight minus the second stage parachute weight) with impact weight. These results show that for this range of impact weights the terminal parachute weight remains a constant percentage of the impact weight (23 percent). This constant percentage results from the fact that the materials which comprise the major percentage of the parachute weight were acceptable for the largest parachute and were the minimum acceptable for parachute fabrication and functional considerations. One factor which influenced the minimum cloth strength is the geometric porosity of the cloth. The particular cloth being used for this study is a 0.9 ounce per square yard dacron material with a geometric porosity of 6 percent. Reducing the strength of this cloth (and hence weight) will increase the cloth porosity to a range where opening characteristics may be impaired. Due to the possibility of impairing the opening characteristics of the parachute, it is not recommended that a lighter material be used for the low impact weights.



Based on the above results the variation of deceleration system weight with impact weight for the range considered can be approximated by the following equation:

$$W = 30 + 0.24 (\text{impact weight}). \quad (\text{in pounds})$$

E. Description of Development Testing and Cost Estimates for Designing and Testing the Decelerator System

The development program which is required prior to performing system tests of the proposed decelerator system is significant. To minimize the cost of the total development program it is mandatory that component testing be performed prior to launching into a full scale system program. Components which must be developed and tests which are required are as follows:

1. Sensing system.
2. Long time vacuum tests to define accurately the rate of degradation with time of Nomex and Dacron materials.
3. Mortar system design.
4. Hyperflo parachute tests behind the entry vehicle shape.
5. Accurate definition of the effect of sterilization and vacuum environment on pyrotechnic charges.
6. Determination of the capability of the proposed second stage parachute to function at the extremely low densities which are expected.

1. Sensing System

As a result of the study performed, the sensing system by far appears to be the most nebulous item listed above. Prior to performing any test program with this item, an error analysis must be conducted to enable the definitions of a satisfactory system. Due to the uncertainties associated with this item, no attempt has been made to define a cost estimate for a testing program.

2. Effects of Sterilization and Long Time Vacuum on Materials

Work has begun on item 2 (Reference 13), however, the results obtained to date do not define accurately the effect of a long duration (6 or 7 months) vacuum environment. Further tests are required to define better the slope of strength degradation with time to enable the selection of proper parachute materials. This vacuum and sterilization program is considered the second most important item for work since without this information it is impossible to define any of the following components.

3. Mortar System Design

The mortar system design listed in item 3 is dependent on the results obtained in items 1 and 2 discussed above and is also influenced by items 4 and 5. This interdependency on the results of other tests hampers the mortar design. Without a knowledge of the limiting errors in the sensing system, the vehicle deceleration range at the time of deployment cannot be assessed; the weight of first stage parachute (to which the energy requirement is proportional) is dependent on the material tests of item 2. Items 4 and 5 influence the size, and thereby the mass ejected, of the parachute and the design of the propellant charge respectively. The theoretical design of the mortar system will depend on the effects of the sterilization tests of the pyrotechnics. However, after a satisfactory propellant type is defined preliminary mortar tests can commence to demonstrate a range in ejection velocities even though uncertainties in the other parameters still exist. It is recommended, therefore, that the tests performed in item 2 also pursue the pyrotechnic problem. The data required for preliminary design of the mortar are the influence of velocity on the peak-to-average pressure ratio. The structure required to hold the mortar at the top of the aft heat shield is dependent on this information.

4. Hyperflo Parachute Tests

Wind tunnel tests of the Hyperflo behind the entry vehicle shape (item 4) are required to assess the performance and stability of this parachute behind a blunt forebody. This information is necessary to determine the actual length of the riser required to obtain satisfactory performance. Potential problems of induced instability due to deploying the parachute behind an oscillating forebody or behind a body with low dynamic stability should also be investigated in the wind tunnel.

Preliminary tests to ascertain the above information should be performed at either the Langley Research Center or Tunnel A at AEDC. In these tests preliminary design parameters should be determined. For validation, a larger scaled model should be tested in the 16 x 16 foot supersonic tunnel at AEDC. This test sequence is considered advisable due to inherent problems of scaling (geometry, weight and stiffness) of a flexible aerodynamic decelerator to a scale compatible with either the Langley or Tunnel A facility. The Hyperflo has been tested in the Cree (supersonic parachute test vehicle) program at both the appropriate density altitude and deployment dynamic pressure which is to be experienced in this program. Therefore, it is felt that if the wind tunnel tests prove successful, free flight testing of the first stage parachute can be limited to system tests described later.

5. Effects of Sterilization and Long Time Vacuum on Pyrotechnic Charges

Item 5 covers the testing of the shaped charges, reefing cutters, and propellents for use in the gas generator. These tests must prove sufficient data

to be able to predict accurately the effects of a 6 to 7 month vacuum environment after being subjected to the sterilization environment. This information should be obtained concurrently, if possible, depending upon test chamber size limitations, with the material tests performed under item 2. Tests performed in Reference 13 indicate that simultaneous testing of both pyrotechnics and material fabrics is feasible.

6. Second Stage Parachute Testing

The testing of the second stage parachute at the low atmospheric densities which are to be encountered in this program (item 6) poses a serious problem. Two types of information are required. The first and most consequential to a non-survival type of payload is the determination of the opening characteristics of the parachute. Data on high altitude testing of parachutes without inflation aids are meager. Data reported in Reference 12 indicate peculiar drag area variations as a function of descent altitude. This limited experience with high altitude operation demands the testing of the second stage parachute at atmospheric densities and dynamic pressures compatible with that to be encountered prior to system tests. For these tests filling time and opening shock data are required. To obtain this information the mass of the system is the critical item as opposed to the system weight. This scaling of mass is beneficial in that weight will be available for force measurement devices. A means by which these data can be obtained is through a rocket launched test vehicle. Other means by which density altitudes of approximately 130,000 feet (H atmosphere 20 degree entry flight path angle) may be obtained are piggy-back tests on the X-15 or A-11 aircraft. High altitude balloon drops may also be feasible. For this phase of testing, the cost estimates are based on 4 tests with rocket launched vehicles due to the unknowns associated with the other methods. These costs are based on using the proven Cree parachute test vehicle data acquisition system as the means of obtaining the parachute load data.

The obtaining of second stage parachute drag information or rate of descent data is complicated by the fact that the canopy loading ($\frac{W}{S}$) must be held a constant. This maintaining of constant canopy loading requires that the system weight must be scaled in proportion to the ratio of the gravitational accelerations (Mars to Earth). This cannot be accomplished by using the same materials in the parachute as specified in the design. An example of this is that in using a second stage parachute weight of 23 pounds its equivalent weight on Mars would be 8.8 pounds, or 14.2 pounds less. Realizing that the total impact weight must be 38.2 pounds, to scale the accelerations of gravity for a 100 pound impact weight, the difference in parachute weight becomes significant. Due to this major difference in canopy effective weights and that the shape of the canopy, hence its drag coefficient, is dependent on this parameter, the materials used in the canopy construction for these tests must be other than those designed. This consideration

can be approximated analytically by assuming the canopy at terminal conditions and operating the forces which act on a segment of the roof at the center of the parachute.

fabric tension component in vertical direction - weight of canopy material in segment of roof + aerodynamic force = 0

$$T_y - \rho A_c + q C_D A_c = 0$$

where

ρ = density of canopy (lbs/ft²)

A_c = surface area of segment of canopy roof (ft²)

q = dynamic pressure (lb/ft²)

T_y = fabric tension component in vertical direction (lbs)

It is seen that when the weight of the segment of canopy material increases and the aerodynamic force remains the same the tension component diminishes. When this occurs the roof of the canopy approaches a flat shape, hence the projected area increases. This increase in projected area would ultimately result in an increased drag coefficient based on a nominal canopy area (S_0).

The feasibility of using materials such as Mylar or silk with the same geometric porosity must be determined to compensate for this difference in effective weight. The tests themselves, once the problem of scaling has been resolved, can be performed using helicopter drops (4) to minimize opening shock forces on the lightweight materials. Data obtained from these tests would be photographic information which would provide stability information and drag coefficient data. It is noted that the terminal velocity would have to be scaled for the effect of density ratio between earth and Mars. The location recommended for these tests is the El Centro test facility where range instrumentation and personnel familiar with parachute testing are available.

7. System Tests

The decelerator system tests required must incorporate at least two tests where the decelerator system has been subjected to the sterilization and long time vacuum environment. Prior to performing these tests at least 3 others should be conducted to assure that all sequencing events are functioning correctly. Test parameters which must be met are maximum loading conditions, maximum deployment Mach numbers and minimum deployment densities. To attain these test conditions it is anticipated that rocket launched vehicles must be used. The

possibility of riding piggy-back on a heat shield system test of the Mars entry vehicle must be assessed when information is available, however. The number of tests (5) proposed is considered a minimum since if all tests function correctly it will provide a reliability figure of 0.87 with a confidence level of 0.50 (Reference 20). The test vehicle used in these tests must be identical in external geometry and possess the same mass and stability characteristics that the Mars entry vehicle would have.

The flight trajectory during the deployment sequence must be carefully considered due to the difference in accelerations of gravity. This effect of gravity on the vehicle trajectory and entry vehicle ballistic coefficient cannot be eliminated from consideration by scaling the entry vehicle mass since the velocity-time history during the filling of the parachute must be identical to achieve the critical opening loads. This requirement of scaling mass can be seen when reference is made to a single degree horizontal equation of motion.

$$m\ddot{x} = C_D A^{1/2} \rho \dot{x}^2$$

where

$$C_D A = f(\text{time}) \text{ during filling}$$

$$\ddot{x} = \frac{C_D A \rho}{2m} \dot{x}^2 = C_0 \dot{x}^2$$

To acquire the proper variation of horizontal velocity (x) the time dependent variable C_0 must be a constant at any given time during the filling operation. The necessity to retain the proper velocity time history stems from the fact that all filling time relationships indicate filling time is inversely proportional to velocity. The higher the velocity the shorter the filling time thereby the higher the peak load. If the vehicle mass were scaled the value of C_0 at the start of inflation would be lower by the ratio of the accelerations of gravity, hence the velocity decay with time would be larger. This increased decay in velocity would result theoretically in a reduced opening load. In a vertical trajectory the influence of gravity is minimized if the value of $C_0 \dot{y}^2$ is large relative to g . This condition is approximated during first stage deployment where maximum loads are predicted. The effect of gravity is most critical in the reefed and disreef deployment sequence. If the entry vehicle is in a vertical flight path for these sequences the design deployment dynamic pressures can only be met with excessive time delays. This can be seen from using the predicted drag area of the Hyperflo at 0.9 Mach number (96 ft²) the entry vehicle weight of 350 pounds, and combining them to obtain the effective earth ballistic coefficient of 3.65 (terminal pressure). This value is approximately 50 percent of the maximum design deployment dynamic pressure and is over twice as high as the value expected on a 20 degree entry in G

atmosphere. The design disreef dynamic pressure (1.70 psf) is slightly more critical since the impact weight of 100 pounds and the predicted reefed drag area of 111 ft² results in a terminal dynamic pressure of 1.1 psf. This terminal value is approximately 65 percent of the maximum design disreefed deployment dynamic pressure. The lowest dynamic pressure of 1.00 encountered in the H atmosphere 20 degree entry angle trajectory cannot be obtained in a vertical trajectory.

The following are cost and manpower estimates for designing and proof testing the decelerator system for the 350 pound entry vehicle. These estimates do not include costs for booster motors or Government-owned facilities nor do they include the cost of the boiler plate system test vehicle.

<u>Function</u>	<u>Cost</u>	<u>Manpower Req'mt</u>
I. Component design and testing		
A. Material and pyrotechnic vacuum and sterilization tests (items 2 & 5)	80,000.00	40 man-months
B. Mortar system design and qualification (item 3)	75,000.00	37 man-months
C. Wind tunnel tests of the Hyperflo parachute (item 4)	30,000.00	15 man-months
II. Development Testing		
A. Second stage testing (item 6)		
1. Opening shock data	120,000.00	60 man-months
2. Drag coefficient and stability data	20,000.00	10 man-months
B. Electrical tests	7,000.00	3.5 man-months
C. Vibration & shock tests	3,500.00	1.5 man-months
D. System Drop tests (item 7)	500,000.00	250 man-months
	<u>835,500.00</u>	<u>417 man-months</u>

SECTION IV

EFFECT OF INCREASING THE ENTRY VEHICLE WEIGHT

The analysis discussed herein deals with the effect of increasing the entry vehicle weight from 350 to 5,000 pounds (earth) on the sizes and weight of a deceleration system. To set the guide lines for the investigation it was assumed that the ratio of entry vehicle weight to impact weight for all entry vehicles would be the same as that used for the 350 pound system (i.e., 3.5) discussed in detail previously. It was also assumed that the optimum system used in the 350 pound analysis would be scaled up to provide the same ballistic coefficient (W/C_{DA}) for higher entry vehicle weights. The vehicle geometry which dictates the ballistic coefficient of the entry vehicle and first stage parachute positioning was assumed to be geometrically similar and scaled in proportion to the square root of the entry vehicle weight.

The scaling of the entry vehicle diameter based on the above assumptions was as follows:

$$\text{Vehicle diameter} = 7.44 \sqrt{\frac{W}{350}}$$

The drag area of the parachute required to provide the same ratio of entry vehicle weight to vehicle plus parachute drag area as that used for the 350 pound system was determined from the following equations:

$$\frac{W}{(C_{DA})_c} = \text{constant} = K$$

therefore

$$W = (C_{D_v} A_v + C_{D_p} A_p)K$$

where the subscripts v and p stand for the vehicle and parachute respectively. The subscript c stands for the composite of vehicle plus parachute.

hence

$$W - K(C_{D_v} A_v) = K(C_{D_p} A_p)$$

Dividing both sides of the equation by $K(C_{D_v}A_v)$ results in the following:

$$\frac{W}{K(C_{D_v}A_v)} - 1 = \frac{C_{D_p}A_p}{C_{D_v}A_v}$$

Recognizing that the left side of the equation is a constant for all entry weights (criteria given above) the ratio of parachute area and vehicle area must be a constant. Substituting the values for Mach 3 results in the following:

$$\frac{C_{D_p}A_p}{C_{D_v}A_v} = \frac{(.61)(113)}{(1.46)(43.4)} = 1.085$$

$$\frac{A_p}{A_v} = \frac{(1.085)(1.46)}{(.61)}$$

Therefore using the equation for the vehicle diameter

$$A_p = \frac{W}{350} (.785)(7.44)^2 (2.60)$$

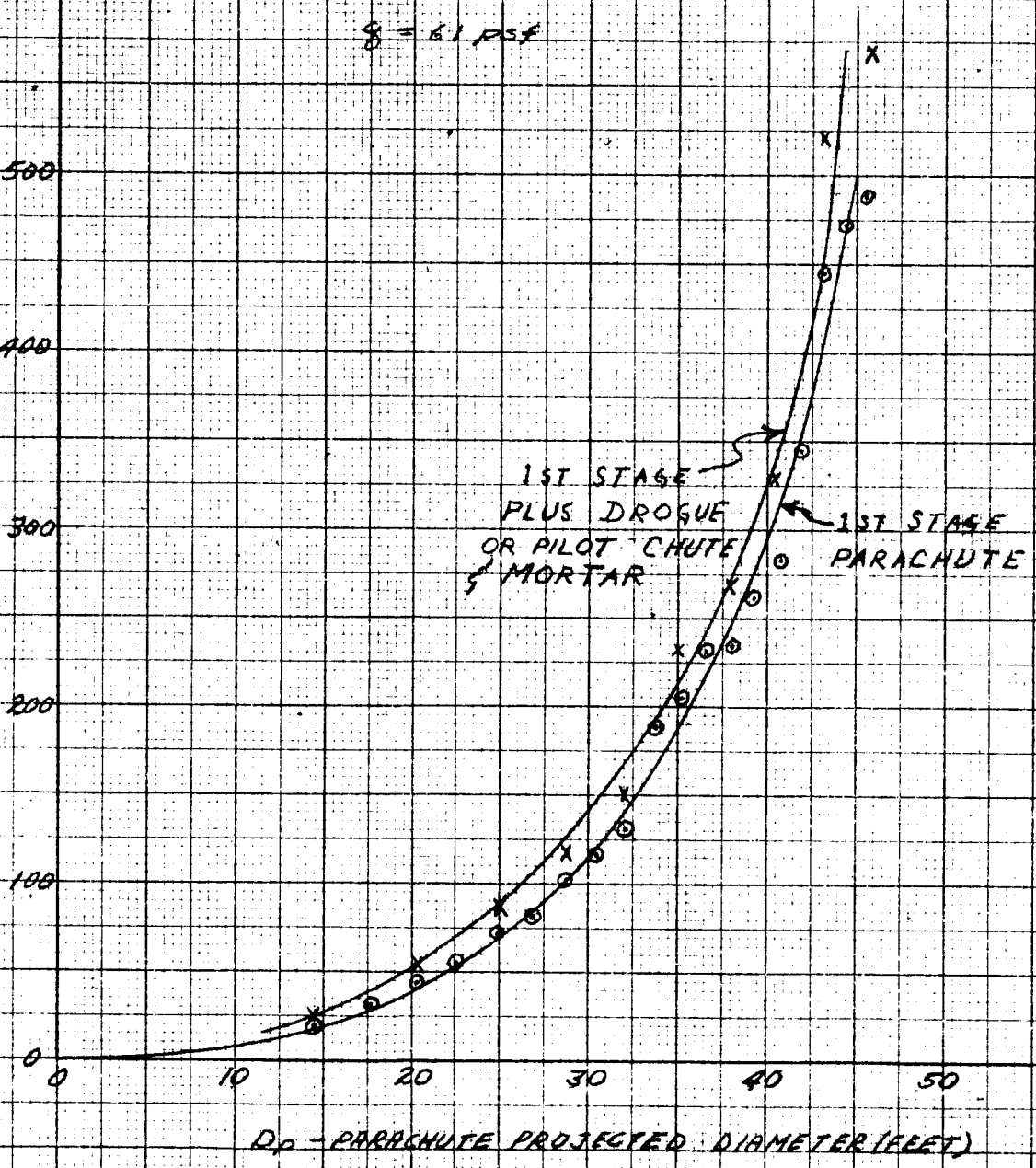
$$A_p = (0.323)W$$

Using the above relationship for area as a function of entry vehicle weight resulted in the Hyperflo parachute sizes given in Table VII. Based on these parachute sizes the weights for these parachutes were calculated for deployment conditions of Mach 3 and a dynamic pressure of 61 psf. In these weight calculations the parachute was assumed to be positioned 6 vehicle diameters behind the vehicle base. Figure 39 gives a graphical presentation of the weight of the first stage Hyperflo as a function of the projected parachute diameter. It is noted that in this figure the points calculated exhibited some scatter from the faired line. This scatter results from the fact that an infinite variation of material strengths are not available, hence when a different material for strength purposes is required for a major component of a parachute, abrupt weight discontinuities occur.

Examination of the variation of parachute weight with parachute projected diameter clearly indicates that the mortaring of parachutes this large is well beyond the present state-of-the-art. Due to the magnitude of first stage parachute weights associated with the large entry vehicle weights it was considered advisable

WEIGHT OF FIRST STAGE PARACHUTE
OR WEIGHT OF FIRST STAGE PLUS DROGUE OR PILOT CHUTE AND MORTAR - LBS

DEPLOYMENT CONDITIONS
MACH = 3.0
 $\rho = 61 \text{ PSF}$



WEIGHT OF FIRST STAGE PARACHUTE AS
A FUNCTION OF PROJECTED DIAMETER AND
WEIGHT OF FIRST STAGE PLUS DROGUE OR
PILOT CHUTE AND MORTAR

TABLE VII

Decelerator Components Description As A Function Of Entry Vehicle Weight

Entry Vehicle Weight (Lb.)	Entry Vehicle Diameter (Ft.)	First Stage Hyperflo Diameter D _p (Ft.)	First Stage Hyperflo Weight (Lb.)	Drogue Hyperflo Diameter (Ft.)	Drogue Hyperflo Weight (Lb.)	Drogue Diameter to Vehicle Diameter	Mortar Weight (Lb.)	Single Parachute D _o (Ft.)	3 Chute Cluster D _o (Ft.)	4 Chute Cluster D _o (Ft.)	5 Chute Cluster D _o (Ft.)	6 Chute Cluster D _o (Ft.)
500	8.86	14.37	19.2	4.1	4.0	.47	.8	71.2				
750	10.90	17.58	30.8					86.9	52.9			
1000	12.60	20.30	44.6	6.3	5.0	.50	1.4	100	61.2			
1250	14.10	22.6	55.6						68.8			
1500	15.45	24.85	71.8	8.0	6.5	.52	2.1		74.9			
1750	16.65	26.80	82.5						81.0			
2000	17.80	28.70	101	9.5	10.4	.53	4.0		86.4	80.3		
2250	18.90	30.40	116						91.6	84.8		
2500	19.90	32.10	131	10.8	13	.55	5.4		96.7	88.6		
2750	20.90	33.70	188							92.7	83.8	
3000	21.80	35.20	205	13.5	20	.62	9.0			96.4	87.2	
3250	22.70	36.60	231								90.5	
3500	23.50	38.0	234	14.4	23	.61	11.2				93.6	
3750	24.40	39.3	262								96.9	
4000	25.20	40.7	283	15.8	28	.63	14.8					86.4
4250	25.90	41.9	345									89.4
4500	26.70	43.1	445	19.8	4.9	.70	27					92.2
4750	27.4	44.4	472									94.8
5000	28.2	45.5	488	20.8	55	.71	30					97.4
												99.5

to sacrifice the advantages afforded by directly mortaring the first stage parachute and it was assumed that a drogue or pilot parachute would be used to extract the first stage. As was discussed previously in the sections dealing with the 350 pound entry vehicle, no data exist for Hyperflo parachutes smaller than the entry vehicle diameter. The following computations are therefore based on engineering judgment and all values are subject to experimental verification.

The determination of the size of the Hyperflo drogue or pilot parachute required for extracting the first stage parachute was determined based on providing a relative acceleration of approximately 1.5 earth acceleration units to the first stage parachute at a Mach number of 3 and a dynamic pressure of 61 psf.

$$\frac{q C_{D_p} A_p}{W_{1st}} = \text{vehicle } g\text{'s} + 1.5$$

$$= 11.3 + 1.5 = 12.8$$

where q equals the dynamic pressure and W_{1st} equals the weight of the first stage parachute.

$$A_p = \frac{(W_{1st})(12.8)}{(61)(C_{D_p})}$$

The drag coefficient value used for the drogue or pilot parachute was arbitrarily assumed to be one-half of that for which parachute data are available for a Mach number of 3.0.

$$A_p = \frac{(W_{1st})(12.8)}{(61)(.305)} = .686 W_{1st}$$

$$D_p = \sqrt{.875 W_{1st}}$$

The drogue parachute sizes based on the above formulations are given in Table VII. The distance to which the drogue parachute must be mortared was then considered. Based on solid cone data with cone to vehicle diameter ratios of 0.89 (Reference 15) that indicate favorable drag coefficients can be obtained at approximately 3.5 vehicle diameters, a value of 4 vehicle diameters has been chosen to minimize the weight of the risers. This position must be verified by wind tunnel tests. The weights of the drogue parachutes were calculated based on the above

riser length assumptions and the assumption that during the extraction process the parachute would acquire a drag coefficient equivalent to that used for larger parachute-to-vehicle diameter ratios. The weights resulting from this sizing are given in Table VII.

The weight of the mortar required to eject these drogue parachutes is the remaining parameter to be assessed. Review of Table III which gives the calculated mortar weight with various parachute weights shows that the weight of a mortar system is directly proportional to the amount of energy delivered. Since the energy required under the assumptions given in Appendix III is directly proportional to the mass of the object and the distance traveled, the weight of the mortars required for the drogue ejections were computed using the following procedures.

Based on the results given in Table III and accounting for the fact that the drogue will be positioned 4 vehicle diameters behind the body result in the following:

$$W_m = 4.45 \times 10^{-4} \text{ kinetic energy} = 2.01 \times 10^{-2} (W_D)(D_V)$$

where W_m equals the weight of the mortar and W_D equals the weight of the drogue parachute.

The weights obtained from the above procedure are given in Table VII. The combined weight of the first stage plus drogue and mortar are given in Figure 39.

The sizing of the second stage parachute or terminal parachute for entry weights up to 5,000 pounds was performed by maintaining the same ballistic coefficient for the impact weight as obtained in the 350 pound case. For the 350 pound case the impact weight (defined as the payload weight, plus the second stage parachute weight) is 100 pounds and the drag area fully inflated is 2,485 square feet. By maintaining the same ballistic coefficient ($W/C_D A$) for the terminal parachute, the fully deployed altitudes and descent times for the increased entry vehicle weights will be approximately the same and will deviate from the values for the 350 pound case due to changes in filling times for the bigger chutes. It is believed these changes will not significantly alter the descent time or the fully deployed altitude since review of calculations performed for parachutes with diameters of 78.7 59.3 and 34.3 feet indicate that the altitude lost in going from reefed inflation to full open are 652, 580 and 339 feet respectively. It is noted that these values are for different $W/C_D A$ terminal values; however, for parachute sizes up to 100 feet in diameter based on the above numbers the loss in altitude will be approximately 300 feet more than the nominal. This loss represents approximately 10 seconds of descent time which, when compared to 12 minutes for the 90 degree G atmosphere case is less than 2 percent. The reduction in fully deployed altitude based on a 300 feet loss is also less than 2 percent.

For all the computations performed it has been assumed that the maximum terminal parachute size is 100 feet D_0 . This limit is based on experience which has shown that parachutes larger than this diameter create fabrication, packing and handling problems. For impact weights which require more drag area than a 100 foot diameter parachute will provide, clustered arrangements have been considered. The type of canopy considered for the clustered arrangement is a solid flat. This canopy has undesirable stability characteristics as a single parachute but is a very stable configuration when clustered. Clustering, however, has some undesirable weight considerations. Based on test data the drag coefficient for a clustered arrangement is lower than for a single canopy. The values used in sizing the clustered chutes are listed below.

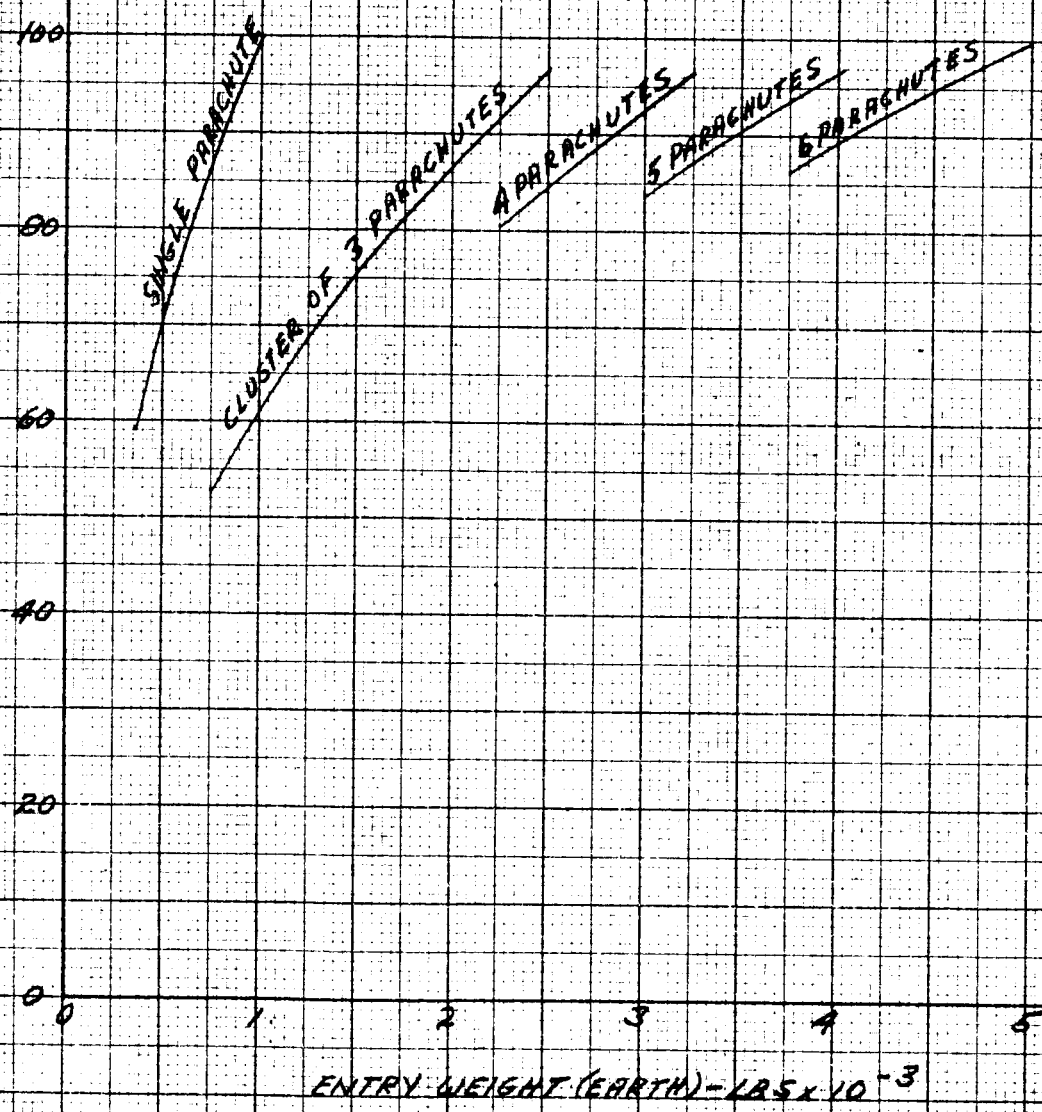
<u>No. of Parachutes in Cluster</u>	<u>% of Single Parachute Drag Coefficient</u>
3	.9
4	.88
5	.86
6	.84

These cluster factors have been determined by personnel associated with parachutes for many years. Although many clustered drops have been performed by the armed services, not many of these have been instrumented; hence, only limited test data are available. This lack of data is especially acute in the range of extremely low canopy loadings which are contemplated for this program. As a consequence of this absence of applicable data from which to scale and the belief that the cluster factor may be significantly dependent on the terminal rate of descent, the above figures are considered at best as engineering estimates and should be experimentally verified.

Aside from the reduction in drag coefficient discussed above, risers must be provided to assure proper operation. The riser lengths used for the weight calculations were based on standard Air Force cargo delivery clustered configurations for 100 foot parachutes. For these systems, clusters of 3 and 4 parachutes use 60 foot risers; clusters of 5 and 6 parachutes use 80 foot risers. Figures 40 and 41 show the size of terminal parachutes required in either a single or clustered arrangement as a function of entry vehicle weight and the weight of these parachutes respectively. In calculating the size of the parachutes the impact weight was assumed to be the entry weight divided by 3.5 as stated previously. It is noted in Figure 40 that parachutes were sized for the same entry vehicle weight for two types of configurations. This overlapping of the configurations coupled with the weight information provided in Figure 41 shows that from a weight consideration it is more favorable to minimize the number of chutes in a cluster rather than to use smaller chutes in a larger cluster arrangement.

Figure 42 shows the payload weight as a function of entry weight. Plotted in the same figure is the maximum possible payload weight (no terminal parachute)

D_0 - NOMINAL DIAMETER OF TERMINAL PARACHUTE - FEET
(INDIVIDUAL PARACHUTE OF A CLUSTER)



NOMINAL DIAMETER OF TERMINAL PARACHUTE AS
A FUNCTION OF ENTRY WEIGHT - FOR BOTH
SINGLE AND CLUSTERED PARACHUTE ARRANGEMENTS

WEIGHT OF TERMINAL PARACHUTE SYSTEM - LBS

100

350

300

250

200

150

100

50

0

DEPLOYMENT CONDITIONS (REF F D 1070)

MACH = 0.9

$q = 7.5 \text{ PSF}$

6 PARACHUTES

5 PARACHUTES

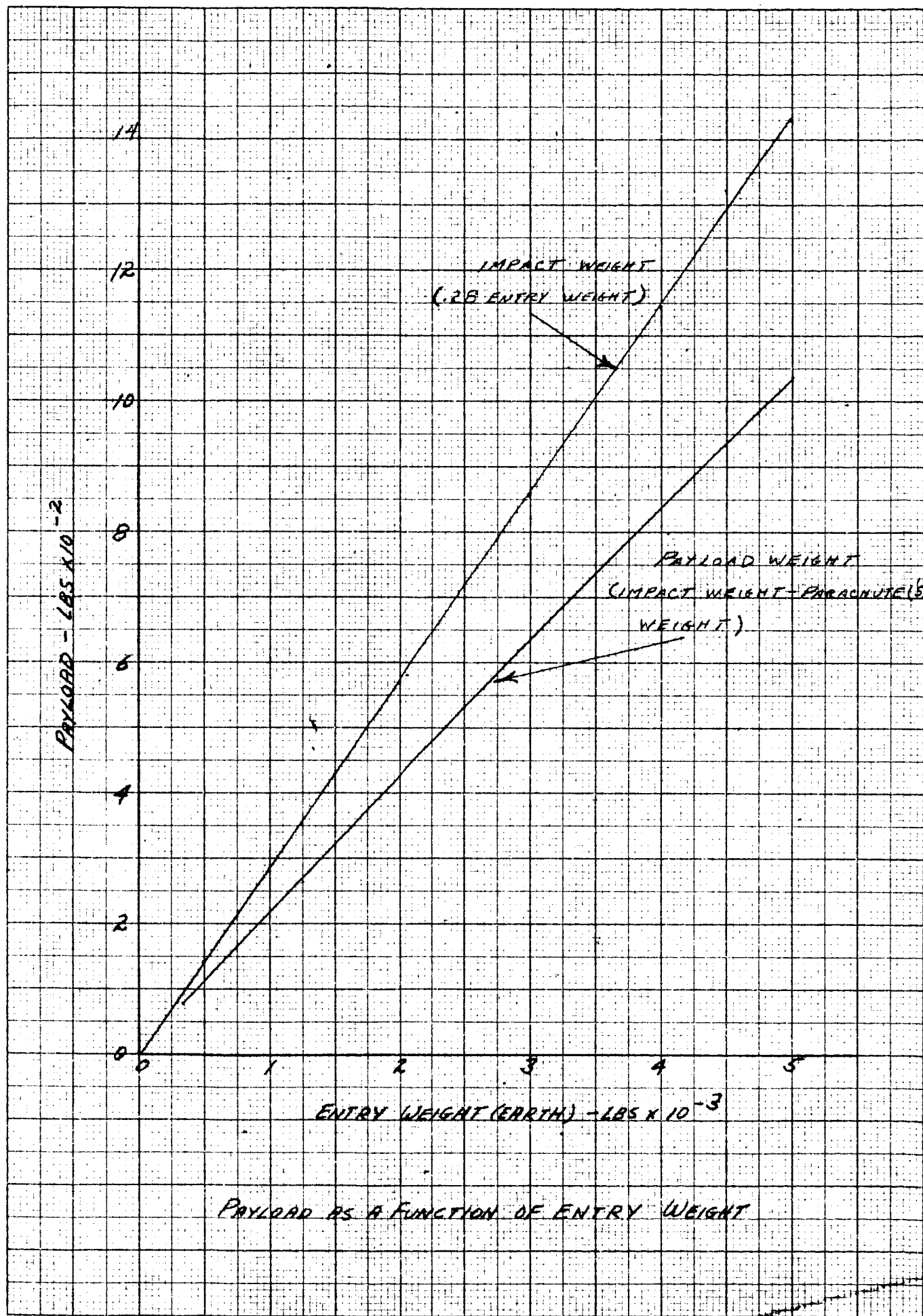
4 PARACHUTES

CLUSTER OF 3 PARACHUTES

SINGLE PARACHUTE

D_0 - NOMINAL DIAMETER OF SINGLE TERMINAL PARACHUTE
OR OF INDIVIDUAL PARACHUTE OF A CLUSTER - FEET

WEIGHT OF TERMINAL PARACHUTE SYSTEM AS A FUNCTION
OF PARACHUTE NOMINAL DIAMETER



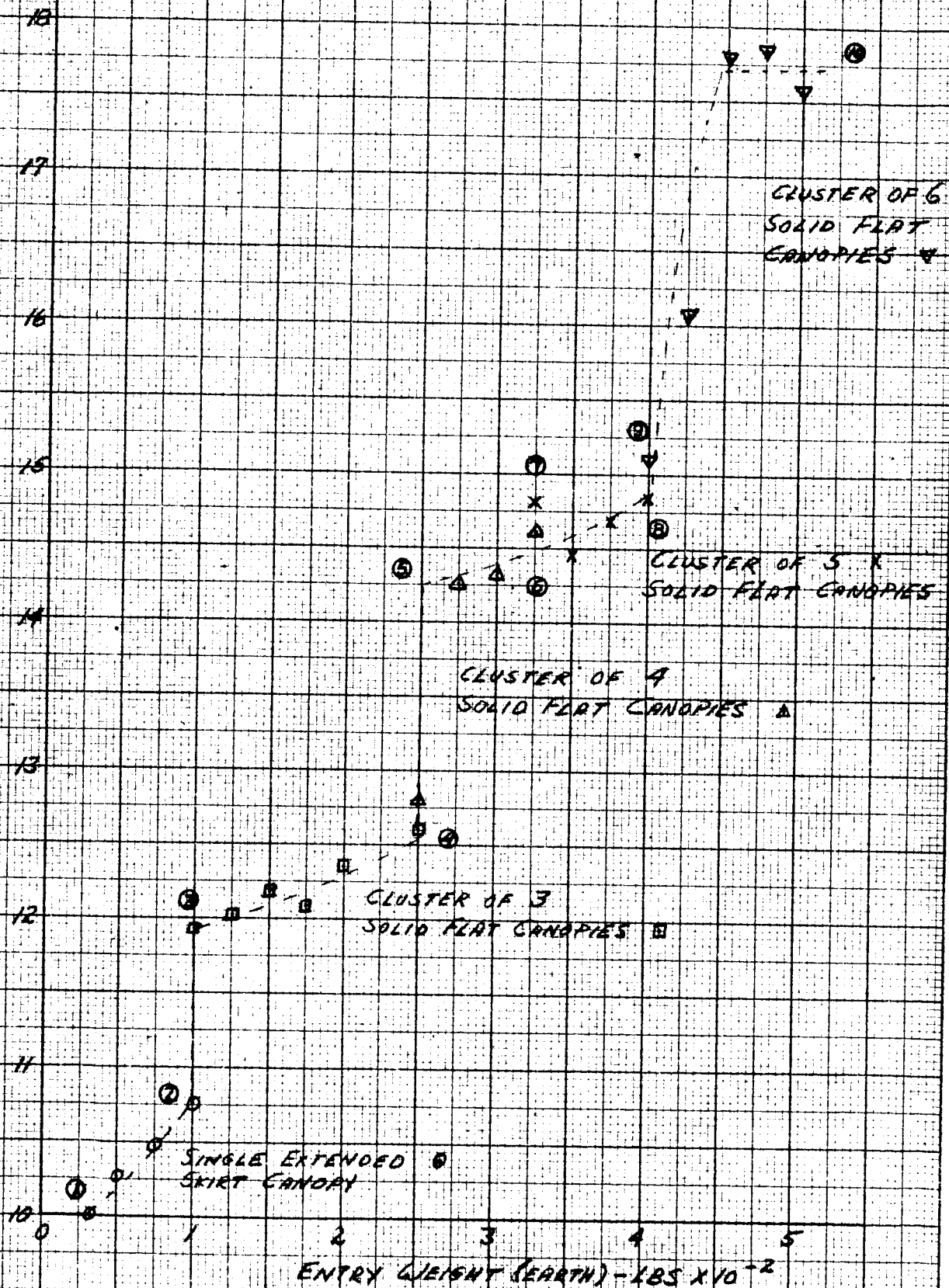
based on the assumption that the impact weight will be 28.6 percent of the entry vehicle weight. Comparison of the impact weight to payload weight indicates the terminal parachutes comprise 27 percent of the impact weight for a 5,000 pound entry vehicle; 26 percent for a 2,500 pound entry vehicle and a minimum of approximately 23 percent for a 350 pound entry vehicle. This variation of approximately 4 percent over the entire entry vehicle weight variation represents a decrease in efficiency with larger parachute sizes and cluster arrangements.

Figure 43 gives the total weight of the first stage and second stage parachutes in percent of the entry vehicle weight for the range of entry vehicle weights considered. In this figure the ranges for the types of terminal parachute arrangements are noted and the numerical designations are given below.

1 to 2	Single Terminal Parachute
3 to 4	Cluster of 3 Parachutes
5 to 6	Cluster of 4 Parachutes
7 to 8	Cluster of 5 Parachutes
9 to 10	Cluster of 6 Parachutes

It is seen that for entry vehicle weights ranging from 350 to 5,000 pounds the first and second parachute weights vary from 10 to approximately 18 percent. This variation of 8 percent is mainly attributed to the increased size of the first stage parachute. This factor of increased weight as a function of size can be seen based on the stress equations given in Appendix II. These equations show that the predicted stress in the canopy inlet and roof are directly proportional to the parachute projected diameter for a given deployment Mach number (C_D) and dynamic pressure. Another factor which does not scale directly with the entry vehicle weight is the weight of the risers. The riser weight for the 350 pound vehicle comprised 17 percent of the first stage weight and for the 5,000 pound vehicle the riser weight to first stage parachute weight was 37 percent. This increase results from the increased strength required in the risers and the decrease in weight efficiency of high strength webbings. For the 350 pound vehicle the first stage weight comprises 3.5 percent of the entry vehicle weight. The weight of the first stage parachute for the 5,000 pound entry vehicle comprises 9.8 percent of the entry vehicle weight or a 6.3 percent increase. It is apparent from these calculations that the decrease in weight efficiency with increased entry vehicle weight is primarily associated with the first stage and the terminal parachute is responsible for approximately 1.5 percent.

TOTAL WEIGHT OF FIRST AND SECOND STAGE PARACHUTES IN PERCENT OF ENTRY WEIGHT



VARIATION OF 1ST & 2ND STAGE PARACHUTE WEIGHT AS A FUNCTION OF ENTRY WEIGHT CONSIDERING BOTH SINGLE AND CLUSTER ARRANGEMENTS FOR THE TERMINAL RECOVERY PHASE

SECTION V

SUMMARY AND RECOMMENDATIONS

The results of the study indicate that a two stage parachute configuration will enable a 22,000 foot descent after all sequencing has been performed in the least dense atmosphere. The impact velocity in this most severe atmosphere is predicted to be 27 fps. To accomplish this deceleration the parachutes which have been selected for the 350 pound entry vehicle are as follows:

1st Stage	A 12.0 foot projected diameter Hyperflo canopy
2nd Stage	A 59.3 fully extended skirt canopy with a 14.3 percent extension reefed initially to 10 percent of its drag area at deployment conditions.

The first stage decelerator must be deployed at a Mach number of approximately 3.0 to obtain the above conditions. The deployment dynamic pressure at this condition is 61 psf and the equivalent earth density deployment altitude is 107,000 feet. The highest equivalent earth density altitude for which this parachute must be deployed based on the computations performed to date is 145,000 feet. This altitude band, Mach number, and dynamic pressure are within the spectrum in which the Hyperflo parachute has demonstrated satisfactory performance in the Cree Parachute Test Program. The predicted aerodynamic heating is extremely low and well within the capability of Nomex material to withstand.

The second stage parachute is in the size range where experimental data and design techniques for 55 and 67 foot configurations can be used. The inflation characteristics of this parachute at the high equivalent earth density altitude is the major unknown. Experimental data are not available for this type of parachute operating at an earth density altitude of 135,000 feet. Based on a reduction in effective cloth porosity which has been predicted for high altitude operation it is felt that the proposed configuration will function satisfactorily. A test program to verify the operation of this parachute is a prime requirement.

The estimated weight of the decelerator system is 54 pounds. The parachutes themselves make up approximately 65 percent of this weight. The explosive disconnect hardware constitutes 16.5 percent and the remaining 18.5 percent is allocated to the sensing system, 1st stage deployment mortar and the accessories associated with the parachutes. For this system the parachutes themselves comprise 10 percent of the entry vehicle weight. The optimum weight of the 1st stage in percent of the total parachute weight, considering both terminal velocity and deployment altitude, was 35 percent.

The weight of parachutes for entry vehicles heavier than 350 pounds was found to vary between 10 and 18 percent of the entry weight. This increase was attributed mainly to the increased weight fraction for the 1st stage parachute. The decreased efficiency of the 2nd stage parachute was computed to be approximately 1.5 percentage points of the 8 percent increase. This increase is primarily due to the inefficiency of clustered arrangements for parachutes where the minimum strength material can be used for all parachute designs.

The major problem area for which no satisfactory answer was derived as a result of this program is the defining of an adequate sensing system. It is felt that the solution to this problem should be foremost in the schedule of new work since the errors associated with sensing may directly influence the parachute structural designs given herein. The two avenues of approach recommended should be studied to ascertain which system would be most accurate.

✓ The second most critical problem area for which further work should be performed is the ascertaining of the Hyperflo's performance characteristics behind an Apollo shape. Coupled with this work is the determination of the effects of vehicle stability on the parachute-vehicle combination. This work, and continued effort in the sterilization and vacuum studies, should be performed immediately since the decelerator system weight is highly dependent on these results.

The third recommended task is the outlining of a complete test program to qualify the decelerator system. This work would be performed in two phases. The first phase would describe a schedule of testing and definitize the exact environment for all tests. This programing is considered mandatory prior to beginning any testing program. Work which would be included in this phase is the determination of the deployment conditions in other atmospheric profiles which were not considered in this study and the effects of errors in the sensing system.

The second phase of this program would be the designing of the test vehicle equipment which would meet the requirements of phase one. This program would definitize the instrumentation required, define the ranges to be used and provide engineering drawings and specifications for the manufacturing of the test equipment.

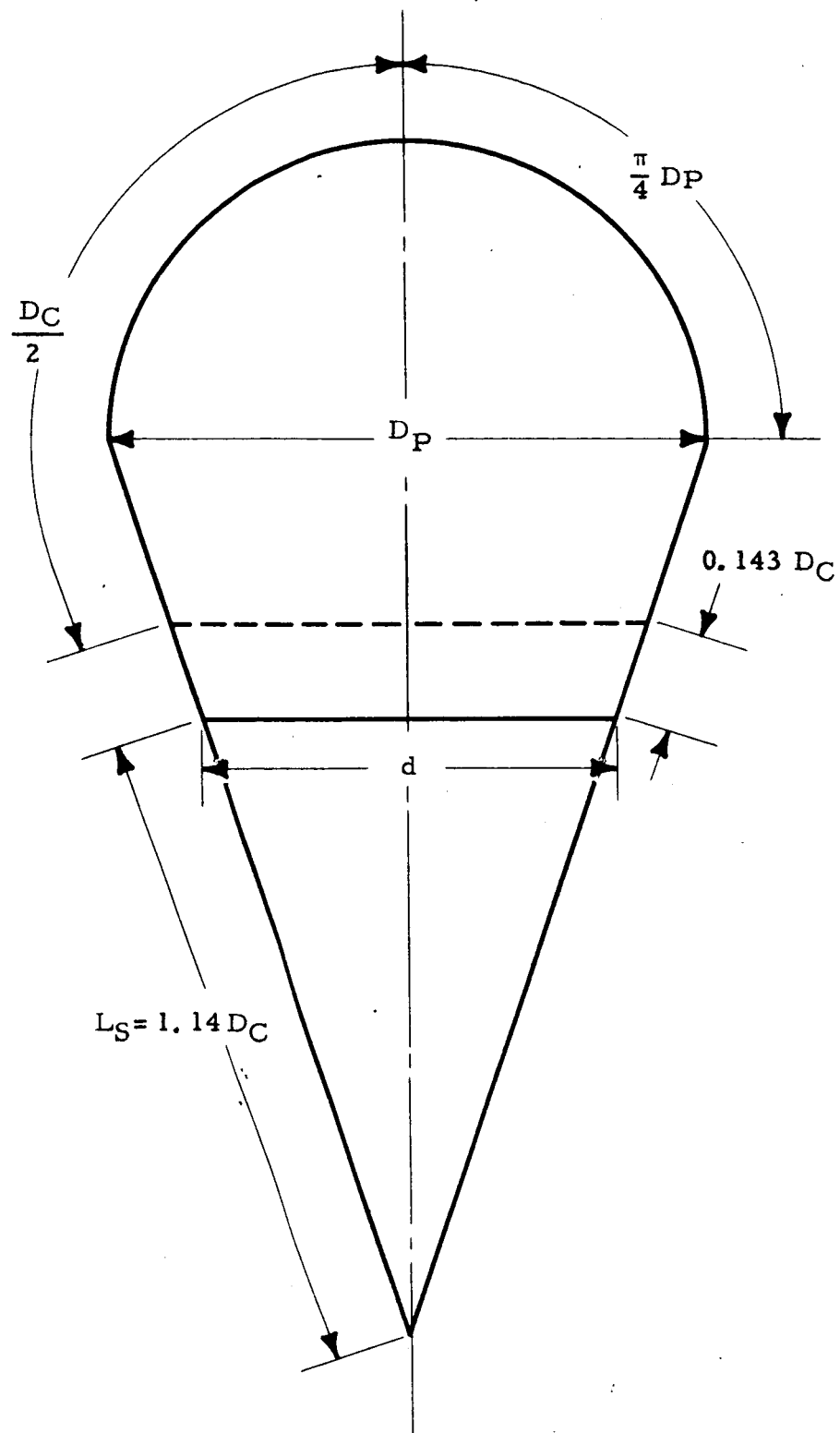
APPENDIX I

EQUATIONS USED IN DETERMINING THE TIME TO FILL FROM REEFED INFLATION TO FULL OPEN FOR A 14.3 PERCENT FULLY EXTENDED SKIRT PARACHUTE

The procedure selected to determine the filling time for the extended skirt canopy during the interval between reefed inflation and full inflation is a modification of the procedures given in Reference 6 for a solid flat canopy. This method of calculating the filling time employs the desirable characteristic of accounting independently for the atmospheric density as well as the instantaneous decelerator velocity. A second factor which influenced this selection is the lack of reliable filling time data for extended skirt canopies in going from reefed to full inflation. This factor is further accentuated by the fact that no data could be found for inflations at densities as low as may be encountered in this program. The above reasons coupled with the fact that the solid flat canopy filling time relationship incorporates all the advanced work since the last USAF parachute handbook, (Reference 21) was published in 1956 suggests its use.

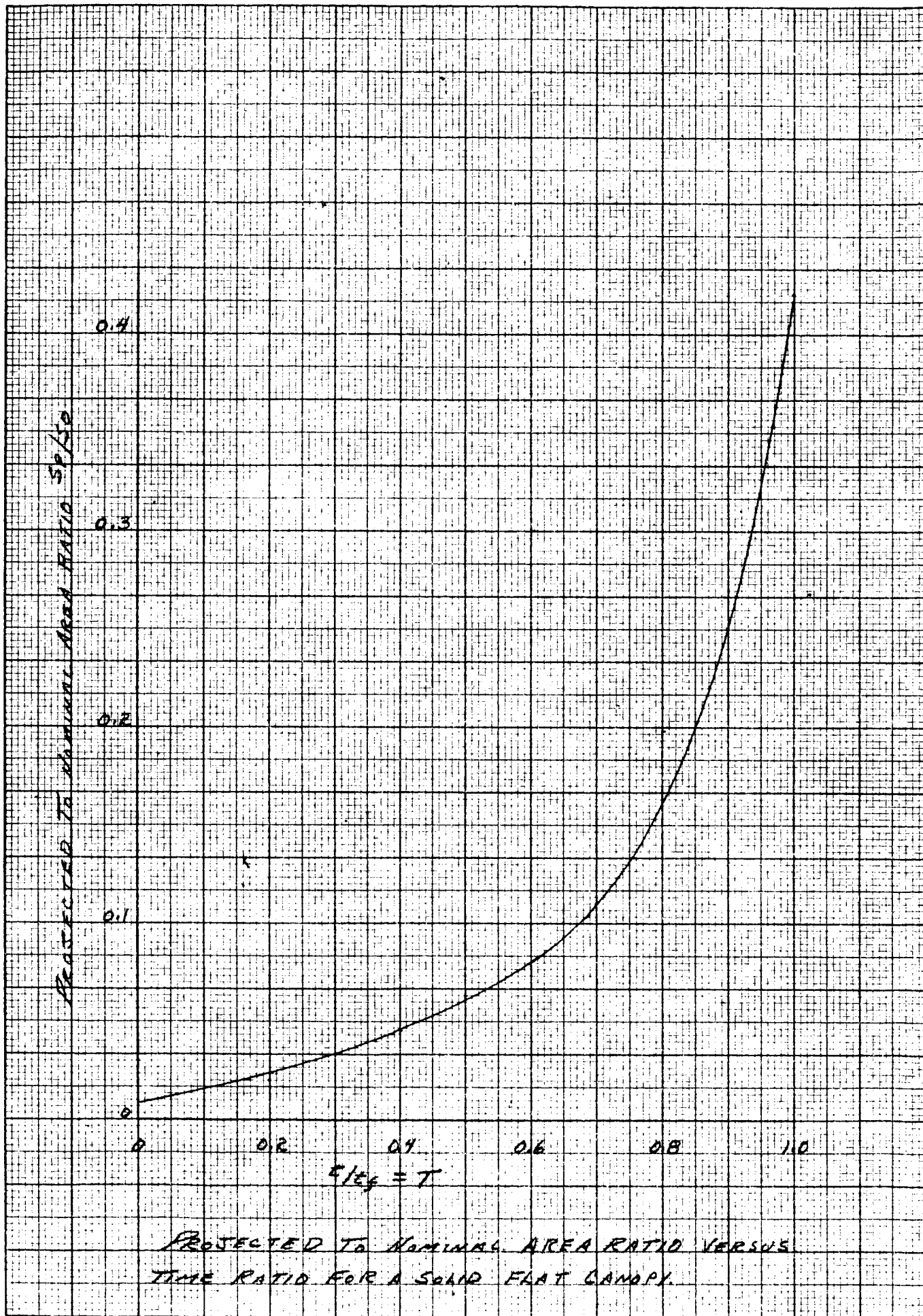
The geometric differences between the solid flat canopy and the extended skirt canopy requires a modification to the model, "idealized canopy shape", described in Reference 6. This shape is assumed to be comprised of a hemisphere of a diameter D_p and a truncated cone with a lower base of d and an upper base of D_p (Figure A 1). Since the fully extended skirt canopy proposed in this study is comprised of a solid flat canopy center section with a diameter D_c and a conical extension of $.143 D_c$, it has been assumed that the extension portion of the extended skirt merely lengthens the truncated cone on the idealized model. This is compatible with the geometry assumed by the fully extended skirt configuration in the inflated state where the inlet diameter of the canopy assumes a diameter less than that of the maximum projected diameter. Based on these assumptions, Figure A 1 shows the shape and nomenclature used for the modified idealized model. The suspension line lengths (L_s) used for this analysis are $1.14D_c$.

The latest information on the variation of projected canopy area as a function of time has been used in the calculations performed. In Reference 6 a linear variation of projected area with time was assumed. Empirical data has shown (Reference 11) that this assumption is not accurate and that the projected area referenced to the surface area of the flat circular parachute (S_0) is better approximated by a fourth order equation for the major portion of the filling time. Figure A 2 shows the variation of S_p/S_c as a function of non-dimensional time (t/t_f). The symbol t is any



IDEALIZED CANOPY SHAPE

100 TO THE INCH
KEUFFEL & ESSER CO.
ALBANY, N.Y.



instantaneous time during the filling process and t_f is the time to fill. The symbol S_c is S_o for a solid flat canopy. The symbol S_o was used in the paper (Reference 11), however, for use in the analysis performed herein S_c is defined specifically as the surface area of a flat circular parachute of nominal diameter D_c . This substitution is based on the assumption that the extension on the solid flat canopy does not alter the projected diameter of the canopy over that which would be obtained by considering the flat circular constituent only. Based on the values that are given in Reference 6, this assumption is less than 9 percent in error.

Using the model given in Figure A-1 and the assumption that the flat circular portion of the extended skirt canopy governs the projected diameter during the filling time, the curve given in Figure A-2 was used directly. It should be noted that for the extended skirt canopy being considered, that D_c is approximately 80 percent of D_o .

From the above geometry description and the mass flow balance given in Reference 6 and shown below, the following equations have been derived.

$$\text{mass in} - \text{mass out} = \text{change in mass flow}$$

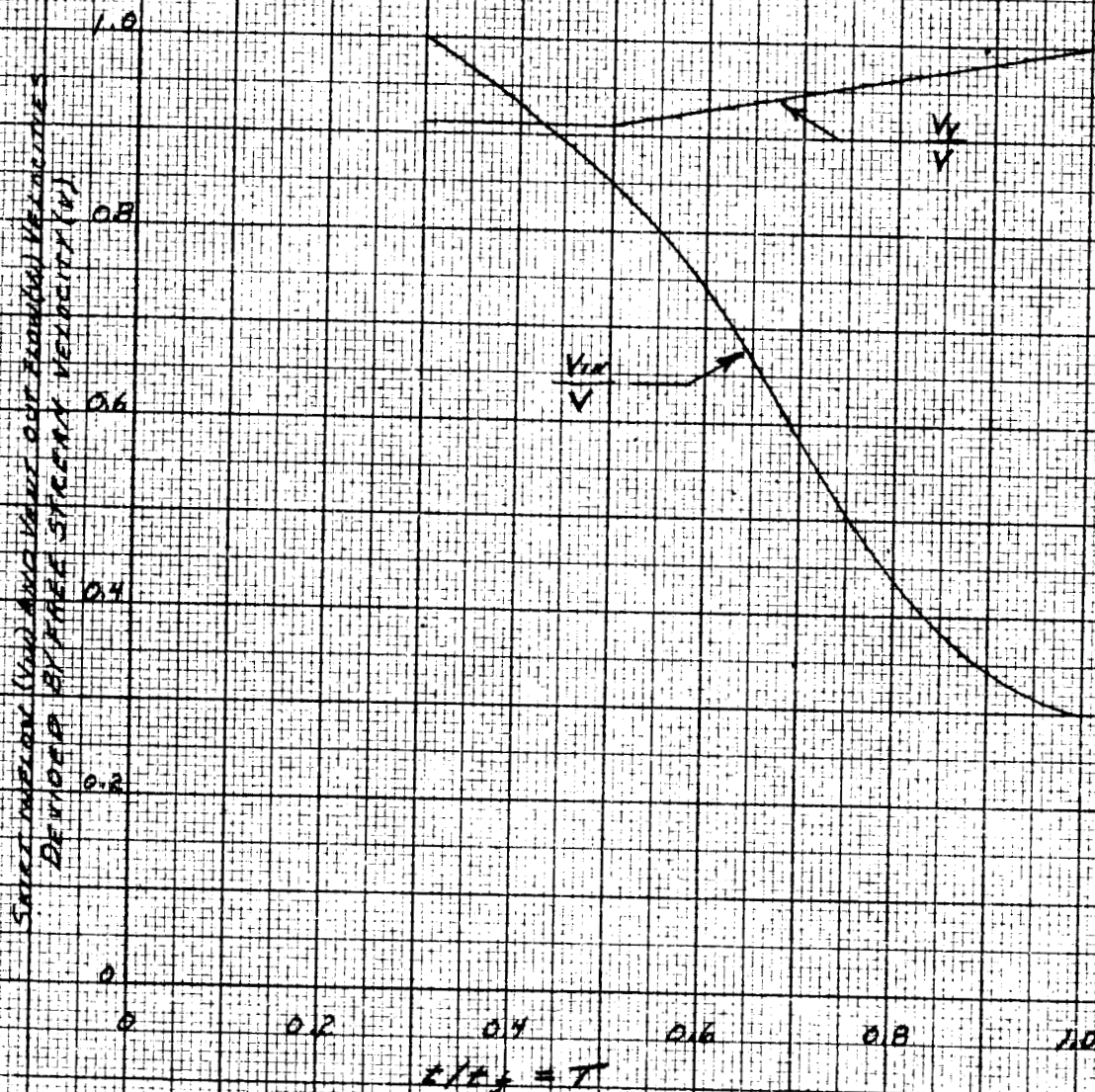
$$(1) \frac{\pi d^2}{4} V_{in} \rho - \frac{\pi D_p^2}{2} U \rho = \frac{d}{dt} (\rho V)$$

Accounting for the area of the vent in equation (1) and that the inflation process takes place over a small altitude range, it has been assumed that the air density remains constant.

Equation (1) thereby takes the following form:

$$\frac{\pi d^2}{4} V_{in} - \left(\frac{\pi D_p^2}{2} - A_v \right) U - A_v V_v = \frac{dV}{dt}$$

At this point in the equation formulation it was necessary to define the inflow (V_{in}) and outflow (U) velocities. Here again the results given in Reference 11 by DeWeese were used as opposed to the linear relationship for inflow used in Reference 6. Figure A-3 shows the ratio of inlet velocity to free stream velocity as reported by DeWeese. This figure also gives the percentage of vent outflow (V_v) with respect to free stream as a function of the nondimensional time T .



RATIO OF SKIRT INFLOW AND VENT OUTFLOW VELOCITIES TO FREE STREAM VELOCITY VERSUS TIME RATIO FOR A SOLID FLAT CANOPY

The remaining term needed is the outflow velocity U. For this term the concept of "effective porosity" given in Reference 6 was used. This concept accounts for the effect of varying density and Mach number on the flow through a fabric material. Unfortunately the data available for the effective porosity term are limited to nylon cloths and densities ratios of greater than 0.1. As a result of this limitation, an arbitrary value of 0.03 was used for the effective porosity term C. This choice was based on using a Mach number of 0.5 for the disreef condition and the limit of the 1.1 oz. per square yard nylon data. Due to the uncertainty of the effect of decreasing the density ratio term by nearly another order of magnitude, coupled with the lack of data for dacron material the value of 0.03 was used for the C term for all computations performed independent of the variation of density ratio from one atmospheric model to another. The resulting equation for the outflow velocity is as follows:

$$(3) \quad U = CV_{in} \text{ or } 0.03 V_{in}$$

By using the above equations and substituting

$$(4) \quad dt = t_f dT$$

equation (1) becomes

$$t_f \left[\frac{\pi d^2}{2} V_{in} - \left(\frac{\pi D_p^2}{2} - A_v \right) (0.03 V_{in}) - A_v V_v \right] = \frac{dV}{dt}$$

Using Figure A-1 the solution for the enclosed volume of the idealized model as a function of T now becomes a geometry exercise of solving for the volume of the hemispherical top of the parachute and the truncated cone as a function of the projected diameter of the parachute, D_p .

To perform the volume calculations the following geometric identities have been used.

$$S_p = \frac{\pi D_p^2}{4} \quad D_c = 0.806 D_o \quad S_c = 0.65 S_o$$

By geometric similarity.

$$\begin{aligned}
& \left[0.25 D_{pmax}^2 + 0.202 D_{pmax}^2 + 0.224 D_{pmax}^2 \right] (1.05) \\
& = 0.262 D_{pmax}^3 + \left[\sqrt{3.86 D_{pmax}^2 - 0.25 D_{pmax}^2} - 1.7 D_{pmax} \right] (0.676 D_{pmax}^2) (1.05) \\
& = 0.262 D_{pmax}^3 + \left[D_{pmax} (1.9 - 1.7) \right] (0.676 D_{pmax}^2) (1.05) \\
& = 0.262 D_{pmax}^3 + (0.2) (1.05) (0.676) D_{pmax}^3 \\
& = 0.262 D_{pmax}^3 + 0.142 D_{pmax}^3
\end{aligned}$$

$$\text{Inflated Volume} = .404 D_{pmax}^3.$$

The remaining variable not described is the area of the vent A_v . Since this area is contingent on the final fabrication procedures vent diameters for 39, 67 and 100 foot parachutes were used to formulate a general expression. It was found that for this parachute nominal diameter (D_o) range the linear equation given below fits reasonably well and was used in the calculations.

$$\frac{D_v}{D_o} = 0.1 - 7.0 \times 10^{-4} D_o$$

The equations and curves discussed above were programmed into the Cook Electric Company 1920 computer and solved by a finite difference technique. To obtain the parachute filling time an iterative scheme was employed. This solution was started by assuming a filling time t_f and computing the volume of the air enclosed in the canopy for this filling time and comparing it to the volume predicted by the idealized model at full open ($T = 1$). Different values of t_f were assumed until agreement between the computed volume and the known maximum volume were within 2 percent. It is noted that in these calculations the interval of T over which this integration was performed was from $T = .45$ ($S_p/S_o = .042$) to $T = 1$. This initial value of T was chosen since it represents the projected frontal area of 10 percent of that fully inflated (Figure A-2). This procedure is consistent with the assumption used in Reference 6, that assumes that the drag coefficient during inflation is a constant, hence for a 10 percent reefed drag area the ratio of S_p reefed to S_{pmax} used was 0.1.

$$\frac{d}{L_s} = \frac{D_p}{L_s + 0.143 D_c + \frac{D_c}{2} - \frac{\pi D_p}{4}} ; \frac{d}{1.14 D_c} = \frac{D_p}{1.14 D_c + 0.143 D_c + \frac{D_c}{2} - \frac{\pi D_p}{4}}$$

$$d = \frac{1.14 D_c D_p}{1.783 D_c - \frac{\pi D_p}{4}} ; d = \frac{D_p}{1.56 - 0.69 \frac{D_p}{D_c}}$$

The volume enclosed within the parachute at any time T is then:

V = volume of hemisphere + Volume of frustum

$$V = \frac{2}{3} \pi \left(\frac{D_p}{2} \right)^3 + \frac{\pi h}{3} \left[\left(\frac{D_p}{2} \right)^2 + \left(\frac{d}{2} \right)^2 + \frac{d D_p}{4} \right]$$

$$\text{Where } h = \sqrt{(1.14 D_c + 0.143 D_c + 0.5 D_c - 0.785 D_p)^2 - \left(\frac{D_p}{2} \right)^2} - \sqrt{(1.14 D_c)^2 - \left(\frac{d}{2} \right)^2}$$

$$V = \frac{2}{3} \pi \left(\frac{D_p}{2} \right)^3 + \left[\sqrt{(1.783 - \frac{\pi}{4} D_p)^2 - \left(\frac{D_p}{2} \right)^2} - \sqrt{(1.14 D_c)^2 - \left(\frac{d}{2} \right)^2} \right] \frac{\pi}{3} \left[\left(\frac{D_p}{2} \right)^2 + \left(\frac{d}{2} \right)^2 + \frac{d D_p}{4} \right]$$

Using the fact that $S_{p \max} = .42 S_c$ (Figure A-2)

$$D_{p \max} = .65 D_c$$

$$D_c = 1.54 D_{p \max}$$

Therefore

$$V = 0.262 D_{p \max}^3 + \left[\sqrt{(2.75 D_{p \max} - 0.785 D_{p \max})^2 - 0.25 D_{p \max}^2} - \sqrt{3.09 D_{p \max}^2 - 0.202 D_{p \max}^2} \right]$$

APPENDIX II

EQUATIONS USED FOR DETERMINING MATERIAL STRESS

FOR FIRST AND SECOND STAGE PARACHUTES

The equations used to determine the strengths of materials for both the first and second stage decelerators are given below. Considering the first stage Hyperflo design, the equations used for determining the fabric stresses in components which comprise the major percentage of the parachute weight are as follows:

The design load for the individual lines

$$(1) \quad L_L = \frac{(1.5) (C_{Dp}) (S_p) q (S.F.)}{n} \quad (\text{in pounds})$$

where

q = the deployment dynamic pressure (lbs/ft^2)

(1.5) = "bounce factor" to account for oscillating loads measured in free flight tests

S_p = projected frontal area of Hyperflo = $\frac{\pi D_p^2}{4}$

C_{Dp} = Hyperflo drag coefficient based on S_p

n = number of gores or lines used in the parachute design

S.F. = Safety factor = 1.5

The criteria used in determining the number of gores was based on free flight and wind tunnel tests

$$n = 4j$$

where j is any integer equal to or larger than 3 which satisfies the following and is the lowest numerical value which can pass the test.

$$(2) \quad \frac{\pi D_p^2}{4j} \leq 2.66$$

The equation used in defining the material strength requirement for the conical inlet of the Hyperflo parachute was as follows:

$$(3) \quad L_{cc} = \frac{C_{D_p} q D_p (S. F.)}{(2) (12)} \quad (\text{in pounds/inch})$$

The above equation determines the hoop stress in the inlet which is considered a cylindrical tube with a diameter of D_p . The internal pressure is assumed uniform and equal to $C_{D_p} q$.

The safety factor used in this computation was the same as that used for the lines (1.5).

The material strength required for the roof of the canopy was determined based on using 3/8 inch wide ribbons in the design. The stress was calculated assuming an elongation of the ribbons to 115 percent of their initial length, and the shape of the roof resulting from this elongation being a segment of a sphere with a diameter equal to $1.27 D_p$.

Therefore

$$(4) \quad L_R = \frac{C_{D_p} q (1.27 D_p) (S. F.)}{(4) (12) (1.47)} = \quad (\text{pounds})$$

Accounting for the geometry of the grid formed by the ribbons and the width of the ribbons assumed in the design, the 1.47 (ribbons per inch) factor appearing in the denominator converts the hoop stress equation into a material strength required.

The results of equation (4), therefore, give the ribbon rated strength needed.

The safety factor used in this equation was 1.5. The 1.27 term in the numerator stems from the elongation of the roof material.

The material strength required for the radial reinforcement bands was determined by the following equation:

$$(5) \quad L_{RR} = \frac{\text{line load}}{2} \quad (\text{in pounds})$$

The value of the line load determined in equation (1) which included the safety factor (1.5) and "bounce factor" (1.5) was used in this equation.

The Nomex materials chosen as a result of these design stresses or loads were materials which were available at the time of commencement of work. It is expected that as time progresses a greater selection of materials will become available. Hence, the parachute weights resulting from this analysis may be reduced when additional material selections are available. The magnitude of this weight reduction will be entirely dependent on the selection of materials available at the time of parachute fabrication.

The procedures used in determining the strength of materials required for the major weight components of the second stage parachute are as follows:

$$F_o = C_{DR} S_o q (\% \text{ Reefing})$$

where

F_o = parachute opening shock

C_{DR} = drag coefficient of reefed parachute = 0.4

$S_o = \frac{\pi D_o^2}{4}$ = Parachute Surface area

$\% \text{ Reefing} = \text{percent of reefed area} = \left(\frac{D_p}{D_{pmax}}\right)^2 = 0.10$

$\left(\frac{D_p}{D_{pmax}}\right)$ = ratio of reefed to fully inflated projected diameter

The strength of the lines required was calculated as follows:

$$L_L = \frac{F_o (S.F.)}{n}$$

where

S.F. = safety factor = 1.5

n = number of gores

The optimum number of gores was determined based on the following criteria.

$$n = 4j \text{ where } j \text{ is any integer}$$

and

$$0.716 D_o \leq n \leq 9.6 \pi D_o$$

The minimum number of gores ($n = 0.716 D_o$) is based on the requirement that the unsupported skirt length or distance between gores for the extended skirt canopy be less than or equal to π feet. This requirement is based on experience which indicates that canopies with fewer number of gores tend to squid (not open properly). The maximum number given is an approximation of the limit which is dictated by the width of the radial seams in the canopy.

The equation used to determine the strength of material needed for the canopy cloth is

$$L_C = \frac{F_o (C) (R) (S. F.)}{12 D_o} \quad (\text{pound per inch})$$

where

C. = canopy factor = 5 for an extended skirt
and 2.5 for a solid flat

R = reefing factor - 2 for a reefed parachute deployment

S.F. = safety factor = 1.5

The total cloth area of the canopy is dependent on the number of gores due to overlapping of cloth to produce radial seams. This dependency of both the canopy roof and suspension line strength, discussed previously, on the number of gores suggest an optimization routine. To obtain the minimum weight system, the number of gores for any parachute size was varied over the practical range limit discussed above. For the second stage parachutes considered in this program the minimum parachute weight was always obtained with the minimum number of gores since the design line loads for this number of gores was always below the minimum usable line strength (100 pound cord).

The procedure used to determine the parachute sizes for a specific parachute weight allowance was as follows:

1. Select a first stage parachute size.
2. Determine the weight of this parachute.
3. Determine the allowable second stage parachute weight by subtracting the first stage weight from the parachute weight allowance.
4. Determine the size of the second stage parachute which would meet within 2 percent the weight allocated to this parachute.

Item 4 above introduced the problem of performing an iterative solution to determine the size of the second stage parachute. It was found in some computations that a minimum weight to drag area ratio could not be obtained with the above criteria. These exceptions occurred when there did not exist a second stage parachute size that would fulfill the exact weight allowed. As stated previously, the minimum number of gores for a given parachute size always provided the minimum weight. However, in some cases there were two solutions of interest. In these cases it had to be determined which of these solutions rendered the minimum weight to drag ratio. These cases occurred where the second stage parachute size (D_o) for a given allowed weight slightly exceeded the maximum parachute size compatible with a minimum number of gores. In these cases to obtain the parachute weight allowance within the set tolerance of 2 percent required using the next higher number of gores. Using this higher number of gores results in a parachute size smaller and heavier than that obtained by using the maximum size parachute compatible with a fewer number of gores. The obvious choice was the second stage parachute using the minimum number of gores, which was lighter than the allowed weight and provided the minimum ratio of weight to drag area.

APPENDIX III

EQUATIONS USED IN DETERMINING MORTAR WEIGHTS

Assuming that the aerodynamic forces acting on the packed parachute produce a negligible decelerative force, the ejection velocity or relative velocity between the vehicle and pack required for moving the packed parachute to a separation distance of X calibers (vehicle diameters) can be approximated by the following equation. This equation assumes that the vehicle deceleration remains constant and for this application produces a conservative value.

$$V_E = \sqrt{2ngDvX}$$

n is the number of g 's that the vehicle is undergoing and X is the number of calibers at which the pack and vehicle will again be traveling at the same velocity.

Assuming that the parachute is packed in a cylindrical shape with a length (L) to diameter (d) ratio of 2 results in the following expression.

$$\text{Vol} = \frac{\pi d^2}{4} L = \frac{\pi d^3}{2}$$

Letting y be the packing density used ($30\#/ft^3$) the volume required is

$$\text{Vol} = \frac{W}{y} = \frac{\pi d^3}{2}$$

Where W is the weight of the parachute plus risers in earth pounds.

Using an energy balance

$$\text{Energy input} = \text{Kinetic Energy} + \text{Work Performed.}$$

$$P \text{ (average)} \frac{\pi d^2}{4} L = \frac{1}{2} mV_E^2 + mngL$$

substituting for L its equivalent 2 d

$$P \text{ (average)} \frac{\pi d^3}{2} = \frac{mV_E^2}{2} + mng2d$$

Assuming a peak to average pressure ratio of 20, a working stress of 40,000 psi, the thickness of the tube side walls based on a hoop stress calculation of a thin wall cylinder is as follows.

$$t = \frac{P \text{ (peak)} d \text{ (S.F.)}}{(2)(40,000)(144)}$$

where

(S.F.) = the safety factor = 1.5

t - wall thickness (ft)

P (peak) peak pressure (#/ft²)

To determine the weight of the mortar, it has been assumed that a 2 inch cylindrical extension below the bottom of the parachute and bottom of the mortar exists for an expansion chamber. For the bottom of the mortar it has been assumed for weight estimates that the area is that of a flat plate with a thickness equivalent to twice that of the cylindrical walls. To account for the weight of the internal baffling, the divider between the expansion chamber and the parachute compartment, and the cover to the mortar, a weight equivalent to the bottom of the mortar has been assumed. The equation used for the mortar weight is as follows.

W = (walls) + (Bottom and cover and divider and baffling) + 2 inch expansion chamber

$$W = \left[\pi d^2 2t \right] \rho + \left[\pi d^2 t \right] \rho + \left[\frac{\pi d^2 t}{12} \right] \rho$$

Assuming aluminum for the material used in the mortar, a density (ρ) of 173 pounds per cubic foot has been used. Substituting this density in the above equation results in the following.

$$W = 543t \left[2d^2 + d^2 + 0.167d \right]$$
$$W = 543t \left[3d^2 + 0.167d \right]$$

The weights obtained from the above calculations could be reduced if higher strength to weight materials were used. The selection of the stress level used in computations was based on using conventional mortar fabrication techniques. If significant weight reductions are to be achieved, the use of higher strength to weight ratio materials such as alloy steels or filament wound glass reinforced plastics would require more elaborate fabrication techniques, hence higher costs.

APPENDIX IV

SUPPLEMENTAL INFORMATION

At the oral presentation of the final report, JPL requested the determination of the effect on descent time if a first stage parachute was allocated the entire parachute weight allowance (100 percent). Since this request was made after the final report had been prepared, this supplementary information is added for information purposes and was not considered during the performance of the study. This particular percentage of first stage weight to parachute weight allowance was not considered during the performance of the study since it was not in keeping with the design objectives of providing maximum descent time.

To determine this effect, the first stage parachute size and weight information given in Table 2 was used to estimate the size of a first stage parachute deployed at a Mach number of 3.0 that would weigh 35 pounds. It was determined that a Hyperflo parachute diameter of 19.4 feet would fulfill this requirement. The terminal velocity for an impact weight of 100 pounds with this parachute diameter was calculated to be 85 fps. Based on the trajectories computed, it was estimated that the altitude where 0.9 Mach number would be achieved would be 27,000 feet and the time of descent would be appropriately 4 minutes. Comparing this result with the computer calculations given in Figure 12 indicate that the information provided can be extrapolated to give a reasonable estimate of descent time for a 100 percent first stage weight allowance.

REFERENCES

1. Sims, L. W. Analytical and Experimental Investigation of Supersonic Parachute Phenomena, ASD-TDR-62-844 (CONFIDENTIAL), February 1963.
2. Cook Research Laboratories, Final Report of the SD-2X Drone Recovery System Test Program, for Aerojet-General Corporation, Contract No. DA 36-039-SC-80230, May 1960.
3. 67.3 Ft. Nominal Diameter 14.3 Percent Fully Extended Skirt Parachute, FTL-55-9, February 1956.
4. Nickel, W. E. and Sims, L. W., Study and Exploratory Free-Flight Investigation of Deployable Aerodynamic Decelerators Operating at High Altitudes and at High Mach Numbers, FDL-TDR-64-35, Vol. I, March 1964.
5. Properties of Nomex, DuPont New Product Technical Information Document NP-33, October 1963.
6. Performance of and Design Criteria For Deployable Aerodynamic Decelerators, ASD-TR-61-579, December 1963.
7. Pedersen, P. E., Study of Parachute Performance and Design Parameters for High Dynamic Pressure Operation, FDL-TDR 64-66, May 1964.
8. Schmarje, D. P., Evaluation of the 67 Ft. D₀ Recovery Parachute, FTC-TDR-62-39, January 1963.
9. Knacke, T. W., Systems Considerations, Proceedings of Retardation and Recovery Symposium, ASD-TDR-63-329, May 1963.
10. Cook Research Laboratories, Test of the 55 Foot Nominal Diameter Fully Extended Skirt and Deployment System, for Rheem Manufacturing Company, Contract No. DA 36-039 SC-75553, February 1959.
11. DeWeese, J. H. Jr., The USAF Research Program for the Validation of Parachute Performance Prediction Approaches, Paper presented at the Symposium on Parachute Technology and Evaluation, 7, 8, and 9 April 1964.

REFERENCES (Con't)

12. Murrow, H. N., Observations of Parachute Characteristics at Altitudes Above 100,000 Feet by Means of In-Flight Photography, a Paper Presented at the Symposium on Parachute Technology and Evaluation, 7, 8, and 9 April 1964.
13. Anderson, A. R., Effect of Biological Sterilization and Vacuum on Certain Parachute Retardation System Components, Cook Electric Company Report, FR 4324, August 1964.
14. Performance of Trailing Aerodynamic Decelerators at High Dynamic Pressures Phases V and VI, WADC TR58-284, February 1962.
15. Coats, J. D., Static and Dynamic Testing of Conical Trailing Decelerators for the Pershing Re-Entry Vehicle, AEDC TN-60-188.
16. Broderick, M. A. and Turner, R. D., Design Criteria and Techniques for Deployment and Inflation of Aerodynamic Drag Devices, ASD Technical Report 61-188, May 1961.
17. Love, E. S., Base Pressure at Supersonic Speeds on Two-Dimensional Air Foils and on Bodies of Revolution With and Without Fins Having Turbulent Boundary Layers, NACA TN 3819, January 1957.
18. Hoshizaki, H., Heat Transfer in Planetary Atmospheres at Super-Satellite Speeds, ARS Journal, Vol. 32, No. 10, October 1962.
19. Allen, J. H. and Eggus, A. J. Jr., A Study of the Motion and Aerodynamic Heating of Missiles Entering the Earth's Atmosphere at High Supersonic Speeds, RM A53D28, August 25, 1953.
20. Lloyd, D.K. and Lipow, Myron, Reliability Management, Methods and Mathematics, Published by Prentice-Hall, Inc., 1962.
21. United States Air Force Parachute Handbook, WADC TR 55-265, December 1956.